The Acylation Cycle – Mechanisms, Specificity, the creation of spatial order and Implications on Ras Signaling

Dissertation
Zur Erlangung des Grades eines
Doktors der Naturwissenschaften
Der Fakultät der Chemie der
Technischen Universität Dortmund

vorgelegt von
Nachiket Vartak

März 2011

The work described in this thesis was performed under the supervision of Prof. Dr. Philippe Bastiaens from February 2007 to February 2011 at the Max Planck Institute for Molecular Physiology, Dortmund, under the auspices and funding of the International Max Planck Research School-Chemical Biology.

First Examiner:

Prof. Dr. Philippe Bastiaens   Dept. of Systemic Cell Biology

Max Planck Institute for Molecular Physiology

Dept. of Chemical Biology

Technische Universitaet, Dortmund

…………………………………………………………………

Second Examiner:

Prof. Dr. Herbert Waldmann   Dept. of Chemical Biology

Max Planck Institute for Molecular Physiology

Dept. of Chemical Biology

Technische Universitaet, Dortmund

……………………………………………………………..

ZUSAMMENFASSUNG

Innerhalb von Zellen ist die Verteilung von Proteinen häufig präzise, das bedeutet mit spezifischer Anreicherung in verschiedenen intrazellulären Kompartimenten. Als Ursache solcher Verteilungen wurden bereits Interaktionen, Rezeptoren oder auch Signalsequenzen beschrieben. In dieser Arbeit wird die Entstehung einer räumlich inhomogenen Proteinverteilung innerhalb von Zellen beschrieben – 'Acylation Cycle' genannt - die auf einem Reaktions-Diffusions-Prozess basiert, welcher die reversible S-Palmitoylierung umfasst. Palmitoylierung läuft am Golgi-Apparat ab, wobei die dort lokalisierten Enzyme kaum oder keine Spezifität für ein konkretes Proteinsubstrat zeigen. Anscheinend benötigen DHHC-Palmitoyltransferasen zur Palmitoylierung lediglich einen membrannahen Cysteinrest. Den gerichteten Transport zur Plasmamembran ermöglicht der sekretorische Weg. Der 'Acylation Cycle' wirkt der entropie-getriebenen Homogenisierung palmitoylierter Proteine im Zellvolumen entgegen. Weiterhin wird die Aufenthaltsdauer palmitoylierter Proteine, wie z.B. Ras, an der Plasmamembran durch die Kinetik des 'Acylation Cycle' beeinflusst, wodurch auch die Menge an Ras, die dem MAPK-Signalweg zur Verfügung steht, verändert wird. Das Unterbrechen des 'Acylation Cycle' durch den neuartigen Inhibitor Palmostatin B bewirkt die durch Entropie getriebene Umverteilung von Ras. Durch Palmostatin B-Behandlung wird die Ras-Signalaktivität nach EGF Stimulierung an der Plasmamembran von der Aktivität am Golgi Apparat entkoppelt. Letztendlich führt die Palmostatin B-Behandlung von mit onkogenem HRasG12V transformierten MDCK Zellen zu einer Unterdrückung ihres konstitutiv-aktiven MAPK-Signals, welches zur Zellteilung führen kann und verursacht so die Reversion des Phänotyps zu einem der untransformierten MDCK Zellen sehr ähnlichen. Der 'Acylation Cycle' ist ein Phänomen, dem viele Proteine unterworfen sind und bietet daher die Gelegenheit die Modulation von Signalaktivitäten therapeutisch auszunutzen.

ABSTRACT

Protein distributions within the cellular environment are often precise, with specific enrichments in different intracellular compartments. Such distributions have previously been described to be generated by specific interactions, receptors or signal sequences. This work describes the creation of a spatially inhomogeneous protein distribution within the cell through a reaction-diffusion process, involving reversible S-palmitoylation – termed as the Acylation cycle. Palmitoylation occurs on the Golgi apparatus, and enzymes participating in the acylation cycle have little or no specificity towards the protein substrate. DHHC Palmitoyltransferases seem to require only a membrane proximal Cysteine residue for palmitoylation. The secretory pathway provides the vectorial transport required to transfer palmitoylated proteins to the plasma membrane. The Acylation cycle counters entropy driven homogenization of a palmitoylated protein within the cellular volume. Further, kinetics of the acylation cycle affect the residence time of palmitoylated proteins such as Ras on the plasma membrane, and thus change the amount of Ras available for MAPK signaling. Interruption of the acylation cycle through a novel inhibitor Palmostatin B, causes entropy driven redistribution of Ras. Under Palmostatin B treatment, Ras signaling from the Golgi apparatus in response to EGF stimulation is uncoupled from its signaling on the plasma membrane. Finally, treatment of oncogenic HRasG12V-transformed MDCK cells with Palmostatin B quenches their constitutively active proliferative MAPK signaling and leads to a phenotypic reversion to one similar to untransformed MDCK cells. The acylation cycle is a phenomenon a diverse array of proteins is subject to, and thus offers an opportunity for therapeutic modulation of signaling activities.

Contents

1   INTRODUCTION

Biological Systems are complex, not just in the colloquial sense of the word, nor as the collective whine of exasperated biologists. They are complex in the pure mathematical designation – the number of interacting nodes in even the best map of all the molecules, structures and behaviors makes them extremely information-rich on all levels – from cellular biology to ecosystem dynamics. This information of course, changes in response to the environment, the internal state of the system and according to predetermined programming inherited from the previous generation of such systems. Focusing on cell biology, one could go so far as to say that biological systems exist *because* they are information rich, for many of the molecules and structures have functions and activities directly antagonistic to each other. In other cases, some structures are so efficient at their function that without the metaphorical handbrake, their activity would spiral out of control. In still others, the simple existence of molecules in the 3D-volume of the cell would not nearly be sufficient to have concentrations high enough that the molecules are able to function as required to maintain the system. To find any semblance of a method to the madness, it is a necessary condition that some sort of information-processing capabilities exist within cells. A common solution to the problem is to have multiple levels of regulation imposed on to specific molecules, tempering their activity to the state of the cell. The regulation may be imposed on the level of activity of the gene, as is seen with transcription factors and the periodic expression of cell-cycle proteins. It may be as seen with protein phosphorylation, or G-proteins, where the activity of a protein is controlled by secondary molecules that are bound to it. While these phenomena have been studied in substantial detail, a simpler, less appreciated method involves protein targeting, i.e., the creation of asymmetric protein distributions within the cell. Receptor-based or signal-sequence based mechanisms to achieve protein targeting are well known, and reaction-diffusion mechanisms in calcium-dependent signaling are known. However, to the knowledge of the author, no known reaction-diffusion mechanism that targets proteins with specific implications on cellular signaling has been described so far. This work describes such a spatial reaction-diffusion cycle, its mechanism and its influence on signaling.

1.1 Emergent Patterns in Biology

In general, asymmetric pattern generation has been the subject of study in mathematical biology (Polack & Stepney, 2005). With a brief description of certain well-understood examples, the author wishes to draw out a central theme in the emergence of spatial patterns.

Cellular Automata: Cellular automata (CA) are isolated abstract universes, with discrete 'cells' (no relation to biological cells), that may transition iteratively between many states (Dasgupta et al, 2001). The rules of these transitions are simple, and usually involve a dependency on cells surrounding the one undergoing the transition, referred to as the 'neighborhood' of the cell. Perhaps the most well-known of CA universes is Conway's Game of Life, which consists of a matrix of cells that transition between 2 states: alive and dead. Transitions between these two states are given simply as follows:

1. Any live cell with fewer than two live neighbors dies, as if caused by under-population.
2. Any live cell with two or three live neighbors lives on to the next generation.
3. Any live cell with more than three live neighbors dies, as if by overcrowding.
4. Any dead cell with exactly three live neighbors becomes a live cell, as if by reproduction.

Conway's Game of Life has been used to model population dynamics in an eco-system. But perhaps the most insightful feature is the occurrence of self-reproducing patterns that achieve a steady-state until perturbed.
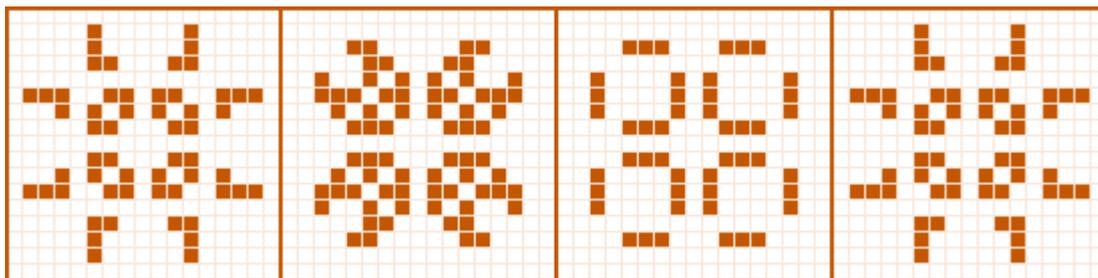
'Pulsar': Snapshots depicting the 4 stages of a self-reproducing steady-state pattern generated from the rules of Conway's Game of Life.

Lindenmayer Systems: Lindenmayer (L)-systems (Lindenmayer, 1968) described simple rules for the generation of strings, with each hierarchical step recorded as the string builds up. When the rules of such strings include a distance and angular component, graphical

representations of the strings may be obtained. Surprisingly, it is possible to reproduce the appearance and branching of nearly every plant by simply varying the distance and angular component. While the biological basis of these components is not understood, it is convincing proof that complex fractal-like spatial expanses such as those of plants and trees may be produced by repetitive iteration of simple rules.
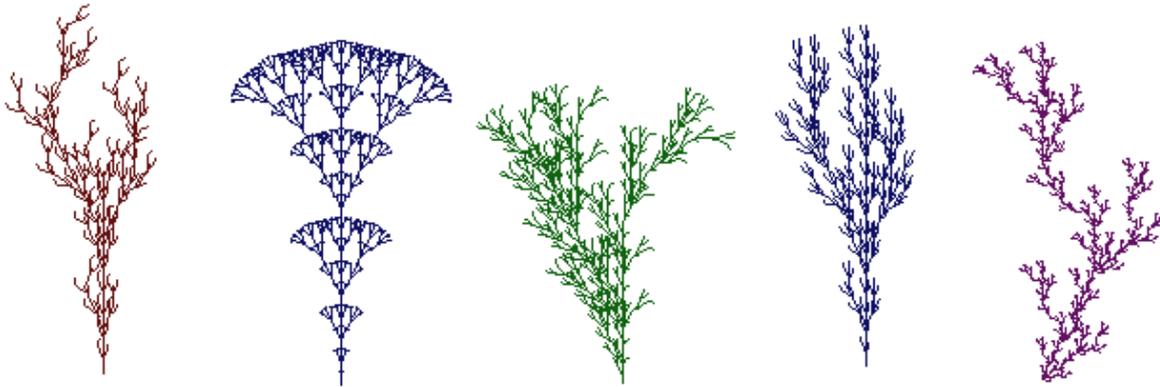
Plants and Fractals: Various L-system generated shapes of plants based on variations of (1) Create line of length 'd'. (2) Change growth angle by φ. (3) Repeat. Reproduced from *Prusinkiewicz P, Lindenmayer A (1990). The Algorithmic Beauty of Plants. Springer-Verlag:New York*

Turing Patterns: Described initially by Alan Turing, Turing patterns are concentrations gradients that arise due to the spontaneous fluctuations in spatially uniform distribution of a molecular activity, when the activity is inhibited over large distances, but enhanced over short distances (Dillon et al, 1994; Benson et al, 1998). In this sense, Turing patterns are classical reaction-diffusion systems and are closest to the spatial cycles described in this work. Turing patterns have been described as models for cellular differentiation during development, and more recently as involved in cellular glycolytic processes, eventually contributing to decisions to commit to the cell division process.

While the systems described above may seem diverse and unrelated, the central theme in all of them is one of discrete agents following simple rules (mathematical, physical or biochemical), such that the interaction of these agents lead to spontaneous steady-state asymmetries in particular contexts. The Acylation Cycle described in this work is a spatial reaction-diffusion cycle that follows similar rules to generate a precise localization of proteins in the cellular environment, emerging from the interaction of localized agonistic

activity, ubiquitous antagonistic activity and a vectorial transport of entities subjected to these activities.
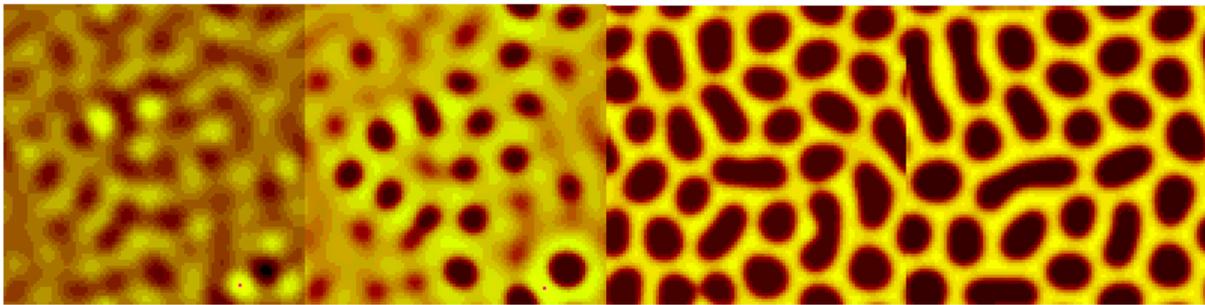
How the leopard gets its spots – Turing pattern generation from spontaneous fluctuations in the 'brown' molecule against a yellow 'inhibitor'. *Reproduced from Rauch et al. Journal of Theoretical Biology, Volume 226, Issue 4, 21 February 2004, Pages 401-40*7

1.2 Protein Lipidation

Protein lipidation involves the post-translational covalent modification of proteins with lipid moieties. It is described here as the biochemistry of the acylation cycle falls within the purview of this broad topic. While a large number of lipid-modified proteins are known, the role of such a modification in each case has been thought to be rather unique to the protein. Lipid modifications are generally categorized according to the nature of the lipid group and its linkage to the protein. However, in the context of this work, it is more suitable to describe lipid modifications as either irreversible, or reversible and dynamic.

Irreversible Lipidation and its roles

Irreversible lipid modifications are those that remain on a protein molecule throughout its life cycle, that is, they are removed only through protein degradation processes. In Eurakryotes, irreversible lipid modifications include N-linked acyl groups (Martin et al, 2011), S-linked isoprenoids (Hougland & Fierke, 2009)and O-linked cholesterols (Milenkovic & Scott, 2010).

N-linked acylations occur at the ε-N of Lys residues, or at the α-N of the first amino acid of proteins via amide bonds. N-linked lipids are typically long-chain fatty acids, of which palmitate and myristate represent the overwhelming fraction. It should be noted however, that N-palmitoylation and N-myristoylation are not redundant, and are catalyzed by separate N-myristoyltransferase and N-palmitoyltransferase in *Drosophila melanogaster*. A mammalian N-palmitoyltransferase is known with a single known substrate – the Hedgehog protein, and there are indications that the biochemical mechanism involved in these modifications may also be different. N-myristoylation describes the addition of myristic acid (C14:0) to a glycine residue with an exposed NH_2 group after cleavage of the immediately adjacent initiating methionine (Resh, 2006; Zha et al, 2000). This process is predominantly post-translational, mediated by soluble enzymes, and has a strict consensus sequence (M**G**XXXS/T)(Maurer-Stroh et al, 2002). N-myristoylation can also occur posttranslationally, notably after caspase-mediated protein cleavage during programmed cell death (Zha et al, 2000). N-palmitoylation is less understood, but is known to require a Cys residue, which is presumably S-palmitoylated first, and then an S-to-N acyl transfer occurs (Buglino & Resh, 2008). In general, N-palmitoylation seems to be common in proteins that are eventually secreted such as *Hedgehog*, and seems to have more profound effects on tissue-level signaling activities. N-myristoylation on the other hand is more common in proteins involved in cellular signaling such as the heterotrimeric G-proteins and seems to have more profound effects on intracellular signaling (Salaun et al, 2010). In either case, myristoylation and palmitoylation seem to confer additional hydrophobicity to protein molecules, allowing them to interact with membranes. A large number of N-myristoylated proteins are peripheral membrane proteins, with well-defined functions on the plasma membrane of cells. Indeed, abolishing these modifications through mutagenesis of the N-myristoylation signal sequence leads to a loss-of-function for most proteins at their cellular expression levels. N-palmitoylated proteins on the other hand are secreted, necessitating a requirement to transgress the plasma membrane, which may be mediated by the membrane-soluble palmitate group. For example, the Hedgehog protein, which is required tissue patterning to establish a concentration gradient in the tissue, fails to be secreted when expressed in a non-N-palmitoylatable mutant form.

Prenylation is the well-studied of the post-translational modifications, owing to the success of prenylation inhibitors in clinical trials (Gelb et al, 2006). Prenylation involves the linkage of farnesyl or geranylgenranyl moieties to the C-terminal of proteins containing the so called CaaX signal sequence as the last 4 aa in the polypeptide chain. The CaaX sequence is first proteolytically processed to remove the terminal the 3 amino acids. Farnesyl pyrophosphate or Geranylgeranyl pyrophosphate, both precursors in the cholesterol biosynthesis pathway serve as respective isoprenyl donors in the reaction catalyzed by farneyltransferase (FTase) or geranylgeranyltransferase (GGTase) (Reid et al, 2004). The prenyl moieties are then linked to the S-atom of the Cysteine residue in the CaaX box via a thioether bond. The role of isprenyl modifications has been elucidated largely for Rab and Ras proteins which are geranylgeranylated and farnesylated respectively. As with N-myristoylation, prenylation increases a protein's hydrophobicity and is necessary for correct localization of these proteins to membranes and docking into cellular membranes (Silvius & l'Heureux, 1994). Comparisons of the CaaX box of these proteins have led to the identification of sequence requirements dictating preference for which of the two isoprenoid groups are acquired by the proteins(Maurer-Stroh & Eisenhaber, 2005). However, some degree of redundancy exists in this preference, as treatment with farnesyltransferase inhibitors leads to geranylgeranylation of Ras. At least the geranylgeranyltransferase, therefore, is specific to the isoprenyl group, but has a much more relaxed specificity when it comes to the specific CaaX sequence.

Finally, at least one example of the *Hedgehog* protein is known where the isoprenoid group attached to the protein is a cholesterol ester. This modification occurs at the carbonyl group prior to a non-terminal Cysteine residue, and is said to mediate secretion of the *Hedgehog* protein (Herz et al, 1997). However, cholesterol modified proteins are not known to possess the acylation cycle described in this work.

Besides the clear mislocalization and loss of function reported for both Ras and Rab proteins when prenylation is inhibited in general (Rak et al, 2003; McGeady et al, 1995; Santillo et al, 1996), several studies suggest that prenylation may affect the partitioning of these proteins to specific membrane domains. Clustering behavior of Ras proteins has been suggested to

exist and derive largely from its farnesyl moiety (Prior & Hancock, 2001; Harding & Hancock, 2008). Solubilization of Ras, Rab and other prenylated proteins such as Rho is mediated by binding of isoprenoid groups to so-called Guanine Dissociation Inhibitor (GDI) proteins (Antonarakis & Van Aelst, 1998). GDIs shield the hydrophobic isoprenoid from the hydrophilic cytosol, thus allowing solubilization. Given the absolute necessity of prenylation for correct localization and solubilization, it is therefore not surprising that FTase and GGTase inhibitors are effective in quenching hyperactive mutants of proteins possessing these modifications.

It has been reported that proteins subjected to the acylation cycle usually require a prenyl group or an N-myristoyl group in order to enter the cycle (Linder & Deschenes, 2007). Since an increase in membrane binding is the common property conferred by these lipid modifications, it seems likely that the acylation cycle requires prior membrane affinity, however weak it may be. As such, these modifications are of special importance to the work described herein.

Reversible Lipidation

Only one known reversible lipid modification is known, the acylation of proteins at the S-atom of Cysteine residues via a thioester bond. Several transmembrane proteins and peripheral membrane proteins are S-acylated. Again, palmitate moieties constitute an overwhelming majority of S-acyl groups on proteins (Martin & Cravatt, 2009; Liang et al, 2002), and hence terms acylation and palmitoylation are used interchangeably.

The repertoire of S-palmitoylated proteins is diverse, include transmembrane receptors such as the β-adrenergic receptor, peripheral membrane proteins such as Gα family and Ras, as well as several synaptic proteins that shuttle between the cytosol and the synaptic membranes (Fukata & Fukata, 2010). Indeed, large scale proteomic analysis in Yeast has revealed several hundred proteins that undergo S-palmitoylation (Roth et al, 2006). Unfortunately, substantial controversy exists around the enzymes that mediate such palmitoylation. Firstly, the only other known S-acylation of a protein occurs during fatty acid biosynthesis (Alberts et al, 1965; Toomey & Wakil, 1966). Much of the mechanism for

protein acylation is thought to be similar to that occurring on the acyl-carrier protein during fatty acid biosynthesis. As such, palmitoyl-CoA is thought to be the acyl-donor during such a reaction. However, incubation of proteins with accessible Cys residues with palmitoyl-CoA shows that the protein acylation reaction occurs spontaneously *in vitro* (Bizzozero et al, 1987a; 1987b), in a reducing environment. Secondly, no consensus sequence could be established for proteins that are palmitoylation substrates. Due to these reasons, the requirement of a palmitoyltransferase (PAT) enzyme has been the subject of debate (Dietrich & Ungermann, 2004).

It could be shown however, that yeast lacking Erf2 and Erf4 genes showed a phenotype that similar to a RAS knockout (Bartels et al, 1999). RAS (yeast homologue of human Ras genes) is expressed in these yeast cells, but localized to the endoplasmic reticulum (ER) instead of its wild-type plasma membrane (PM) localization. The presence of lipid anchors is known to allow PM binding in other proteins and as RAS is a palmitoylated protein, the activity of the Erf2/Erf4 complex to palmitoylate Ras proteins was assayed in the presence of palmitoyl-CoA. Indeed, the presence of the Erf2/Erf4 proteins led to a modest increase in Ras palmitoylation. Positional mutagenesis showed that a particular 4 amino acid stretch within Erf2/Erf4, henceforth called the DHHC domain was essential for this palmitoyltransferase activity. Formally named the DHHC-zinc finger-like cysteine rich domains (zDHHC-CRD), 7 proteins in yeast were identified (Roth et al, 2002). The DHHC proteins are multipass polytopic transmembrane proteins, while their substrates are often cytosolic or peripheral membrane proteins, suggesting that the reaction they catalyze occurs at the membrane cytosol interface. Further, most proteins undergoing S-palmitoylation have prior N-myristoyl or prenyl modifications within the region of the palmitoylatable Cys residue, which grant them weak membrane affinity. Presumably, at least a weak membrane affinity is required for Cys residues in a protein to gain access to DHHC proteins and acquire palmitate groups. A small subset of proteins such as GAP43 is exclusively S-palmitoylated (Liang et al, 2002) – however, these proteins may possess weak membrane affinity through other non-lipid based mediators.

A comprehensive proteomics study of protein palmitoylation in yeast ascribes PAT activity to each of these proteins, though perhaps the most insightful finding this study is the overlapping and varying specificity of these PATs (Roth et al, 2006). Pfa3 for example, was said to be a general palmitoyltransferase with minimal specificity towards the protein substrate (Nadolski & Linder, 2009), while Erf2/Erf4 mentioned earlier were thought to be specific Ras PATs.

In mammalian systems, 25 DHHC proteins have been identified. As with the yeast DHHC proteins, mammalian proteins display very little sequence similarity beyond the presence of the DHHC domain. Unfortunately, limitations of knockdown methodologies for such a large number of genes in mammalian cells make it difficult to tease out the specificity of these DHHC proteins with the approaches used in yeast systems. Based on comparisons with substrate specificity with those of yeast DHHC proteins, the DHHC9/GOLGA7 complex is thought to be the mammalian equivalent of the yeast Erf2/Erf4 RasPAT (Swarthout et al, 2005). It should be noted that hDHHC9 and Erf2 have only 31% sequence similarity, barely above the 'homology-threshold'. Similarly, DHHC3 and DHHC8 and thought to be general low-specificity PATs, much like the yeast Pfa3. Various studies on the specificity of DHHC proteins have unfortunately led to only partial agreement regarding the substrate specificity of DHHC proteins (Hou et al, 2009).

On the other hand, the tissue specific expression of mammalian DHHC proteins and their intracellular localization has been studied in greater detail (Ohno et al, 2006). The fact that all DHHC proteins do not have ubiquitous expression, while many palmitoylated proteins do has added more credibility to the hypothesis that DHHC proteins must have overlapping specificity. DHHC9, the supposed RasPAT, for example, is not detected in the thymus, spleen and peripheral blood leucocytes. Nonetheless, its substrate Ras is expressed in all mammalian tissues. Clearly, Ras palmitoylation must be mediated by other proteins in the tissues where DHHC9 is absent. The intracellular localization of DHHC proteins, as studied with microscopy of fluorescent fusion constructs indicates that most DHHC proteins localize to the Golgi apparatus or on the ER, with 2 reported to localize on the plasma membrane.

The localization of DHHC9 to the Golgi apparatus is at least consistent with studies indicating that the palmitoylation of Ras occurs on the Golgi apparatus in mammalian cells.

Whatever the exact substrate specificity of DHHC proteins, or their PAT activity, it is certain that these proteins seem to affect the function of their proposed substrates. It is unclear however, if this effect is a direct result of catalyzing palmitoylation of these proteins, or an indirect effect due to an unknown function of these DHHC proteins.

Functions of Reversible S-palmitoylation

S-palmitoylation has shown to be dynamic, consistent with the labile nature of the thioester bond linking the lipid to the protein (Iwanaga et al). A protein may undergo several palmitoylation turnovers during its existence in the cell, suggesting a role for the palmitoylation status of the protein in its cellular functions.

Palmitoylation is known to be essential for the structural stability of proteins such as rhodopsin (Maeda et al). Palmitoylation prevents the inactivation of rhodopsin, presumably by stabilizing the protein tertiary structure. Such structural palmitoylation is postulated to stabilize G-protein coupled receptors as well. It is unclear if such palmitoylation is indeed dynamic, or if it used to regulate signaling via these proteins.

It is well-established that palmitoylation controls the localization and activity of proteins. Receptors such as estrogen-receptor or the AMPA receptor require palmitoylation in order to enhance their membrane residence time (DeSouza et al, 2002; Gonnord et al, 2009; Hayashi et al, 2009). Since such receptors are transmembrane proteins, clearly palmitoylation is not required to enhance membrane binding. However, palmitoylation may facilitate the interaction of the transmembrane domains of these proteins with the local lipid environment, and thus increase their average residence time in the membrane. On the other hand, palmitoylation could regulate ubiquitin-mediated protein degradation, as is the case for the yeast SNARE protein Tlg1 (Valdez-Taubas & Pelham, 2005). The roles palmitoylation plays in the function of a protein may be convoluted. For example, both the

ligand-dependent activation and regularized internalization of synaptic AMPA receptors is dependent on palmitoylation of the protein. In AMPA membrane receptors, palmitoylation controls regularized internalization, but causes inhibition of the receptor. Palmitoylation therefore seems to have direct effects on a protein's activity or indirect effects by regulating its localization and degradation.

For peripheral membrane proteins such as Ras and heterotrimeric G-proteins, palmitoylation increases membrane binding of these proteins by increasing the hydrophobicity. Any effects on cellular signaling, so far have been ascribed to mislocalization of the respective protein. However, the palmitoylation of transmembrane receptors occurs over tens of minutes, while the palmitate turnover of peripheral membrane protein occurs over a time scale of seconds (Rocks et al, 2005). It is likely that limitations of conventional biochemical approaches which typically involve *in* vitro purification, isolation and then equilibrated assays have prevented the elucidation of fast-time scale effects of palmitoylation on the activity of these proteins. Indeed, part of this work describes a mode of signaling regulation of Ras that results from the dynamics of the Ras acylation cycle.

1.3 Depalmitoylation and Thioesterases

While S-palmitoylation is dynamic, autohydrolysis of the thioester bond in the reducing environment of the cell is unlikely. Enzymes that catalyze the depalmitoylation of proteins are simply thioesterases. Fortunately, thioesterases are at least more familiar than the enzymes which catalyze the palmitoyltransferase reaction. Mammalian systems contain only 3 known genes that encode for a acyl-protein thioesterase activity: Palmitoyl-Protein Thioesterase 1 (PPT1), Acyl-Protein Thioesterase 1 (APT1), and Acyl-Protein Thioesterase 2 (APT2) (Hirano et al, 2009a). As PPT1 is a lysosomal enzyme, it is thought to be involved in depalmitoylation during degradative processes and certainly does not have access to the vast array of palmitoylated proteins present in the cell (Dawson et al, 2010). APT1 and APT2 on the other hand are expressed ubiquitously and have cytoplasmic localization, making them good candidates as protein depalmitoylating thioesterases. APT1 was shown to

depalmitoylate Gα protein and Ras *in vitro* (Duncan & Gilman, 1998). However, *in vivo* demonstration of the activity of APT1 was lacking thus far. APT2 is less studied; however, the high sequence similarity (66%) suggests that APT2 is indeed a functional thioesterase. APT2 has now been shown to be an active thioesterase, depalmitoylating the GAP43 protein (Tomatis et al). In either case, the role played by these enzymes in the activity of palmitoylated proteins remains to be elucidated. Regulatory mechanisms have been described, wherein nitrosylation or proline isomerization on substrate proteins (Ahearn et al, 2011; Baker et al, 2000), as well as PKC mediated control of APT1/2 localization affects their activity in certain cell types (Wang et al, 2000). In this work, these proteins are described as components providing the infrastructure for the acylation cycle and thus affecting Ras signaling. The reader may note that APT1 and APT2 were discovered initially as having lysophospholipase activity and may be denominated LYPLA1 and LYPLA2 respectively. This nomenclature is changed to its current form after the publication of this work, corroborated by *in vitro* data indicating that the acyl-protein thioesterase activity of these proteins is far more efficient than their incidental lysophospholipase activity (Uniprot Database Version 25, http://www.uniprot.org).

1.4 The Ras proteins and biochemistry of the GTPase cycle

Ras has the significant distinction of being the first oncogene to be discovered (Parada et al, 1982). The Ras gene was known to be part of the Harvey virus, which caused the rapid formation of sarcoma tumours in Rats. Isolated as tumorigenic fragments from at least thrice from independent samples of human cancerous tissue, its significance in oncogenic transformation was solidly established when Luis Parada reported the tumorogenic fragments to be homologues of the transforming gene in the Harvey virus, thus christening them to be RAS (Rat Sarcoma). Subsequent studies by identified Ras to be a single molecule GTPase akin to the heterotrimeric G-proteins. Over the years, Ras has evolved in scientific literature from single viral protein to a superfamily of related proteins (Wennerberg et al, 2005). The original Ras proteins are now known to occupy a central node in cellular

signaling, and in turn affect a wide variety of cellular processes ranging from cell proliferation, apoptosis, cytoskeletal remodeling etc (Bourne et al, 1991; Shields, 2000).

All Ras proteins are Guanine nucleotide binding proteins – consisting of the G-domain which binds GTP or GDP with affinities as near as makes no difference (Vetter & Wittinghofer, 2001). Substantial changes occur in the tertiary structure of the G-domain when bound to GTP, as compared to when bound to GDP. The two resulting conformational states can be distinguished by 'effector' domains on other proteins that recognize only the GTP-bound form of Ras. In short, the ability to bind different nucleotides and reflect its 'loading state' turns Ras into a molecular switch. Of course, a switch of this sort is not very useful until it is regulated. In order to switch from a GDP-bound state to a GTP-bound state, Ras proteins require interaction with proteins called Guanine Nucleotide Exchange Factors (GEFs). GEFs pry the structure of Ras, allowing the release of GDP. Since the cytoplasmic GTP concentration is much higher compared to GDP (GTP:GDP ratio is ~10), GTP replaces GDP, thus changing the loading state of Ras (Antonarakis & Van Aelst, 1998; Zhang et al, 2005).

Conversely, G-domains are weak GTP-hydrolases (GTPases), possessing an active site that lacks a critical Asp residue (Wittinghofer et al, 1997). Interaction with the aptly named GTPase Activating Proteins (GAPs) completes the active site, and causes the hydrolysis of the bound GTP to GDP and inorganic phosphate. Thus Ras is switched to the GDP-loaded state.
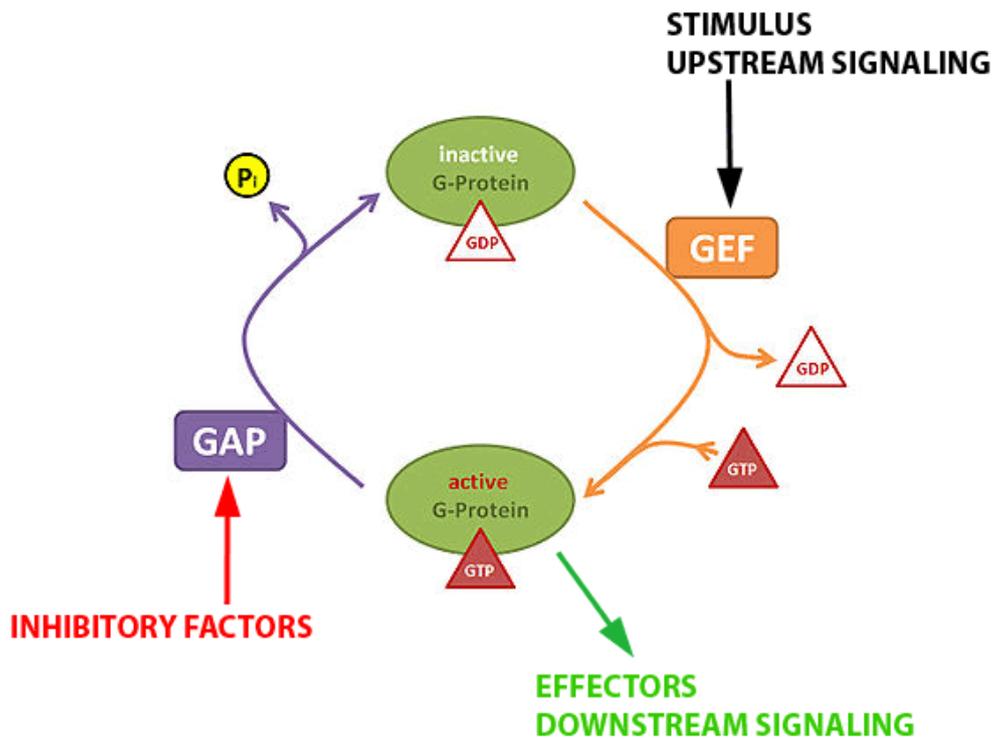
The GTPase Cycle. G-proteins transition between GTP-bound and GDP-bound states, catalyzed by GEFs and GAPs that respond to upstream stimuli. GTP-bound G-proteins are considered 'active' and they can bind downstream effectors and continue the signal transduction cascade.

This transition scheme between GTP and GDP loaded states of Ras is known as the GTPase cycle, and occurs in response to activation of GEFs and GAPs from upstream signaling events. Typically, downstream effectors bind Ras when it is GTP-loaded, furthering the transmission of the signaling event. Since upstream GEF and GAP activators represent a wide variety of cellular receptors and proteins, it is clear that Ras serves as an integration point in various signaling networks, facilitated by the GTPase cycle.

1.5 Ras Signaling in the Context of the MAPK Pathway

Ras signaling in the context of the Membrane Associated Protein Kinase (MAPK) pathway has received significant attention for a number of reasons. Firstly, it is the first pathway describing a linear signaling cascade from extracellular ligands to gene expression. Secondly, the pathway was discovered to signal proliferation of cells. The discovery of Ras, which itself was known to be an oncogene, as a component of this pathway was an epiphany in mechanisms of signal transduction. In particular, the role of Ras in MAPK pathway is important for this work, since it is the proliferative effects of oncogenic Ras that can be quenched by manipulating the acylation cycle.

The MAPK pathway is activated by one of several extracellular ligands, each binding to different plasma membrane bound receptors. One such ligand is the Epidermal Growth Factor (EGF), which binds the transmembrane Epidermal Growth Factor Receptor (EGFR). The cytoplasmic domain of these receptors is a receptor tyrosine kinase (RTK), which undergoes activation upon ligand binding of the extracellular domain. The kinase activity autophosphorylates tyrosines present in the activation loop of the protein (Lemmon & Schlessinger, 2010). Adaptor proteins containing Src-Homology (SH2) domains, which can themselves be phosphorylated bind to phosphorylated Tyrosines, for example Grb2 (Chen§ et al, 1996; Lowenstein, 1992), which in turn recruits GEFs such as SOS (*son of sevenless*). SOS then interacts when GDP-loaded Ras to 'activate' it, exchanging the GDP to GTP. GTP-loaded Ras can then be bound by the downstream Serine/Threonine kinase Raf, activating it (Freedman et al, 2006). Raf then activates Mek by phosphorylation. Mek is itself a Ser/Thr kinase which in turn activates another downstream Ser/Thr kinase Erk by phosphorylation (Peyssonnaux & Eychène, 2001). Upon phosphorylation, Erk translocates to the nucleus (Brunet et al, 1999), and phosphorylates Elk and nuclear transcription factor by phosphorylation. Elk then activates expression of several genes required for cell proliferation.

This linear description of the MAPK pathway is of course oversimplified. Several complexities exist within the details of MAPK signaling. Besides adaptor proteins such as Grb2, the interaction of several of the kinases is facilitated through scaffold proteins such as

KSR or Ste5 (in yeast) (Kolch, 2005; Zhong et al, 2003; Rocks et al, 2006). The ligand sensing RTKs on the membrane are known to cluster, and exhibit regulated internalization (Hofman et al, 2010; Wang et al, 2005). Network analysis of MAPK systems have shown that the fidelity with which the involved kinases act on each other differs depending on the upstream extracellular ligand, eventually affecting the output of the signal transduction process (Santos et al, 2007). Numerous positive and negative feedback loops exist within the MAPK infrastructure. At the level of Ras, the previously mentioned GEF SOS does not simply activate Ras, but its activity can be allosterically enhanced by activated Ras (Waters et al, 1995; Freedman et al, 2009). In other words, SOS asserts positive feedback on itself, making it an effector as well as GEF for the Ras protein.
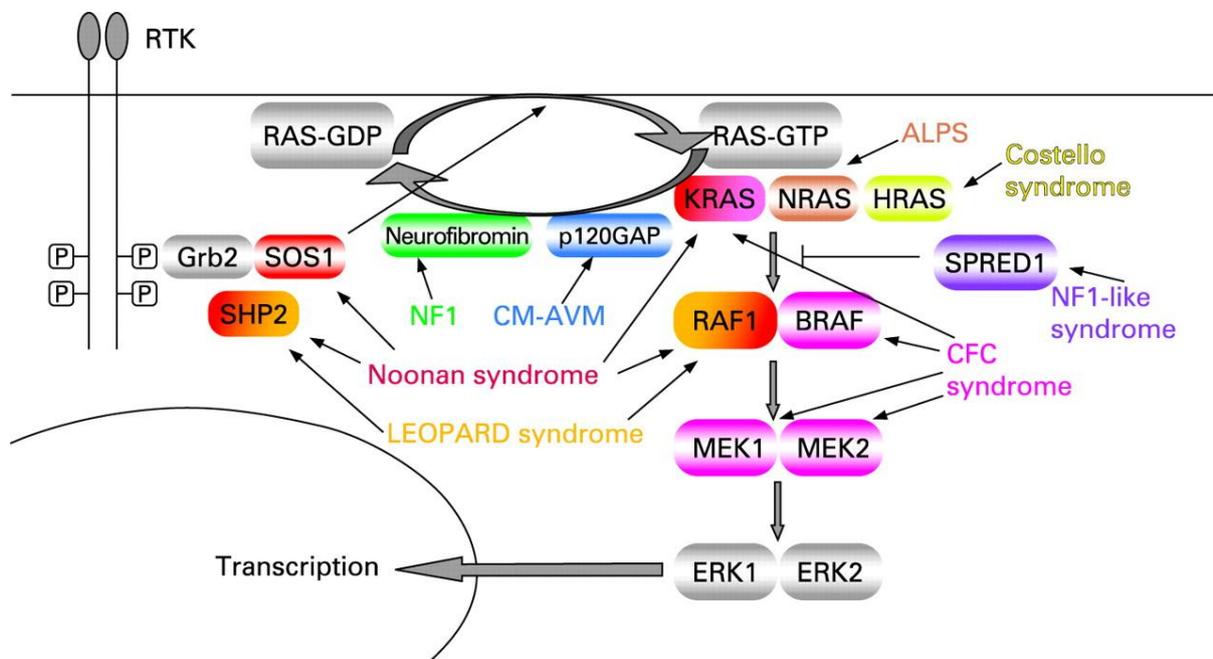
MAPK pathway and Ras coupling to RTKs. Signal transduction in a highly simplified depiction of the MAPK pathway is itself full of complex interactions surrounding the Ras GTPase cycle. Additionally, a plethora of syndromes associated with alterations in MAPK components highlights the prominent role of the MAPK cascade in cellular signaling.

In the background of such complexity, the Ras protein forms a nodal point where MAPK signals are integrated. Due to its role in cellular proliferation, differentiation and a host of

other cellular processes, it is no surprise that nearly every protein-coding gene that contributes to the MAPK cascade, including Ras is a potential oncogene. Unfortunately, attempts to design inhibitors that affect the GTPase cycle of Ras in order to control oncogenic effects of the MAPK mutations, have met with failure. The GTPase cycle, which is the intended target of such inhibitors, is far to general a mechanism. The G-domain is an all-purpose protein domain that is present in proteins involved in protein sysnthesis, such as Ef-Tu, in the entire Ras superfamily (protein secretion, sorting, proliferation, cytoskeleton remodeling, vesicular transport etc.), in proteins that form the basis for alternative forms of signaling such as G-protein coupled receptors. As a result, designing specific inhibitors for the MAPK/Ras GTPase cycle is challenging and almost always results in massive toxicity and pleiotropic effects (Morris et al, 2010; Newton et al, 2000; Caron et al, 2005; Klohs et al, 1997; Arredondo et al, 2006). In this work, the acylation cycle is shown to be a target candidate for modulation of Ras activity while avoiding such unwanted effects.

1.6 Ras Isoforms and Localization

So far, this document has referred to Ras as a single protein entity. However, mammalian genomes contain three isoforms of Ras – Harvey (H)-Ras, Neuroblastoma (N)-Ras and Kirsten (K)-Ras. HRas and KRas are named after their homology viral oncogenes that induce sarcomas after infection (Ulsh & Shih, 1984; Norton et al, 1984). NRas is known from its homology to the oncogene identified in a human neuroblastoma cell line (Ireland, 1989). The KRas gene product occurs in two splice variants KRas4A and KRas4B, with differences in the C-terminal region of the protein. As KRas4B is similar to HRas and much less abundant than KRas4A, the term 'KRas' typically refer to the KRas4A variant (Pan et al, 1990).

The Ras proteins are 189 amino acids in length of which the first 165 constitute the conserved G-domain. This region is nearly identical between all of the three Ras isoforms displaying >95% sequence similarity. The effector binding region of the G-domain is exactly identical, indicating that that H, N and K-Ras do not differ in their ability to bind effectors or in their GTPase cycles. The three isoforms are indistinguishable in *in vitro* assays of GTPase

activity and effector binding (Gulbins et al, 1994). The C-terminal 25 amino acids however, display only 10-15% sequence similarity between the three isoforms and is hence referred to as the Hypervariable Region (HVR). However, biological studies show that KRas activates Raf more effectively, while H and NRas show more potent activation of PI3-kinase, representing an alternative downstream signaling branch. Further, gene knockout studies in mice show that KRas is essential for mouse development, but H an NRas seem to be dispensable at this stage (Johnson et al, 1997). Since the phenotypic effects of oncogenicity of these genes are distinguishable and tissue-specific and developmental changes in the expression of the three isoforms has been reported (Quinlan & Settleman, 2009), the HVR is clearly responsible for differences in the signaling mediated by the three Ras isoforms.

The HVR terminates in a CaaX box – each of the three Ras isoforms is prenylated. More specifically, Ras isoforms are Farnesylated and methyl-modified at the C-terminus. This confers weak membrane affinity to the Ras proteins. In addition, HRas contains 2 Cys residues (position 181 and 184) which are S-palmitoylated. N-Ras contains only a single S-palmitoylated Cys residue (position 181). HRas also contains proline residues in the HVR , which have been reported to affect the reversibility of the S-palmitoylation on HRas (Ahearn et al, 2011). KRas is not S-palmitoylated, but instead contains a sequential polybasic stretch of 6-lysine resides, conferring a strong positive charge onto the KRas C-terminus.

The features on the HVR are shown to be responsible for the differential localization of H,N and KRas. HRas and NRas localized to the PM and Golgi apparatus, a result of mediated by palmitoylation on the Golgi apparatus which increases its membrane affinity (Rocks et al, 2006). HRas however, is doubly palmitoylated, which is correlated with its more prominent PM localization. Artificially, increasing the number of palmitoylatable Cys residues is known to confer a a bias towards PM localization for H and NRas, shifting their partitioning away from the Golgi apparatus (Rocks et al, 2005). KRas, on the other hand, is not detected on the Golgi (as is expected from its lack of palmitoylatable Cys residues). KRas localization is almost exclusively towards the plasma membrane, mediated by the interaction of the polybasic stretch towards the negatively charged phospholipids and the electrical polarity in the PM (Yeung et al, 2008; Crouthamel et al, 2008; Quatela et al, 2008). Additionally, KRas

contains a Ser residue adjacent to the polybasic stretch, which is a phosphorylation substrate for Protein Kinase C (Bivona et al, 2006). Phosphorylation of the adjacent Ser can neutralize the positive charge of the polybasic stretch, and shifts KRas localization away from the PM onto internal cellular membranes, due to the weak affinity of the prenyl group. Such an effect is also seen for H- and NRas, where treatment with 2-bromopalmitate (2-BP), an inhibitor of palmitoylation causes a change in localization of H and NRas to all internal cellular membranes (Jennings et al, 2009; Dekker et al, 2010). The prenylated forms of the three Ras isoforms are indistinguishable in their cellular localization. The palmitoylation and polybasic stretch are the key features that generate differences in localization between H,N and KRas.
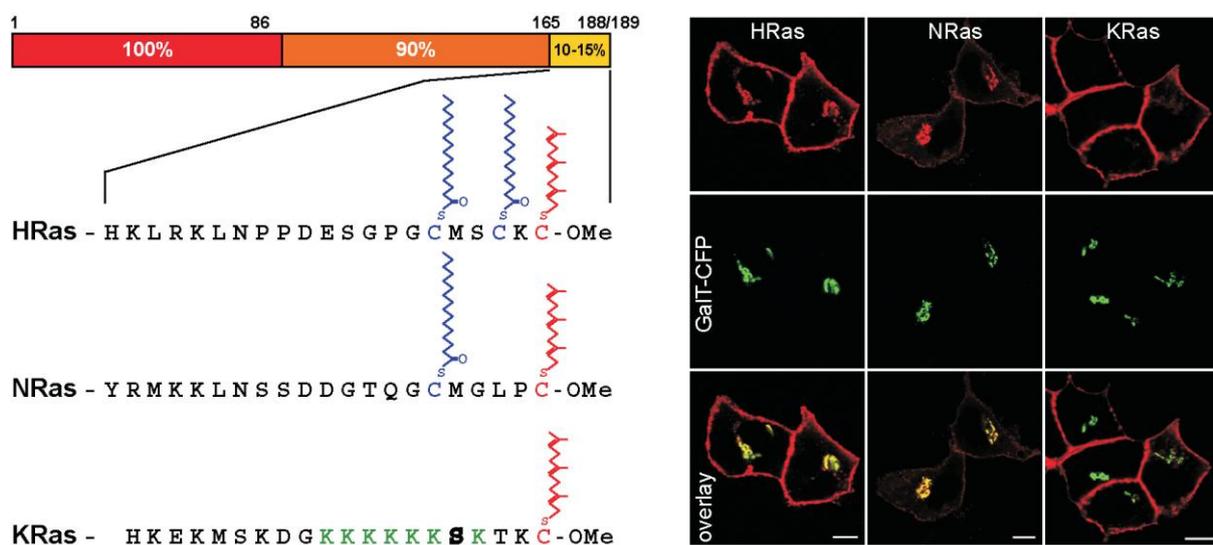
Localization and Lipid Modifications of Ras Isoforms: All Ras isoforms are farnesylated (red). H- and N-Ras are palmitoylated (blue) at cysteines, while K-Ras contains a polybasic stretch of lysines (green). These distinct features modifications result in the differential partitioning of Ras isoforms. H-Ras and N-Ras stain the Golgi apparatus and plasma membrane, albeit to different degrees. K-Ras stains the plasma membrane almost exclusively. Gal-T-CFP is a Golgi marker. Reproduced from Rocks et al. 2005

The dynamic nature of H and NRas palmitoylation is known from FRAP studies conducted by Rocks et al. However, exactly how this reversible S-palmitoylation leads to the observed PM/Golgi localization, and what effects it has on Ras dependent signaling is unclear. Considering what is known about the similarities and differences between the Ras isoforms,

this reversible palmitoylation is clearly a critical factor in the biological functions of these proteins. This work provides a mechanistic explanation for how localization is generated from spatially separated palmitoylation and depalmitoylation activities for H/N-Ras, resulting in an acylation cycle that eventually modifies their signaling activities.

2   SCOPE

It is clear that the cell is not simply a 'bag of enzymes'. Proteins within the cell have precise activity profiles that vary over time and space. It is of interest to determine how such precise activity profiles emerge from the kinetics of basic biochemical reaction processes when coupled with molecular mobility. Spatial modulation of protein activity is a critical for a variety of phenomenon – some obvious, such as the establishment of cell polarity or orientation of the mitotic spindle. In other cases, spatial modulation takes place over subcellular compartments. The acylation cycle for peripheral membrane proteins, such as Ras, can be thought of as a reaction-diffusion cycle that generates asymmetry along the radial axis of the cell, with enrichment at the Golgi and the PM, and fast, constant, low-intensity flux of the protein on the endoplasmic reticulum or cytosol. The ensuing study results seek to answer the following questions regarding the acylation cycle of peripheral membrane proteins:

1) The repertoire of proteins subjected to the acylation cycle is substantial. Is the acylation cycle then a case of independent convergent molecular evolution of these proteins, or is it a general mechanism that recruits various proteins into its scope? Equivalently, is there specific machinery for the acylation of each protein, or is it aspecific machinery that can act any protein that satisfies the minimal criteria for acylation?

2) How does the acylation cycle generate the spatial asymmetry that is so prominent? What are the minimal criteria that a protein must satisfy in order to enter the acylation cycle? What are the mechanics of the process, and more importantly, what is the basic 'infrastructure' – proteins, subcellular structures etc. required to operate the acylation cycle?

3) Howsoever the acylation cycle functions, what exactly is the influence of such a cycle on proteins that are subjected to it? Teleological reasoning suggests that it is unlikely for such a widely conserved mechanism to exist without function. Is the purpose of

the acylation cycle merely protein targeting, or does it entwine with other aspects of the proteins' activity to generate more complex phenomenon?

4) Finally, is it possible to perturb or modulate such a reaction-diffusion cycle for therapeutic benefits?

The Ras proteins exist in three isoforms, each differentially susceptible to the effects of the acylation cycle. They are peripheral membrane proteins with a single, well-defined biochemical activity that stems from their GTPase domain. They form integral nodes in the well-studied MAPK cascades; the functioning of which can be assayed with well-established biochemical, molecular and phenotypic readouts. As oncogenes, the biology of Ras proteins has definite clinical implications. As such, Ras proteins and their signaling represent a convenient model with which the answers to the above questions might be attempted. The results however, may be readily extended to other proteins, taking into account the respective proteins' idiosyncrasies.

3 EXPERIMENTAL PROCEDURES

3.1 Materials

3.1.1 Consumables and Kits

PRODUCT	MANUFACTURER
QIAPrep Spin Plasmid Miniprep Kit	Qiagen
HiSpeed Maxi Plasmid Kit	Qiagen
RNAeasy Spin Kit with gDNA Elminator	Qiagen
OneStep RT-qP CR SYBR Green Kit	Qiagen
Glass Bottom Cell Culture dishes (35mm)	MatTek Corp (Ashland, USA)
Polylysine/Collagen coated Glass Bottom dishes	MatTek Corp (Ashland, USA)
Femtotip- II Gold Microcapillary Needles	Eppendorf
Glass Slides (76x26 mm)	Menzel (Braunschweig)
Coverslips (18x18 mm)	Menzel (Braunschweig)
6-well and 24-well Cell Culture Plates	Nalgene
Cryogenic Vials	Nalgene
Odyssey Blocking Buffer	LI-COR Biosciences Inc.
White-Background RT-qPCR 96-well plates	BioRad
Quickchange-XL Site-Directed-Mutagenesis Kit	Stratagene

3.1.2 Reagents

PRODUCT	MANUFACTURER
Effectene Transfection Reagent	Qiagen
Lipofectamine LTX Transfection Reagent	Invitrogen
RNAiFect Transfection Reagent	Qiagen
2-Bromopalmitate	Sigma-Aldrich

Cycloheximide	**Sigma-Aldrich**
Human Epidermal Growth Factor	**Cell Signaling Inc.**
Bradykinin	**Cell Signaling Inc.**
FITC-labelled Dextran	**Sigma-Aldrich**
Dynasore	**Sigma-Aldrich**
Phorbol Myristate Acetate	**Sigma-Aldrich**
Triton X-100	**Sigma-Aldrich**
Pluronic	**Sigma-Aldrich**

3.1.3 Antibodies and related products

PRODUCT	MANUFACTURER
Anti-Erk1 Monoclonal Mouse IgG	**Cell Signaling Inc.**
Anti-PhosphoErk1 Monoclonal Rabbit IgG	**Cell Signaling Inc.**
Anti-Erk2 Monoclonal Mouse IgG	**Cell Signaling Inc.**
Anti-PhosphoErk2 Monoclonal Rabbit IgG	**Cell Signaling Inc.**
Alexa-488 labelled Anti-E-Cadherin Mouse IgG	**Cell Signaling Inc.**
Anti-E-cadherin Mouse IgG	**Cell Signaling Inc.**
IR-Dye 700 labelled Goat Anti-Mouse IgG Secondary	**LI-COR Biosciences Inc.**
IR-Dye 800 labelled Goat Anti-Mouse IgG Secondary	**LI-COR Biosciences Inc.**
IR-Dye 700 labelled Goat-Rabbit IgG Secondary	**LI-COR Biosciences Inc.**
IR-Dye 800 labelled Goat-Rabbit IgG Secondary	**LI-COR Biosciences Inc.**
IR-Dye 700 labelled Streptavidin	**LI-COR Biosciences Inc.**
Anti-N-Ras Mouse IgG	**Sigma-Aldrich**

3.1.4 Commonly Used Buffers and Solutions

NOMENCLATURE	CONSTITUENTS
PBS (Phosphate Buffered Saline)	**137 mM NaCl,2.7 mM KCl,10.2 mM Na_2HPO_4, 1.8 mM**

	K_2HPO_4
RIPA Cell Lysis Buffer	50mM Tris-cl pH 7.4, 150mM NaCl, 1% NP40, 0.25% Na-deoxycholate, 1mM PMSF, 1x Roche complete mini protease inhibitor cocktail, 1x Pierce phosphatase inhibitor cocktail
Methanol Fixation Buffer	100% Methanol at -20°C
50x Tris-HEPES Buffer	100mM Tris, 100mM HEPES, 3mM SDS
50x TAE Buffer	2M Tris/acetate, pH 8.5, 50 mM EDTA
6x Gel Sample Buffer	30% (v/v) Glycerol, 0.25% (w/v) Bromophenol blue, 0.25% (w/v) Xylenecyanol in TAE Buffer

3.1.5 Cell Culture Media, Supplements and Solutions

PRODUCT	MANUFACTURER
Dulbecco's Modified Eagle Medium (DMEM)	Invitrogen
Trypsin/EDTA for cell culture	Sigma-Aldrich
Fetal Bovine Serum	PAN Biotech GmBH
100X Penicillin-Streptomycin-Glutamine solution	Invitrogen
OptiMEM I w/ Glutamax	Invitrogen
OptiMEM I Reduced Serum Media w/ HEPES	Invitrogen
Dimethyl Sulfoxide (DMSO)	Sigma-Aldrich
HL-5 medium	Invitrogen

3.1.6 Eukaryotic Cell Lines

MDCK (ATCC: CCL-34)

The MDCK cell line was derived from a kidney of an apparently normal adult female cocker spaniel, September, 1958, by S.H. Madin and N.B. Darby. The cells are positive for keratin by

immunoperoxidase staining and display an epithelial phenotype. MDCK cells are strongly adherent, contact inhibited and non-tumorigenic.

MDCK-F3

The MDCK-F3 cell line is a subclone of an MDCK cell line subjected to adenoviral neoplastic transformation with an oncogenic HRas-G12V gene (Karaguni et al, 2002). MDCK-F3 cells are cytokeratin positive and display a mesenchymal-like phenotype. MDCK-F3 cells have constitutively active canonical MAPK pathways, lack contact inhibition and are tumorigenic. The MDCK-F3 cell line was kindly provided by Dr. O. Müller (MPI for Molecular Physiology, Dortmund).

HeLa (ATCC: CCL-2)

HeLa cells are human cervical cancer cells isolated from a patient Henrietta Lacks pre-mortem in 1951. HeLa cells are epithelial-like, are contact inhibited but are tumorigenic. Hela cells contain the Human Papilloma Virus.

Dictyostelium discoideum (Dictybase: AX2)

Dictyostelium discoideum is a species of soil-living amoeba belonging to the phylum Mycetozoa. D. discoideum, commonly referred to as slime mold, is a eukaryote that transitions from a collection of unicellular amoebae into a multicellular slug and then into a fruiting body within its life time. The strain used in this work is a neomycin-susceptible axenic strain, maintained in the amoeboid stage.

3.1.7 Plasmids

Mammalian Plasmids

Mammalian expression plasmids used in this work are derived from the pEGFP vector. pEGFP encodes a F64L,S65T monomeric variant of wild type from *Aequorea victoria* Green Fluorescent protein, with its sequence optimized for expression in mammalian cells. The

backbone contains a human cytomegalovirus (CMV) promoter and Simian Virus 40 (SV40) polyadenylation signal downstream of the coding sequence. Bacterial selection is mediated by a kanamycin resistance gene in *E.coli.* The EGFP sequence could be interchanged with that of several other fluorescent proteins to generate multiple colors of fluorescent fusion proteins. ECFP and mCerulean are cyan fluorescent proteins, the latter being a brightness optimized variant of ECFP. Similarly, EYFP and mCitrine are yellow fluorescent proteins, the latter being a pH-stable version of EYFP. mRFP, and mCherry are red fluorescent proteins, the latter being an optimized version of mRFP for faster maturation and photostability. EpaGFP and EpaCherry are kind gifts from J. Lippincott-Schwartz and encode photo-activatable versions of EGFP and mCherry respectively. These proteins undergo glutamate decarboxylation at the fluorophore upon exposure to UV light of 340-440 nm, resulting in the formation of an alternative fluorophore that is ~40 fold brighter. Most plasmids were obtained from the central plasmid bank at the Dept. of Systemic Cell Biology.

H-Ras, N-Ras and K-Ras plasmids were kind gifts from Dr. Oliver Rocks and all mutations in these plasmids of upto 12 amino acids were derived through site-directed mutagenesis. Fyn sequences were a kind gift from Dr. Margaret Frame (Edinburgh Cancer Research Centre). PCR fragments of Fyn were inserted into the pEGFP vector backbone using the EcoRI/BamH1 restriction sites. Myr, Gα(1-11), tH constructs were created through direct chemical synthesis of nucleotides, followed by ligation into mammalian expression vectors. Constructs were validated using forward and reverse sequencing.

Dictyostelium plasmids

Plasmids for expression in Dictyostelium were derived from the pDM vector, which was a kind gift from Dr. Arjan Kortholt (Max Planck Inst. Dortmund). pDM vectors pDM317 and pDM134 represent N-terminal labeling vectors containing EGFP (green) and mRFPmars (red) fluorescent proteins respectively. The vectors contain the DIctyostelium act15 promoter upstream of the expressed sequence, and a cabA terminator sequence downstream of the expressed sequence. Additionally, ampicillin resistance is encoded for selection in *E.Coli*,

while neomycin resistance is encoded for selection of stable transfectants in Dictyostelium. PCR fragments of human HRas and its mutant HRasC181S,C184S where cloned into the pDM vectors using the XhoI/EcoRI restriction sites, to generate GFP and mRFP fusion variants. Constructs were validated using forward and reverse sequencing.

3.1.8 Oligonucleotides

Fluorescent fusions of short truncated sequences of upto 15 amino acids (for C-termini or HRas and KRas, N-termini of G-alpha proteins and Fyn) were generated using chemical synthesis of the relevant truncated 5'-phosphorylated DNA oligonucleotide with flanking partial restriction sites and direct ligation with restriction enzyme treated vector. The oligonucleotides were purchased from MWG-Biotech and sequences are provided below :

Name	Sequence
MyrSer	5'atgggatccacactgagcgctggctccgctgnttntgcgggtagcgcgcgggatccgcc ggttcagcagggagtgctggctcggcaggatctgcgcgc 3'
Fyn(1-11)	5'atgggctgcgtgcagtgcaaagataaagaagcg 3'

3.2 Molecular Biology Techniques

In general, wherever kits were utilized, the protocol recommended by the manufacture was followed.

3.2.1 Plasmid Preparation

Cultures of transformed bacteria were centrifuged to form a bacterial cell pellet. The pellet was then homogenized and lysed with SDS-buffer provided in the HiSpeed Plasmid Maxi prep kit (Qiagen). The SDS was then precipitated with a pH shift and centrifuged out, while the supernatant of applied to a DNA-binding mini-column. The column pore-size excludes

genomic DNA. After a series of washes with binding buffer (supplied), the DNA was eluted in
in Nuclease-free water.

3.2.2 DNA Restriction and Ligation

Restriction enzymes (New England Biolabs) are typically supplied with optimized buffers. Plasmid DNA and restriction enzymes were mixed in a ratio of 1 unit/mg of plasmid DNA in the appropriate buffer and incubated at the optimal temperature (37 or 55°C) for the restriction enzyme for 1h. When more than one restriction was required, the enzymes added simultaneously to the reaction provided optimal buffers and temperatures were identical. Plasmids in the open conformation or restriction fragments were isolated with subsequent agarose gel electrophoresis and purification on a DNA-binding column.

Prior to ligation vectors were treated with Shrimp Alkaline Phosphatase to remove 5' phosphate groups and thus avoid self-ligation. For sub-cloning procedures, restriction fragments or oligonucleotides were incubated with the vector backbone in molar ratios of 3:1, 5:1 and 10:1 with DNA ligase for 1h. The entire reaction mixture was then used for transformation in bacteria.

3.2.3 Bacterial transformation and selection

200 μL of dense chemically competent E.coli cultures were treated 1mM DTT and incubated with plasmid DNA or ligation products on ice for 10 min. The culture was then allowed to recover in Super Optimal Broth (SOB) for 1h at 37°C. Finally, the culture was plated on LB-agar plates containing 20 μg/mL Kanamycin or 50 μg/ml Ampicillin, depending on the selection marker on the plasmid DNA, and incubated overnight at 37°C. Individual segregated colonies were picked and added to flasks containing LB-medium with the selection marker as on the agar plates. Steady state cultures obtained after overnight growth at 37°C were then used for plasmid preparation.

3.2.4 Sequencing

Sequencing was outsourced to GATC Biotech GmBH. Sequences were obtained using Forward and Reverse primers on three independent runs of standard Sanger methods.

3.2.5 RNA Preparation

Confluent cells were placed on ice and lysed with scraping and lysis buffer immersion. The lysate was passed through gDNA eliminator columns for removal of genomic DNA. Flow-through was then loaded on to RNA-binding columns from the RNAeasy Extraction kit. The column was then washed with buffers containing DNAse, and RNA was finally eluted with nuclease-free water at room temperature. Samples were immediately measured spectroscopically to determine RNA concentration by absorbance at 260 nm and placed on ice.

3.2.6 PCR , RT-qPCR and relevant Data Analysis

PCR was performed using standard protocols, and Pfu polymerase (New England Biolabs). Primers were designed using Primer3, with T_m (melting temperature) typically between 55-62 deg C. PCR products were purified with agarose gel electrophoresis and used for further procedures. A sample protocol for PCR is identical to the one shown below for RT-PCR, eliminating the reverse transcription and optical measurement steps. PCR was typically performed on 100 ng of purified templates and thus the number of cycles was retricted to 25. For site-directed mutagenesis, mismatched primers including the required mutation were used, ensuring that the ration of mismatches to matches between primer and template did not exceed 1:8. The protocol was modified to expand the extension time to 5 minutes to allow replication of the entire plasmid.

Quantitative RT-PCR was performed on total RNA extracts from mammalian cells using the Quantifast One-step RT-PCR kit (Qiagen) in 96-well format on a Bio-Rad iQ5 thermocycler equipped with an imaging unit consisting of a CCD-camera, xenon excitation lamp and

necessary filters. Primers for RT-qPCR were designed with a melting temperature (T_m) between 55-72 °C , and spanned at least one intron-exon boundary to avoid amplification of trace genomic DNA. Quantification of double stranded DNA was based on binding of the fluorophore SYBR Green – I , which is fluorescent only upon binding to double stranded DNA. Reverse transcriptase and a Master mix containing dNTPs are provided in the kit. A typical reaction mixture is as follows :

Description (cycles)	Volume per Reaction(μl)	Final Concentration
RNAse free water	Variable	-
5X PCR Buffer	5.0	1X
dNTP Mix	1.0	400 μM per dNTP
Forward Primer	Variable	1.0 μM
Reverse Primer	Variable	1.0 μM
Enzyme Mix	1.0	-
Template RNA	Variable	100 ng/reaction
Total	25.0	-

In all cases, control samples were prepared as follows :

1. Template RNA negative : To detect possible primer-dimers.
2. Primer negative : To detect possible self-amplification of total RNA
3. Reverse transcriptase negative : To detect possible amplification of trace genomic DNA.

A typical RT-qPCR thermocycler protocol is as follows:

Description (cycles)	Temperature (°C)	Time
Reverse Transcription (1X)	50	30 min
Hotstart PCR Activation (1X)	95	15 min
3 Step Cycling (45X)		
Denaturation	94	1 min
Annealing	50-68 (Primer T_m-5)	0.5 min

Optical Measurement	Same as annealing	0.5 min
Extension	72	1 min
Final Extension	72	10 min

Since RT-qPCR was used only for validation of RNA interference, only relative changes in mRNA expression were measured in this work using Pfaffl's modified Δ(ΔCt) method (Pfaffl, 2001).

$$\Delta(\Delta Ct) = \left(Ct_{Control}^{MOCK} - Ct_{Control}^{RNAi} \right) - \left(Ct_{YFG}^{MOCK} - Ct_{YFG}^{RNAi} \right)$$

Fold Change $= \left(E_{[gene]} \right)^{\Delta(\Delta Ct)}$

% Knockdown $= \left(1 - \dfrac{1}{E^{\Delta(\Delta Ct)}} \right) \times 100$

Where:

- Control represents primers for amplification of a housekeeping gene that is not affected by RNAi

- YFG represents the gene of interest against which RNAi is directed.

- Ct_{gene}^{sample} represents the threshold half-cycling time for gene amplification in sample.

- $E_{[gene]}$ = Primer amplification efficiency for a particular gene primer. We assume $E_{GAPDH} = E_{APT1} = 2.00$.

3.3 Cell Culture Techniques

3.3.1 Mammalian Cell Culture and transfection

MDCK and MDCK-F3 were routinely maintained in MEM containing antibiotics and glutamine, supplemented with 10 % and 5% fetal bovine serum respectively. Cells were

typically cultured upto 90% confluency in T75 flasks before trypsinization and splitting 1:4 into a new flask. Prolonged incubation at confluency is to be avoided since MDCK cells tend to differentiate under these conditions. Frozen stocks were prepared with confluent trypsinized cells in MEM with 5% DMSO. Cells were routinely checked for infection with mycoplasma by MycoAlert (Cambrex, USA) following the recommendations of the manufacturer. If cell lines were found to be contaminated, they were discarded and new cells were thawed from frozen stocks.

For live cell microscopy, cells were cultured on 35-mm glass bottom dishes (MatTek) and transferred OptiMEM I (Invitrogen) without phenol red supplemented with 25 mM HEPES pH 7.4, or with OptiMEM 1 without HEPES in a CO_2 controlled chamber. In the case of experiments monitoring Ras activation, MDCK cells were starved in MEM without fetal calf serum for 6-7 hours before experimentation. For bright field imaging, cells were cultured in 24-well plates.

Transfection was performed with plasmid DNA and Effectene transfection reagent with the following protocol:

1) MDCK and MDCK-F3 cells must be seeded at 1:5 dilution at least 5.5 hours before transfection. HeLa cells maybe transfected immediately after seeding.
2) Add 0.25 ug DNA per plasmid construct in Buffer EC to final volume of 100 ul.
3) Add [8 x Net amount of DNA used (ug)] ul of Enhancer reagent.
4) Vortex for 1 second.
5) Incubate for 2-5 minutes at RT.
6) Add Effectene Transfection Reagent, 5 ul per 35 mm Mattek dish (amount of DNA is irrelevant)
7) Incubate the transfection mix for 5-10 min at RT. While incubation proceeds, replace
8) medium in 35 mm dishes with 1.5-2.0 ml OptiMEM w/Glutamax.
9) Vortex for 10 seconds after incubation and add OptiMEM to transfection mix.
10) Pipet up and down twice.
11) Add transfection mix to cells gently
12) Incubate dishes at 37 deg C. Cells express protein 7-8 hours post transfection.

3.3.2 RNA Interference

For the experiment, ~6×10^3 cells were seeded and cultured as described above. 5.5 hours after seeding, cells were transferred to OptiMEM I + GlutaMax I (Invitrogen) and cells were transfected with upto 2 μg siRNA or Non-targeting control siRNA , using RNAifect reagent (Qiagen). For determination of siRNA transfection efficiency, cells were transfected with non-targetting Cy5 labeled-siRNA and the efficiency was quatified optically. After incubating cells for at least 6 hours in the transfection mix, the transfection mix was aspirated and replaced with fresh OptiMEM I + Glutamax I (Invitrogen). Cells were then transfected with DNA expression constructs (if required) using Effectene transfection reagent (Qiagen). Total RNA was then extracted from cells and used for RNAi quantification by RT-qPCR or Westernblot as described elsewhere.

3.3.3 Dictyostelium Cell Culture

Dictyostelium discoideum AX2 cells were cultured in HL5 medium under sterile conditions in 60 cm petri-plates at 22° C. Cultures were passaged every 3 days into fresh medium. The culture was not allowed to reach starvation conditions in order to prevent differentiation.

3.3.4 Stable Transfection of Dictyostelium

Transformation of *D.discoideum* amoebae was accomplished by electroporation using supercoiled plasmids. All transformants were selected in HL5 medium containing Neomycin G418 (50 μg/ml) for 2 seeding cycles and then maintained in HL5 medium containing G418 (20 μg/ml).

3.4 Immnunohistochemistry and Western Blotting

For anti-E-cadherin immunostaining, cells were fixed in methanol at -20° C. After blocking for 1h with 1% BSA solution in PBS, cells were stained with FITC conjugated Mouse Anti-E-cadherin antibody (BD Tranduction Technologies Cat no : 612130) and imaged under confocal or widefield fluorescence microscopes. For brightfield contrast staining, cells were fixed with formalin (3.7%), and subsequently stained with Celestine blue (Sigma) and visualized by means of an automated microscope.

MDCK-F3 cells were plated at a density of 1.5×10^5 cells/dish in 3.5 cm dishes and incubated for 36 h. The cells were then treated with Palmostatin B (novel inhibitor), U0126 (Calbiochem) or DMSO at the indicated concentrations for the indicated time periods. After treatment, cells were washed once with ice-cold phosphate buffered saline (PBS). 100 μl of RIPA-buffer (50 mM Tris-HCl (pH 7,4), 1 % NP-40, 0.25 % Na-deoxychelate, 150 mM NaCl, 1 mM EDTA, 1 mM PMSF, 1 μg/ml aprotinin, 1 μg/ml leupeptin, 1 μg/ml pepstatin, 1 mM Na_3VO_4, 1 mM NaF) containing protease inhibitors (complete protease inhibitor tablets, Roche) was then added to each dish. After 10 min of incubation on ice the cells were scraped and the lysates were centrifuged at 10000 g for 10 min at 4°C. The supernatants were kept at 4 °C. Total cellular lysates (50 μg) of each sample were mixed with sample buffer and resolved onto SDS-polyacrylamide (10 %) gels by electrophoresis. The gel was blotted with a semi-dry electroblot onto a polyvinylidene diflouride (PVDF) membrane. The membrane was then blocked with Blocking Buffer (Licor) for 1 h at room temperature and then incubated with the ERK1/2 or p-ERK1/2 antibody (Cell Signaling) diluted (1:1000) in Blocking Buffer (Licor) overnight at 4 °C. To detect the primary antibody the IRDye 700 or IRDye 800 (Licor) goat anti- rabbit IgG antibody was used at $1:2 \times 10^5$ dilution in Blocking Buffer (Licor). Antibody binding was detected using the Licor Odyssey Infra-Red imaging scanner.

Acyl exchange assay for detection of palmitoylated protein (Drisdel & Green, 2004)

MDCK cells were plated at a density of 5×10^5 cells/dish in 3.5 cm dishes and incubated for 6h. The cells were transferred to 2ml OptiMEM I + GlutaMax I (Invitrogen) and transfected with YFP-NRas DNA (0.5 µg/ml) using the Effectene transfection reagent (Qiagen) and incubated for 24 h. The cells were then treated with Palmostatin B (30 µM), 2-bromopalmitate (50 µM) or an equivalent amount of DMSO respectively for 1h in D-MEM (Invitrogen). After treatment cells were washed once with ice-cold phosphate buffered saline (PBS). 300 µl of lysis buffer (5 mM EDTA, 1 % Triton X-100, 50 mM N-ethylmaleimide, 1 mM PMSF, 1 µg/ml Aprotinin, 1 µg/ml Leupeptin, 1 µg/ml Pepstatin, 1 mM Na3VO4, 1 mM NaF in PBS pH 7,4) was then added to each dish. After 3 min of incubation on ice the cells were scraped and the lysates were homogenized by passing the lysate through a 20-gauge needle, attached to a sterile plastic syringe. The homogenized lysates were rotated for 1 h at 4 °C and then centrifuged at 10000 g for 10 min at 4°C. Supernatants were stored ovenight at 4 °C. To remove proteins that bind non-specifically to sepharose the lysates were incubated with Sepharose G (Sigma). All samples were centrifuged and the supernatants were rotated with Living Colors® Full-Length A.v. Anti-GFP polyclonal antibody (Clontech) for 30 min at 4 °C. The protein-antibody complex was precipitated with Sepharose G by rotation for 1 h at 4 °C. The purified protein was then additionally treated with 50 mM N-ethylmaleimide for 1 h at room temperature to ensure quenching of reactive cysteines. After treatment and centrifugation, the pellets were washed twice with PBS and each sample was divided into two fractions. One fraction was subsequently treated with 1 M hydroxylamine (pH = 7.4) by rotation for 1 h at room temperature, to release palmitate groups. The other fraction was treated with PBS and served as control sample. Samples were then treated with 1-biotinamido-4-[4´-(maleimidomethyl)cyclohexanecarboxamido]butane BMCC™ (Pierce 320 µM) and rotated for 1 h at room temperature to complete the exchange chemistry. After washing the samples twice with PBS the samples were resolved by SDS-PAGE and Western Blotting was performed with the Mouse Monoclonal anti-GFP N-terminal antibody (Sigma) or Mouse Monoclonal anti-pan-Ras (Ab-2) (Calbiochem) to detect total YFP-NRas. The primary antibody staining was visualized by using IRDye 680 Goat anti-mouse IgG Antibody (LI-COR),

while biotinylated protein (representing palmitoylated protein) was visualized with IRDye 800CW Streptavidin (LI-COR) on the Odyssey® Infrared Imaging System (LI-COR).

3.5 Microscopy and Imaging Techniques

3.5.1 Equipment

Confocal Microscopy

Confocal microscopy was performed on a Leica SP5 microscope equipped with a set of objectives with magnifications ranging from 10x-60x as air, water and oil based objectives. The automated DMI6000 microscope stage is automated and enclosed in a CO_2/Humidity/Temperature controlled incubator. The scanner unit of the microscope is coupled to an Argon laser, UV Diode laser and Helium Neon lasers. In addition, the microscope in equipped with an experimental super-continuum laser with output wavelengths ranging from 476-800 nm. The excitation wavelength is selected by acousto-optical tunable filters (AOTF), scanned over the sample at frequencies ranging from 100-1400 Hz in standard mode, and 8000 Hz in resonant mode. Emission signals from the sample are also selected for using AOTFs or through rapid switching of the excitation frequency (Sequential mode) to enable multiplex imaging of fluorophores. The emission signal is passed through a pinhole to control confocality. Detection of the signal is on PMTs, whose sensitivity can be adjusted by manipulating the applied gain voltage.

Fluorescence Lifetime Imaging Microscopy

The Fluorescence Lifetime Imaging Microscope is an in-house built custom unit, a basic outline of the construction is provided here. (Grecco et al, 2010).

The desired excitation wavelength and power is selected with an acousto-optic tunable filter (AOTF, AA, AOTFnC-VIS-TN). The AOTF as a fast shutter by connecting its blanking input to the exposure out TTL of the camera. Intensity modulation is achieved by creating an oscillating diffraction grating with a standing wave accousto optic modulator (AOM,

IntraAction, SWM-804AE1-1) powered with a sinusoidal wave of frequency $f/2$, which deflects the light from the zero order at a frequency f. The modulated beam is selected by placing an iris diaphragm (Thorlabs, ID25/M) in the optical path.

The laser is coupled into a vibrationally isolated inverted microscope (Olympus, IX81) using a multimode fiber (Schaeffter Kirchhoff GmbH, #46688-03). The spatial coherence of the laser is disrupted by vibrating the fiber using a rotating eccentric wheel attached to the fiber. This results in a randomly moving speckle pattern, which averages out during detection. Homogeneous (Koehler) illumination at the sample plane is achieved by imaging the fiber core in the backfocal plane of the objective. A 12-bit CCD camera using a 0.5X magnification is used to record images.

To perform phase-sensitive homodyne detection it is important that: (1) the frequencies of the modulation and detection are precisely matched and (2) the phase between the two signals can be shifted.

Total Internal Fluorescence Microscopy: Total Internal Fluorescence Microscopy is performed on a Olympus IX81 microscope equipped with 60x NA=1.8 TIRFM APOCHROMAT oil objective. The microscope is coupled into Argon lasers passing through condensers that allow manipulation of the incident angle of the light onto the specimen.

Microinjection: Microinjection was performed directly at the Leica SP5 DMI6000 microscope using an automated micromanipulator (Eppendorf 5171), coupled to the Eppendorf Femtojet pressure generator.

3.5.2 Confocal Microscopy

For live cell experiments, confocal laser scanning microscopy was performed on a Leica TCS SP5 DMI6000 microscope equipped with a HCX PL APO 63x 1.4-.6 NA Blau CS objective and an environment control chamber which maintained temperature at 37°C, and 5% CO_2. For anti-E-cadherin immunostaining experiments, a N PLAN L 20x/0.40 Air objective was used. For contrast-staining experiments, cells were imaged on a Zeiss Axiovert 200M equipped

with a 'Plan Apo. 20x/0.5 Air objective. Fluorescent fusion-proteins with Cyan Fluorescent Protein (CFP), Citrine and conjugates with the dye fluorescein were excited using the 458nm, 514m and 488nm Ar- laser lines respectively, while fusion-proteins with Cherry and conjugates with the dye Cy3 were excited using the 561nm HeNe laser line. Spectral filtering of emission bands was achieved using an acousto-optical tunable filter. Detection of fluorescence emission was restricted as follows - CFP: 468-504 nm, Citrine: 524-551 nm, Cherry: 571-650 nm, Fluorescein: 498-550nm, Cy3: 571-650 nm . In all cases, scanning was performed in line-by-line sequential mode with 2x line averaging. Confocality was controlled by limiting pinhole-size to between 1.0 and 1.5 Airy units.

3.5.3 Microinjection

Injection needles were prepared from borosilicate glass capillaries from Harvard Apparatus (Kent, UK), using a micropipette puller (Sutter Instruments P-97). Probes destined for microinjection were diluted in buffer (65 mM Tris, pH 7.5, 1 mM $MgCl_2$) to a final concentration of 2 mg/ml. Fresh aliquots were thawed for each experiment. After centrifugation at 13000 g and 4 ºC for 15 minutes the supernatant was immediately used for injection.

3.5.4 Fluorescence Recovery after Photobleaching (FRAP), Fluorescence Loss after Photoactivation (FLAP)

FRAP experiments were carried out at 37 ºC on a Leica SP5 confocal microscope with settings similar to those described in 'Confocal Microscopy', typically with a 63x oil immersion objective. Cells transfected with relevant constructs were allowed to equilibrate in the incubation chamber on the microscope and imaged with laser settings adjusted to minimize photobleaching. A custom routine was setup that followed through the three steps of FRAP/FLAP analysis: (1) Pre-bleach imaging, (2) Bleaching/Photoactivation and (3) Post-bleach imaging. Pre-bleach and post-bleach imaging was typically performed at similar

settings, with durations optimized by preliminary experiments for obtaining complete stability and recovery curves respectively. Bleaching/Photoactivation was performed in a pre-defined Region of Interest (ROI) for either specific organelles such as the Golgi apparatus, which were identified with expressed markers, or in a circular ROI of radius 1 μm in the cytosol or nucleoplasm. The laser scanner on the microscope was set to restrict illumination to the ROI, with high laser intensity for 1 second. This was found sufficient to provide >80% bleaching or 50-fold photoactivation in the ROI without diminishing or increasing total fluorescence intensity regions outside the ROI. For FRAP/FLAP experiments on the Golgi apparatus where durations of the post-bleach imaging extended into several minutes, cells were treated with 50 μg/ml cycloheximide at least 2h prior to the experiment.

For experiments relating to protein diffusion, the method proposed by Soumpasis (see FRAP Analysis techniques, page 48) was utilized. As such, imaging parameters were adjusted to conform to the assumptions implicit in such an analysis: namely, widefield imaging and activation of the smallest possible ROI to approximate the transverse section of a cylindrical volume where height >> width.

3.5.5 Total Internal Reflection Fluorescence (TIRF) Microscopy

MDCK cells were transfected with Protein Kinase Cα-C1 domain- eGFP fusion protein and mCherry and starved for at least 2 hours prior to experiments. After treatment with Palmostatin B or vehicle control DMSO, MDCK cells were observed in Total Internal Reflection Fluorescence (TIRF) microscopy on an Olympus CellR Microscope. Fluorescence excitation for GFP and Cherry was provided by the 488nm Ar- and 561 HeNe-laser excitation lines, respectively. For stimulation, 10 μM Bradykinin (Merck) was added to the cell media and translocation of the PKCα-C1-GFP to the basal membrane was observed in response to diacylglycerol production (Feng et al, 1998). GFP/Cherry ratiometric analysis was performed to quantify the fold increase of PKCα-C1-GFP on the basal membrane of cells in response to bradykinin. Multiple response curves showing PKCα-C1-GFP recruitment to the plasma

membrane over time were averaged for comparison of Palmostatin B- and vehicle control (DMSO) treated cells.

To determine if unpalmitoylated Ras proteins had access to the plasma membrane, MDCK cells were transfected with the non-palmitoylated mCitrine-HRasC181S,C18S mutant and imaged in TIRF. The distributions on the plasma membrane were compared to that of free floating mCherry imaged simultaneously. Since the penetration depth of the TIRF field is greater than the width of the plasma membrane, the cytoplasmic mCherry provided a control for the amount of cytoplasmic protein that contaminates the signal in the TIRF field, at the same time accounting for any intensity differences that may arise due to the invaginations and non-uniformity of the plasma membrane in the TIRF field.

3.5.6 Fluorescence Lifetime Imaging (FLIM) and relevant Data Analysis

Fluorescence Lifetime Imaging Microscopy was performed with MDCK cells expressing GFP-APT1, which were incubated with a various concentrations of Rhodamine-labeled inhibitor. Live cells in indicator-free HEPES buffered medium were imaged on an Olympus FV1000 microscope equipped with a 100x 1.6 NA PLAN APO Oil Objective, with a frequency-domain FLIM imaging setup as described in equipment. In order to prevent bleed through of the excitation laser and acceptor, an extremely narrow band 515/10 emission filter was used. In order to prevent precipitation of the inhibitor and facilitate its entry into cells, 0.001% Triton X 100 was added to the medium. MDCK cells expressing untagged GFP or incubated with free Rhodamine served as biological controls. Calibration of the instrument was performed with a mirror in focus that allowed the characterization of the machine response. Lifetimes were calculated with pixel-wise global fitting of the homodyne wave after images where passed through the standard image processing pipeline (described below).

3.5.7 Image Processing and Analysis Techniques

Standard Image Processing : During image acquisition, 8,12 or 16-bit TIFF images were obtained from microscopes Background subtraction was performed by detecting the low-level background intensity from a image histogram, and an subtracting peak value plus two standard deviations, assuming a Gaussian background distribution. The images were then median-filtered with a 1-pixel neighborhood and converted to 32-bit floating point TIFFs without interpolation. Thresholding was then performed to convert background zero-values to Not-a-Number (NaN).

Time lapse Sequences: Time lapse sequences of images stacked after standard processing and mean intensities or ratios of various image channels were calculated, after defining an ROI if necessary. For tracking intensities on specific compartments such as the Golgi apparatus or plasma membrane, expressed fluorescent markers in alternative channels were used to generate binary masks. Typically, mean intensities in a defined compartment where obtained through the time-lapse stack.

FRAP/Photoactivation: For FRAP and photoactivation, ROI coordinates were retrieved from metadata stored in the microscope data file. After standard image processing, mean intensities yielded FRAP recovery or Fluorescence loss curves, which were normalized to the relevant marker to account for changes structure and intensity in the ROI resulting from the dynamic nature of live cells. For measuring half-time of recovery or loss on organelles in the ROI, these curves were then fitted to the following exponential change equation that accounted for multiple processes contributing to the change in intensity.

$$I = I_0 + \sum_{i=0}^{i} Ce^{t_i \tau_i} + k_b t$$

Where I is the intensity, C is the exponential constant, t is time, τ is the exponential time-constant, and k_b is the bleaching constant.

In the case of protein diffusion measurements, diffusion constants were calculated according to the method of Soumpasis (Soumpasis, 1983). Accordingly, fluorescence decay or recovery curves where fitted to the following equation:

$$f(t) = Ae^{-2\varepsilon/t}\left[J_0\left(2\tau/t\right) + J_1\left(2\tau/t\right)\right] \quad \text{and} \quad D = \frac{(2r)^2}{\tau}$$

where $f(t)$ is the normalized intensity at time t, $J_0()$ is the modified Bessel function of the first kind of order 0 and $J_1()$ is the modified Bessel function of the first kind of first order to find only parameters A and τ, the diffusion time constant. r is the radius of the cyndrical bleaching or activation volume and D is the diffusion constant.

Disparity measurements in TIRF: In order to determine if unpalmitoylated proteins had access to the plasma membrane, the ratio of TIRF intensity maps of the solely farnesylated non-palmitoylatable mutants with those of cytoplasmic fluorophores where calculated. The contrast or disparity in the resulting ratio map provided an estimate of differences arising from unpalmitoylated mutants that could bind to the membrane and did not represent purely cytoplasmic contamination in the TIRF signal or differences in the structure of the plasma membrane. Note that in this case, the absolute mean value of the ratio is simply an indication of the amount of protein expressed ectopically in cells, and only internal variation within the ratio map is indicative of differences in membrane binding.

Ratiometric imaging for membrane partitioning measurements: For steady state measurements where differences in the two simultaneously imaged intensity channels was to be measured, the ratio of mean intensities over compartments isolated through binary masking was calculated. Thus, complete equivalence in partitioning represents a value of 1, while deviations from this value reflect a difference in compartmental partitioning. For time-lapse measurements where one channel represented an organelle marker, ratiometric imaging was performed as a simple division of the intensities in the two channels.

Colocalization analysis: Colocalization of two intensity images obtained from confocal microscopy was performed using Intensity scatter plots of the two channels and with Manders' coefficients (Manders et al, 1993). Manders' coefficients are independent of the relative intensity differences between the two channels, as they are normalized to the mean intensity in the respective channels. Manders' coefficients, range from are determined as :

$$M_1 = \frac{\sum R_{i,coloc}}{\sum R_i} \qquad\qquad M_2 = \frac{\sum G_{i,coloc}}{\sum G_i}$$

where R and G are the two intensity channels.

Morphology analysis: For morphology analysis, a custom algorithm was developed to be applied to brightfield images. Brightfield images were subjected to standard image processing, and local contrast equalization based on a neighborhood of 2 pixels was applied. Following which, a watershed operation was used to binarize and segregate individual cells based on contrast. Grayscale morphology operations were then used to determine area and circularity of the cells under various treatment conditions. The algorithm was automated to deal with large numbers of images of cells.

3.6 Bioinformatics

3.6.1 siRNA Design

The canine APT1 transcript sequence was retrieved from the Ensembl database with transcript ID ENSCAFG00000006978. Three Anti-APT1 21-mer siRNAs were designed from transcript sequence using the HiPerformance siRNA Design Algorithm (Qiagen). The sequences were tested for their efficacy in down-regulating APT1 and the candidate with the highest efficacy was identified as 5'-ACCAGTTATGCCTATAACATT-3' , henceforth referred to as the anti-canine APT1 siRNA.

3.6.2 Hidden Markov Modelling and Consensus Sequence Extraction

Sequences for human DHHC proteins were derived from the UniProt database (Version 23, http://www.uniprot.org) and aligned using the MUSCLE algorithm (Edgar, 2004). The alignment consisting of previously reported Ras palmitoyltransferases was then used as an input for statistical derivation of a Hidden Markov Model (Garber et al, 2009) matrix using HMMer (http://hmmer.janelia.org/). The HMM matrix so obtained was then calibrated through jack-knifing the sequence set, and a distribution of scores of all DHHC proteins was obtained. Reported RasPATs obtained high scores at least 2σ away from the mean score. The HMM was then used to output several 'fictional' sequences that conform to the constraints of the HMM matrix. Position-based frequencies of amino acids in these generated sequences were calculated to obtain the 'consensus sequence' that formed the defining feature of the HMM.

The consensus sequence so obtained was transliterated into a ProSite pattern and scanned against all available genomes (http://www.scanprosite.org). Results so obtained were used to determine ideal test cases for absence of putative Ras palmitoyltransferase activity.

3.6.3 Phylogenetic Analysis

Sequence alignments of human, yeast and fungal DHHC proteins based on the HMM generated previously was used to derive an unrooted distance-tree using nearest neighbor statistics (Smyth, 1997) in Jalview (http://www.jalview.org) or with the MATLAB Bioinformatics Toolbox. Yeast DHHC proteins were chosen due to the substantial amount of literature available on yeast homologs of human DHHC proteins. Fungal DHHC proteins by contrast served as a evolutionarily distant organism to humans, but closer to yeast, that contributed 'noise' to the dataset. The expectation to be realized was that a correct cladal analysis would group fungal DHHC proteins closer to yeast, than to humans.

4 RESULTS

4.1 Molecules with a single covalent lipid anchor have rapid mobility in the cytosol

Since proteins with covalently attached lipid or isoprenyl groups have substantially increased hydrophobicity, they are expected to have high membrane affinity and thus reduced diffusibility through the cytosol.

To investigate the localization and mobility of such proteins, we expressed mutant solely farnesylated HRasC181,184S and solely myristoylated MyrSer (32 aa peptide) (Navarro-Lerida et al, 2002) that cannot get palmitoylated, fused with photoactivatable GFP to follow their diffusion kinetics. Steady state distribution of such proteins showed a staining of all cellular membranes, merely reflecting membrane densities without any enrichment in a particular membrane compartment (Figure 1A). The same proteins were expressed as PA-GFP fusions, which could be photoactivated in a specific region with UV light under a confocal microscope. Upon photoactivation, both proteins rapidly redistributed over all membranes, reaching steady-state within the first seconds after photoactivation (Fig. 1B, C). The diffusion constants for both proteins were measured to be 1.1 ± 0.1 $\mu m2/s$.

This is a clear indication that proteins possessing single irreversible lipidations have a weak membrane affinity, none the less; they are rapidly mobile within the cellular environment. This observation is inconsistent with the presence of receptors for mono-lipidated proteins on specific membrane compartments (Choy et al., 1999), which would show some sort of enhanced fluorescence in the compartments where such receptors are present. Instead it seems that mono-lipidated proteins sample all cellular membranes. Further lipid modifications, such as palmitoylation, of course alter physicochemical properties of such molecules and could their mobility, as is discussed later in this work.

4.2 Unpalmitoylated Ras proteins have access to the Plasma Membrane

To confirm that the mono-lipidated proteins also had access to the PM, TIRF microscopy was performed on the wild-type and mono-lipidated mutant proteins. The TIRF fluorescence distributions, which are devoid of cytoplasmic fluorescence to a much greater degree than confocal and widefield imaging, were compared to that of free-cytosolic fluorescent protein mCherry which would reflect the topography of the cellular membrane, and thus its coupling into the TIRF field.

As expected, the fully lipidated wild type proteins clearly showed an enrichment at the PM (Fig. 1D), as measured by the disparity between the TIRF distribution of the lipidated and free cytosolic proteins. Both mono-lipidated mutants also exhibited clear PM localization establishing that they have access to this membrane. Proteins with only one attached lipid seem to rapidly sample all membranes and clearly additional processes are required to develop enrichment of the wild-type forms of these proteins on specific membrane compartments.

Figure 1
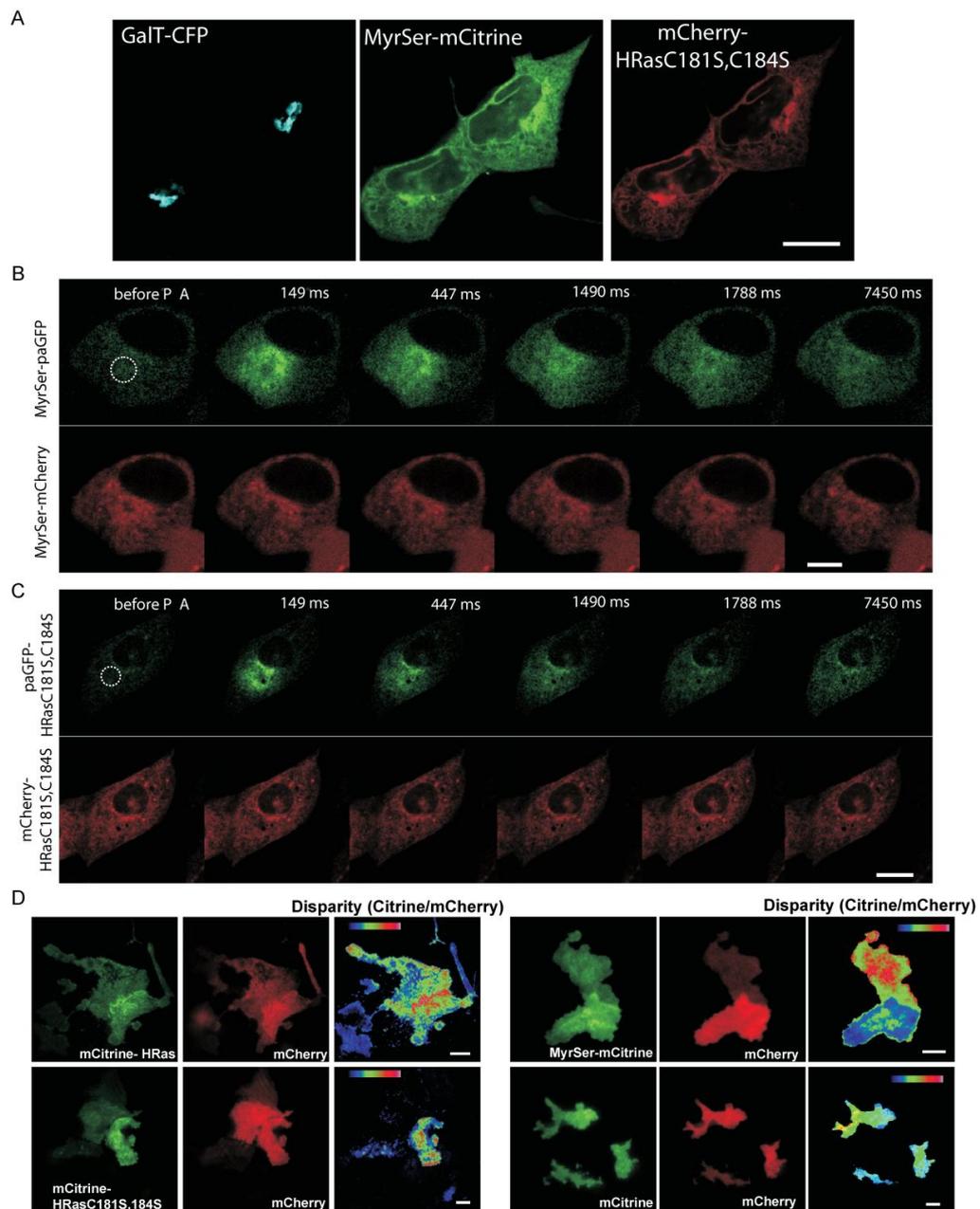
Figure 1: Rapid and random partitioning of monolipidated proteins **A**. Steady state localization of MyrSer is similar to that of HRasC181S,C184S. **B** Fluorescence loss of photoactivated MyrSer-paGFP and **C** paGFP-HRasC181S,C184S at the perinucleus in MCDK cells, showing that both single lipidated proteins rapidly and indiscriminately sample different cellular membrane systems with comparable membrane residence times. **D** Total internal reflection fluorescence (TIRF) images of MDCK cells expressing Citrine-HRras or Citrine-HRasC181S,C184S and MyrSer-Citrine. The fluorescence signals from the lipidated proteins were normalized to soluble mCherry to show the disparity in contrast reflecting their PM localization. Free mCitrine/mCherry images are shown as controls, showing disparity arising due to differences in optical parameters of the TIRF field. Scale bars: 10 μM, Color bar indicates normalized range of pixel ratios from minimum (blue) to maximum (red).

4.3 Stage 1: Palmitoylation at the Golgi

Microinjection of semi-synthetic Cy3 labeled-Ras proteins CysFar and PalFar in previous studies has shown that the Golgi apparatus is the site of palmitoylation (Rocks et al, 2005). CysFar is an N-Ras protein chemically linked to a synthetic prenylated N-Ras terminus lacking the palmitate modification. Immediately after microinjection, CysFar diffuses throughout the cell (consistent with data on monolipidated protein mobility), but enrichment is seen within seconds on the Golgi. Control experiments with SerFar , which is equivalent to a mutant NRas lacking the palmitoylatable Cys does not show this enrichment. Similarly, PalFar is a version of CysFar that already possesses the palmitate modification. PalFar also accumulates on the Golgi after microinjection, but with slightly slower kinetics as compared to CysFar. Presumably, PalFar must be depalmitoylated before it can be repalmitoylated at the Golgi (Figure 2A). However, the depalmitoylation of PalFar all over the cell provides the first indication that depalmitoylation activity is ubiquitous within the cytoplasm. In both cases, over a period of minutes, Golgi enrichment is transferred to the PM and eventually reaches the steady-state indicated by expressed wild-type mCherry-NRas.

HDFar is a semi-synthetic NRas identical to PalFar in all respects, except that the palmitate group is covalently bound to the Cys residue via a thioether linkage (instead of the biological thioester linkage). The thioether linkage cannot be hydrolyzed within cells, and thus HDFar represents a permanently palmitoylated protein. HDFar displays uniform membrane staining enrichment in any particular membrane compartment (Figure 2B). This reaffirms previous reports that the dynamic nature of the S-palmitoylation on Ras is essential to generate the typical wild type localization of NRas (seen as red channel images in Figure 2).

In order to investigate what kind of substrates such a palmitoylation reaction at the Golgi might accept, the flexibility of the semi-synthetic approach was exploited. Truncated NRas proteins D-CysFar and β-CysFar, coupled with C-termini constructed of the unnatural D-amino acids or β-amino acids respectively, were injected into cells. Surprisingly, both these artificial constructs display Golgi accumulation with kinetics indistinguishable from that of the wild-type like CysFar construct (Figure 3). These data indicate that the palmitoylation

machinery has very little local substrate specificity for palmitoylated proteins. As reported earlier, the minimum requirement for a protein to undergo palmitoylation seems simply to have a membrane-proximal Cys residue.

Figure 2
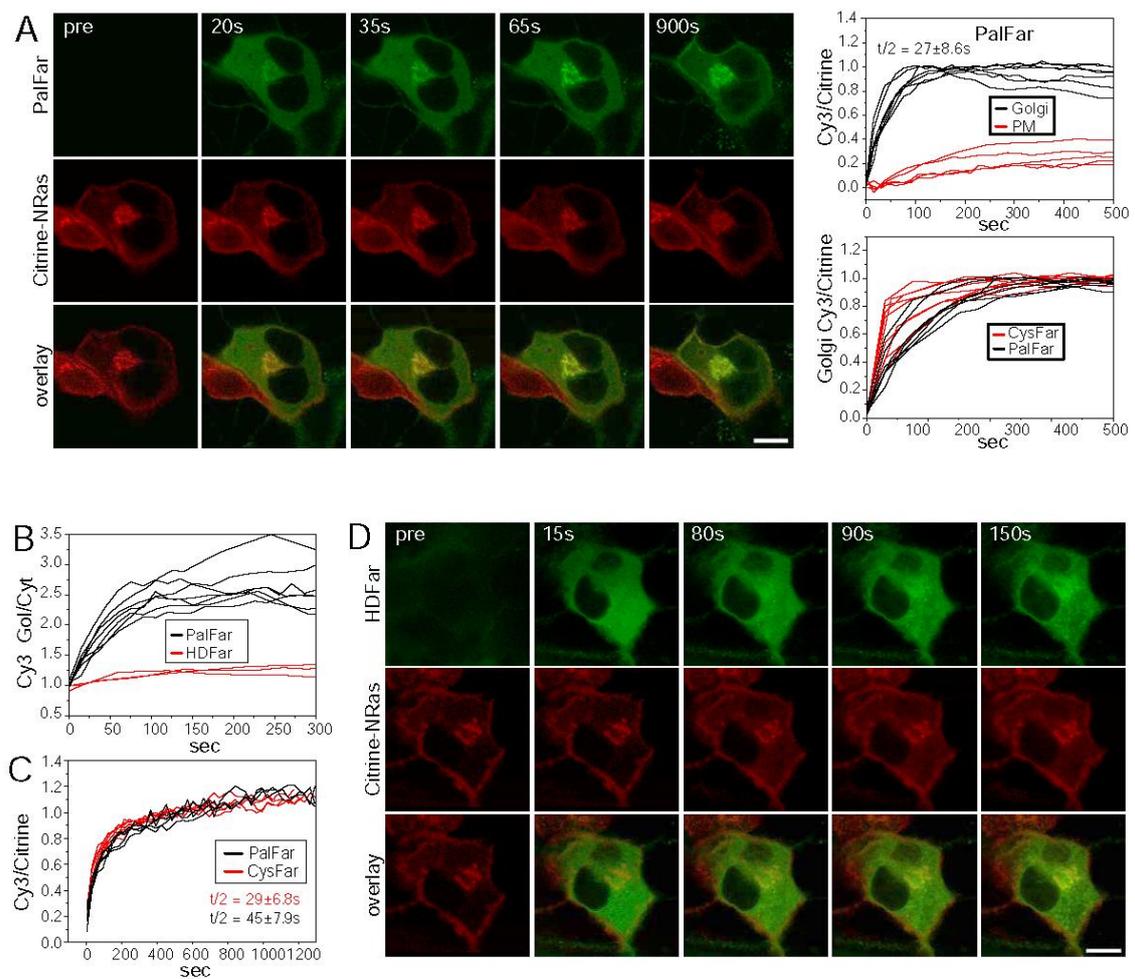
Ras palmitoylation must be reversible to generate localization and occurs on the Golgi apparatus: A. Time lapse confocal images of Cy3-labeled PalFar (green), showing it approach the steady state localization of Citrine-NRas (red channel). Upper graph shows ratiometric quantification of PalFar localization to the Golgi and PM. Lower graph shows faster kinetics of CysFar accumulation on the Golgi compared to PalFar, in similar microinjection experiments **B.** Ratiometric quantification of PalFar and HDFar accumulation of the Golgi versus the cytosol. **C.** Ratiometric quantification of CysFar and PalFar approach to a common wild-type steady state **D.** Confocal time-lapse images of Cy3-labeled HDFar injections (green), showing uniform distribution to endomembranes, as compared to expressed Citrine-NRas. Scale bar: 10μm

Figure 3
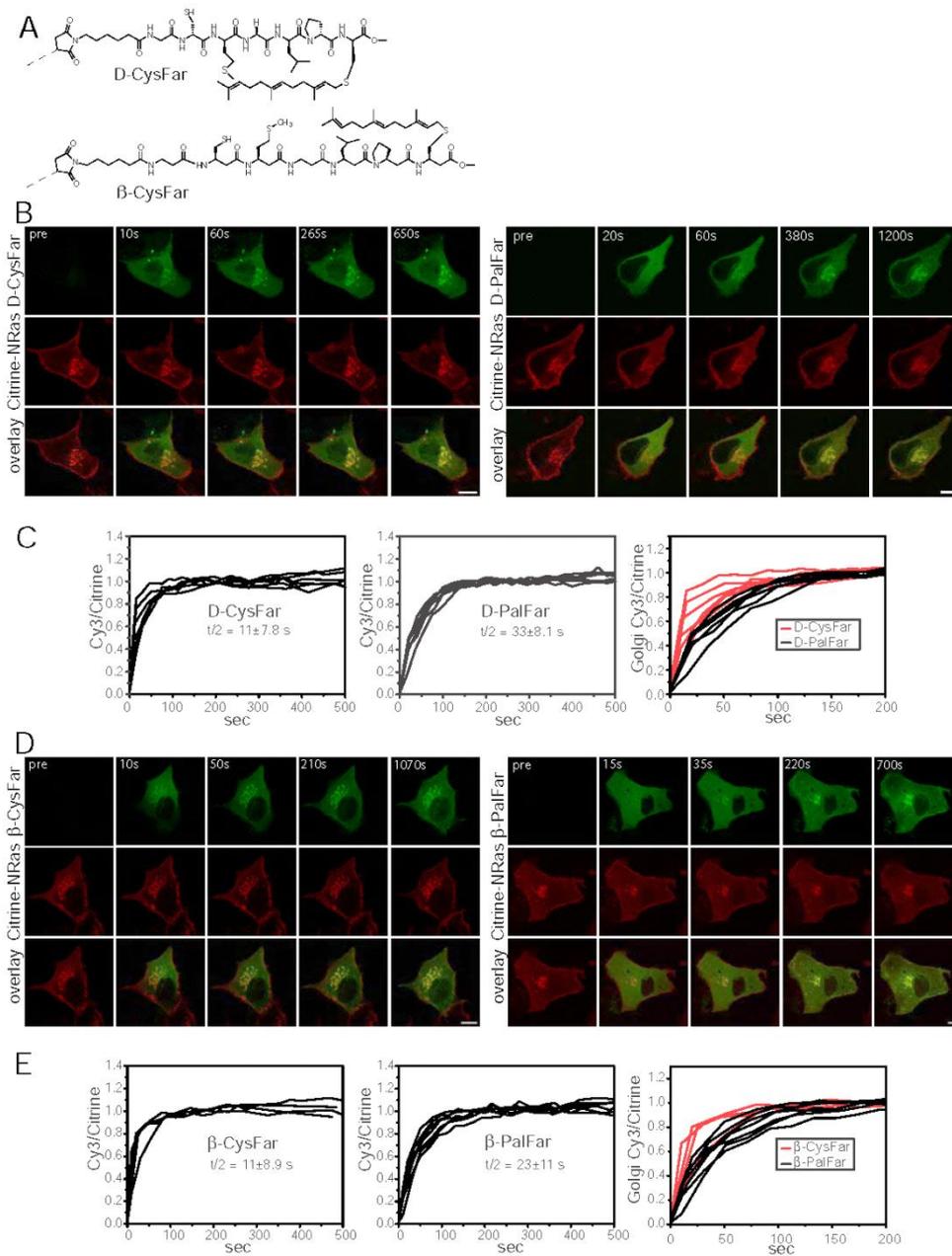
The Palmityolation machinery lacks stereospecificity and backbone specificity towards the protein substrate: Structure of the D-CysFar and β-CysFar (A). Confocal Time-lapse images and ratiometric quantification of D-CysFar and D-PalFar (**B,C**) , as well as β-CysFar and β-PalFar (**D,E**) showing indistinguishable accumulation kinetics and approach to steady state with CysFar and PalFar (see Figure 2). Scale bar: 10μm

4.3.2 The Specificity of Palmitoyl transferases

It is possible however, that the reported specificity of the palmitoyltransferases that are reported to constitute the palmitoylation machinery comes from off-site recognition of putative motifs on the Ras-G-domain distal to the target palmitoylated cysteine. In order to investigate this, we compared the steady state distributions of YFP-tH, a YFP fusion of the only the minimal C-terminal membrane targeting sequence of HRas (aa 175-190) and full-length mCherry-HRas. Differences in the kinetics and fidelity of substrate recognition for these protein constructs would reflect in the steady state localization which is generated from the palmitoylation of these proteins. YFP-tH and mCherry-HRas exhibited an identical steady-state partitioning over the PM and the Golgi (Figure 4D). They therefore must have identical palmitoyl turnover kinetics arguing against recognition of the Ras G-domain by the palmitoylation machinery. The G-domain which forms the globular core of NRas seems to be dispensable for recognition by the palmitoylation machinery as well as for generating the observed cellular localization of wild type NRas.

This apparent lack of specificity led us to explore claims of previously reported specific PAT activity of some DHHC proteins (Linder and Deschenes, 2007; Roth et al., 2006; Tsutsumi et al., 2008). In particular, Human DHHC9 and Yeast Erf2 have so far been identified as Ras PATs based on biochemical assays (Lobo et al., 2002; Swarthout et al., 2005), evidence also exists for DHHC17 and 18 (Fukata et al., 2004; Huang et al., 2004). However, FRAP studies where the Golgi apparatus was bleached and recovery of HRas monitored under shRNA-mediated knockdown of DHHC9 showed no detectable effect on Ras palmitoylation. The steady state localization of HRas in DHHC9 knockdown cells also did not display any differences when compared to cells transfected with control nonsense shRNA (Figure 4A-C).

These data strongly argue for a lack of specificity either on the Ras substrate or on the DHHC proteins (if they are indeed PATs). A bioinformatics analysis of the esoteric DHHC protein family was undertaken, in hopes of finding clues to alleviate the conflict with previously published conflicting reports.

4.3.1 Bioinformatics of DHHC proteins

Attempts to classify DHHC proteins based on their predicted membrane topology, or from basic sequence alignments were not fruitful owing to the large sequence diversity present in this family. A Hidden Markov Model (HMM)-based bioinformatics approach (Smyth, 1997) was therefore used to classify the 25 human DHHC proteins into different classes. DHHCs reported as RasPATs were used to seed and construct an HMM. The statistical model could then be used to extract a consensus sequence and construct a phylogenetic tree Indeed, the HMM indicated close relationships (Figure 5A) between these particular DHHC proteins, as compared to other human, yeast and fungal DHHC proteins. Each of these proteins contained the conserved consensus sequence 'W-X(4)-L-X(12)-TTNE' , located in the cytoplasmic loop predicted to be topologically adjacent to the DHHC-CRD domain. Such a sequence could be inferred to be correlated with *in vitro* RasPAT activity. Scanning of multiple genomes with this consensus sequence showed that the HMM could identify the putative RasPAT DHHC proteins 9, 17, 18 etc. in all mammalian species with high fidelity (Figure 5B). This finding was consistent with biochemical assays of RasPAT activity, and now in conflict with our own microinjection data that showed lack of specificity. Through a detailed search of genomes, we identified the organism *Dictyostelium discoideum* which contained only homologs of human DHHCs 1-8. This organism has at least 11 Ras isoforms, all of which are prenylated, but none of which contain a palmitoylatable cysteine. We hypothesized that if indeed Ras specific PAT activity exists, human HRas should not become palmitoylated when expressed in *Dictyostelium discoideum.* Human HRas was however palmitoylated in Dictyostelium cells as indicated by its clear enrichment at the PM and certain internal membranes including endosomes, as compared to the largely endomembrane/cytosolic localization of its non-palmitoylatable mutant HRasC181S,C184S (Fig. 4E). Endosomes originate from the PM is abundantly present in *Dictyostelium* cells (Gerisch et al., 2004). The enrichment of HRas on the PM and endosomes was lost upon inhibiting palmitoylation with 2-bromopalmitate, a general inhibitor of palmitoylation and palmitate synthesis (Coleman et al, 1992; Jennings et al, 2009). Finally, FRAP kinetics showed that the relatively slow motility of HRas in *Dictyostelium* cells (Figure 4F) was consistent with that of palmitoylated HRas ($t_{1/2}$=183.3±3.8s) as observed in mammalian cells

(Rocks et al, 2005). In summary, it seems that while some correlation in the sequences of DHHC proteins reported to have RasPAT activity exists, the putative PAT activity of these proteins is certainly redundant when other DHHC proteins are present.

Figure 4
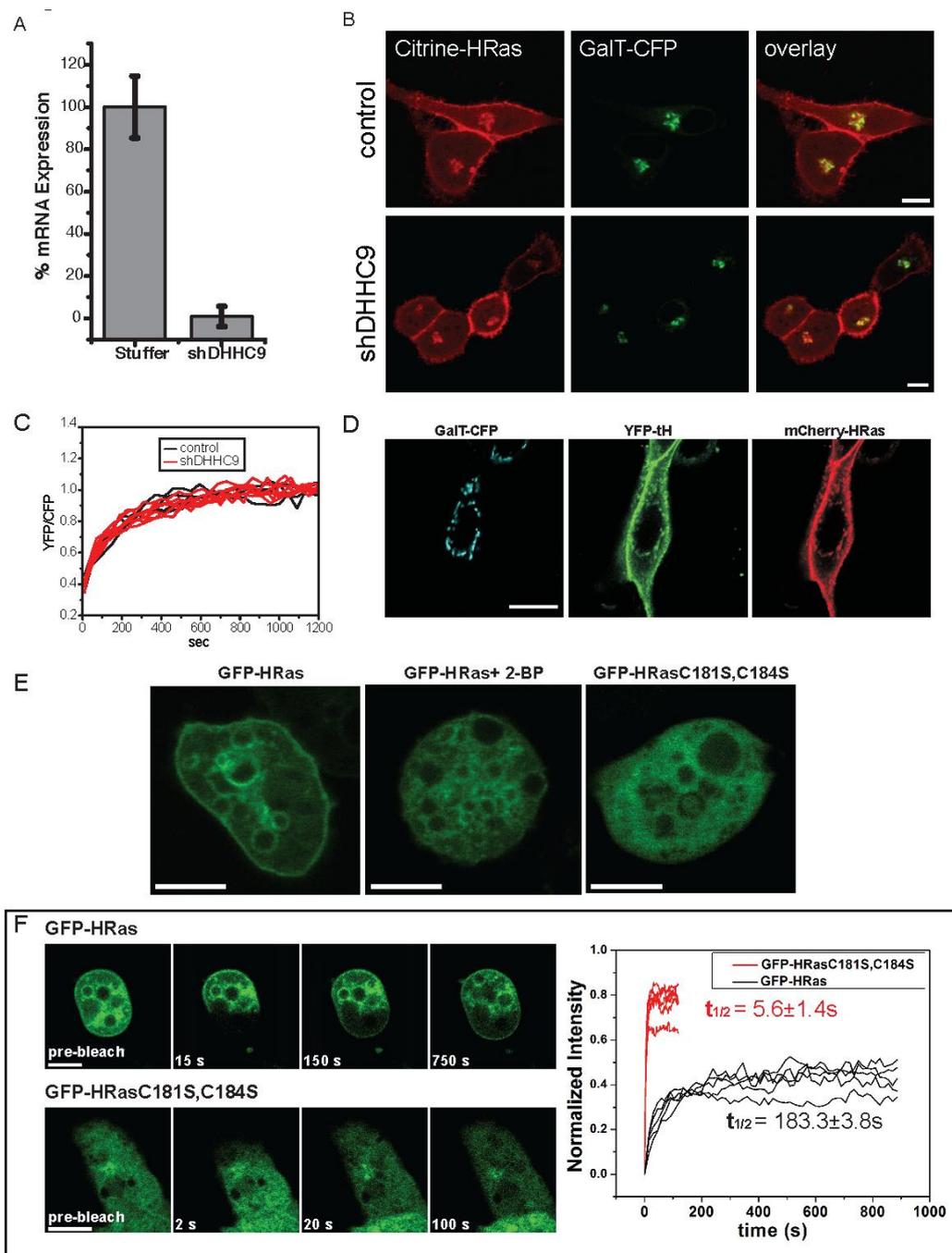
HRas does not require distal recognition or specific PATs for correct localization A Lentiviral shRNA-mediated downregulation of DHHC9 expressions in HeLa cells analyzed by quantitative RT-PCR using Actin B RNA as reference. Error bars represent standard error of mean of percentages calculated from $\Delta(\Delta Ct)$ values in three independent runs. **B** Steady-state localization of HRas in DHHC9 knock down and control HeLa cells. **C** Fluorescence recovery after photobleaching of HRas at the Golgi in DHHC9 knock down (n=7) and control cells (n=4). The recovery of local fluorescence was ratiometrically quantified using GalT-CFP as a Golgi reference. Plateau values were normalized to one. **D** Comparison between the localization of full length HRas fused to

mCherry and the c-terminus of HRas fused to YFP. Equivalent distribution of the fragment versus full-length protein has a theoretical value of 1. Quantification of the experiment shows complete equivalence of both constructs (value of 1.02 +/- 0.04). **E** Representative images of Dictyostelium cells (1 of 20 each) expressing HRas and HRasC181S,C184S. HRas shows clear enrichment on the PM, which is lost upon treatment with 2-bromopalmitate. Scale bars: 5μM. **F** FRAP sequences of HRas and HRasC181S,C184S with representative examples (5 each) in *Dictyostelium* cells showing the slower recovery of HRas, indicating its palmitoylated state. Scale bars: 5μM. See also Suppl. Fig. 7.

Figure 5
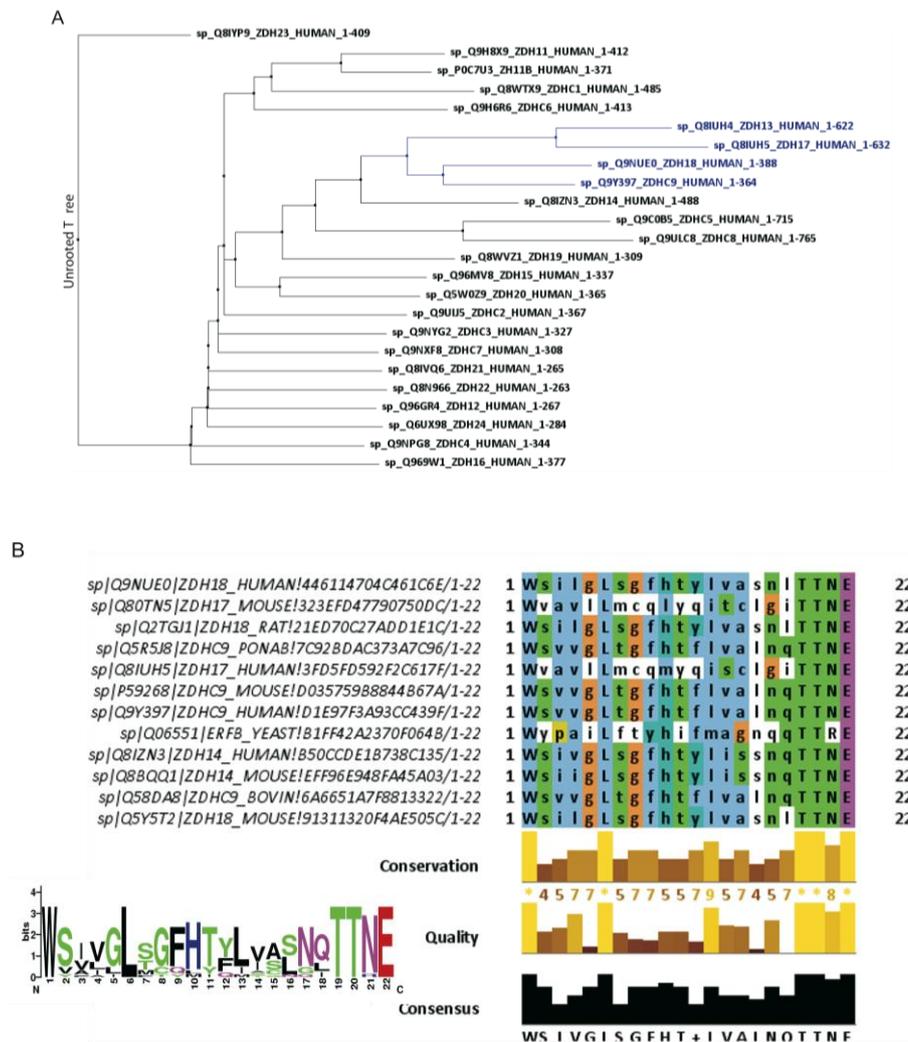
Bioinformatics analysis of DHHC proteins. A Phylogenetic tree showing human DHHC proteins as classified by the HMM. The tree is unrooted since no assumptions of an ancestral DHHC sequence have been made. The clade containing biochemically ascribed RasPATs is indicated in blue. **B** Alignment in the region of the consensus sequence of mammalian and yeast genome hits identified by the PROSITE scan of 'W-X4-L-X12-TTXE' , showing high degree of conservation and fidelity.

4.4 Stage 2: From Golgi to the Plasma Membrane

As the results presented here and those reported earlier show, palmitoylation of Ras occurs at the Golgi apparatus. While this explains the enrichment of palmitoylated Ras on the Golgi apparatus, it does not explain how this enrichment is transferred to the plasma membrane. Partitioning over the Golgi apparatus versus the plasma membrane depends on the reversible palmitoylation. While the core Ras G-domain does not affect this partitioning, additional domains on other palmitoylated proteins could quantitatively shift this partitioning. Fyn is a Src-family kinase that is N-Myristoylated and palmitoylated at Cys residues at positions 3 and 6. At 37°C, Fyn displays strong PM enrichment but almost no enrichment on the Golgi apparatus. Examples such as these have been used to suggest that perhaps palmitoyltransferase is not localized only to the Golgi apparatus, but may also be present on the PM. It should be noted that Fyn is large multi-domain peripheral membrane protein that functions in focal adhesion formation and can interact with several other proteins localized independently to the plasma membrane (Sato et al, 2009). As such, our alternative hypothesis is that Fyn, like all other palmitoylated proteins is also palmitoylated at the Golgi, however, due to its additional features, its steady-state localization is strongly shifted towards to the PM. Incidentally, trafficking of palmitoylated proteins HRas and TC10 to the plasma membrane via exocytic vesicles has been previously reported (Apolloni et al, 2000; Watson et al, 2003). The canonical secretory pathway provides a unidirectional route for the high-affinity membrane bound forms of palmitoylated proteins to reach the plasma membrane. To test this hypothesis, we performed imaging at 16°C, a temperature at which the mammalian vesicular secretory pathway is blocked due to motor-protein dysfunction. In corroboration with our hypothesis, blocking the secretory pathway resulted in a strong enrichment of Fyn at the Golgi apparatus, indicating that the protein does get palmitoylated at the Golgi apparatus (Figure 7). Similar results could be obtained from a secretory pathway block for other palmitoylated proteins- TC10, RRas that do not show Golgi localization at 37°C (Rocks et al, 2010).

As confirmation of this result, microinjection experiments reported in Section 4.3 were repeated at 16°C. As expected, both PalFar and CysFar show enrichment at the Golgi

following microinjection, but this enrichment is not transferred to the PM under the secretory pathway block (Figure 8, compare with Figure 2). Thus, despite quantitative differences in their steady state localization: (1) palmitoylated proteins are palmitoylated at the Golgi apparatus and not at the PM and (2) The secretory pathway is responsible for transferring palmitoylated proteins from the Golgi apparatus towards the plasma membrane.

Figure 7
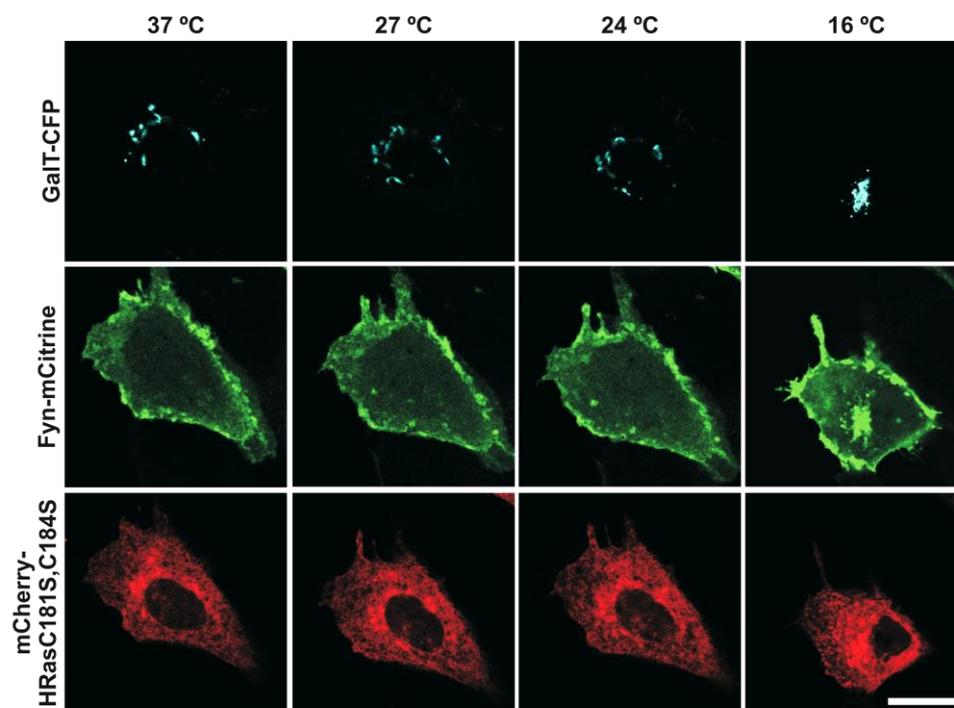
Steady state localization of Fyn wt-mCitrine in MDCK cells at various temperatures. GalT-CFP serves as a Golgi marker, and mCherry-HRasC181S,C184S serves to indicate distribution of non-palmitoylated proteins. No substantial differences in Fyn localization are observed as cells are cooled to from 37°C to 19°C. At 16°C, a vesicular transport block causes the accumulation of Fyn at the Golgi apparatus, with steady localization similar to HRas wt. Scale Bar : 10μM.

Figure 8
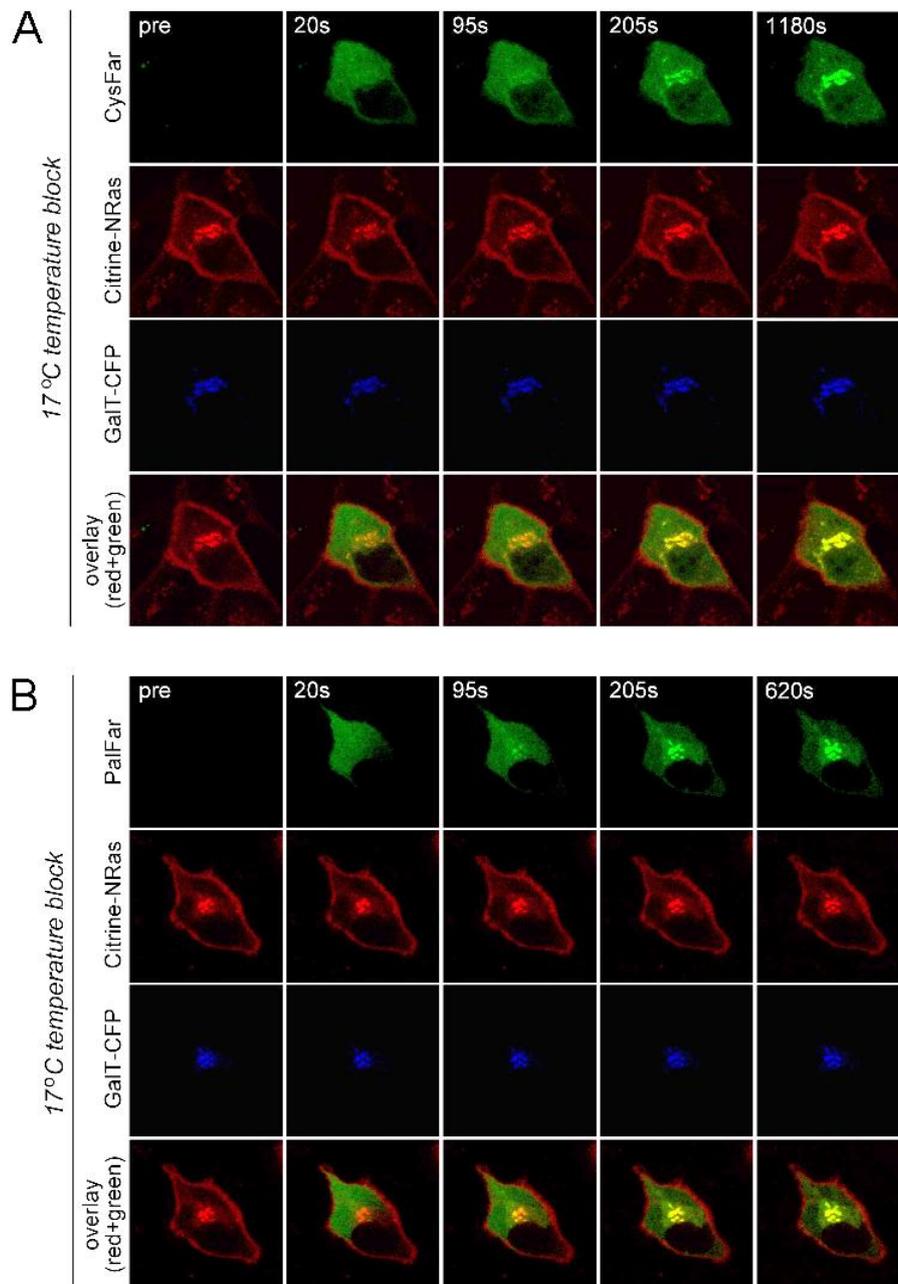
Temperature block of the exocytic pathway inhibits accumulation of semi-synthetic Ras probes CysFar and PalFar at the plasma membrane. Time-lapse images of MDCK cells maintained at 17°C for 10 min prior and after microinjection of CysFar (a) or PalFar (b), in the green channel. Citine-NRas (red channel) and GalT-CFP (blue channel) show the steady state NRas distribution and the Golgi apparatus respectively. This experiment shows that the secretory pathway re-directs palmitoylated Ras proteins to the plasma membrane.

4.5 Stage 3: Depalmitoylation by APT1 and Interrupting the Acylation Cycle

So far, the work described here discusses the palmitoylation of proteins and the mechanism of their transport to the plasma membrane. To maintain a steady state distribution, it Is necessary that proteins so transported be also removed from the PM. One mechanism, albeit inefficient, would be the degradation of such proteins. Moreover, palmitate turnover kinetics as measured by FRAP recovery at the Golgi apparatus is far too rapid to be explained by *de novo* protein synthesis. It was hypothesized that thioesterases such as APT1 (or APT2 as the only 2 candidates) depalmitoylate acylated proteins, returning them to their mono-lipidated rapidly diffusing form, and allowing them to be repalmitoylated at the Golgi apparatus. In order to investigate this phenomenon, we adopted a chemical biological approach, involving treatment of cells with a newly-developed APT1 inhibitor.

4.5.1 Development of an APT1 inhibitor

Collaborators at the Department of Chemical Biology developed a potent inhibitor for APT1 employing 'Protein Structure Similarity Clustering' (PSSC) as a knowledge driven bioinformatics based strategy (Dekker et al, 2005). In PSSC the ligand-sensing core of a given protein is identified and extracted from its structure *in silico*. Databases are then searched for proteins with structurally similar ligand-sensing cores, i.e. similar folds around the binding site, irrespective of similarity in sequence. Compound classes known to inhibit such similar proteins are then used as starting points for the design and synthesis of compound collections that are likely to yield inhibitors for the protein of interest (Fig. 1a). Acyl protein thioesterase 1 (APT1, PDB code 1FJ2) is a α/β-hydrolase with a catalytic triad of Ser-114, His-203 and Asp-169. Based on similarities with a gastric lipase, and screenings with several β-lactone compounds, Palmostatin B (Figure 9A) was identified as a potent APT1 inhibitor and was selected for further investigation *in vivo* (Dekker et al, 2010).

### 4.5.2 Palmostatin B inhibits depalmitoylation of Ras in cells

In order to confirm that treatment with Palmostatin B and the resulting APT1 inhibition directly inhibits depalmitoylation of Ras *in vivo*, the level of Ras palmitoylation was measured in MDCK cells expressed YFP-NRas using the Acyl-biotin exchange assay (Drisdel & Green, 2004; Martin & Cravatt, 2009). Immunoprecipitation of YFP-NRas and quantitative labeling of palmitoylation sites revealed a marked increase of palmitoylated YFP-NRas in the presence of Palmostatin B (Fig. 9B). In contrast, levels of palmitoylated YFP-NRas were reduced upon treatment with 2-bromopalmitate, the general inhibitor of palmitoylation and palmitate synthesis. These results provide direct evidence that Palmostatin B increases Ras palmitoylation levels in cells by inhibiting the depalmitoylating thioesterase.

Further evidence was provided through a repetition of the microinjection experiments with CysFar and PalFar, in cells treated with Palmostatin B. CysFar, which is a substrate for palmitoylation showed enrichment on the the Golgi apparatus, similar to control cells treated with the delivery vehicle or untreated cells. PalFar, however, did not show this enrichment, as PalFar must first be depalmitoylated, the very process that Palmostatin B inhibits (Figure 10). These results demonstrate that Palmostatin B selectively inhibits the cellular de-acylation reaction without affecting the acylation reaction.

Finally, we investigated if Palmostatin B directly binds to APT1 in cells though Fluorescence Lifetime Imaging Microscopy. Firstly, intensity images of APT1 confirmed the reported (Hirano et al, 2009a) cytoplasmic ubiquitous localization of APT1. FRET between a fluorescent labeled (TAMRA) analog of Palmostatin B and GFP-tagged APT1 was detected indicating the molecular proximity of the fluorescent tags, and in turn, confirming APT1 as the cellular target of Palmostatin B (Figure 11).

Figure 9

A
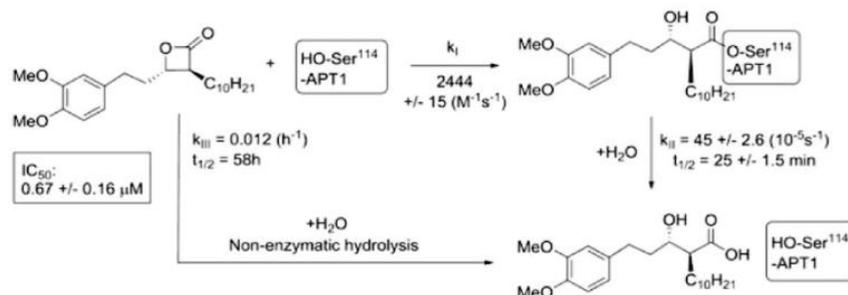
B
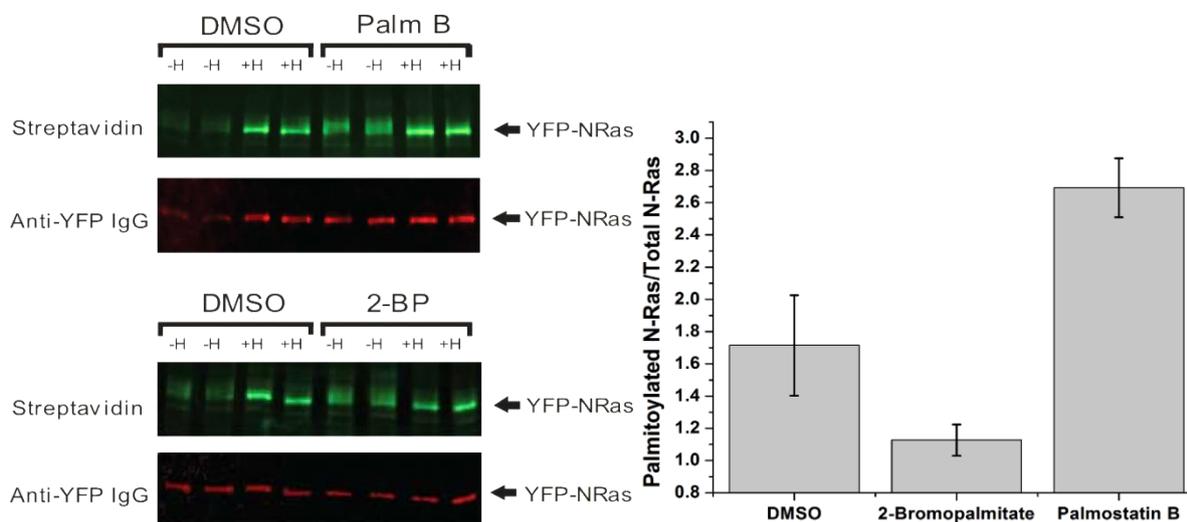
Palmostatin B specifically inhibits depalmitoylation. A Structure and synthesis scheme of Palmostatin B. **B** Thioesterase inhibition by Palmostatin B increases the fraction of palmitoylated NRas in live cells, as measured by the Acyl-Biotin exchange assay. 2-BP, an inhibitor of cellular palmitoylation is shown as negative control. Quantification of Western blots (arbitrary fluorescence units using IR-dye labeled antibodies) represents data from 4 independent experiments with 8 independent runs per treatment.

Figure 10
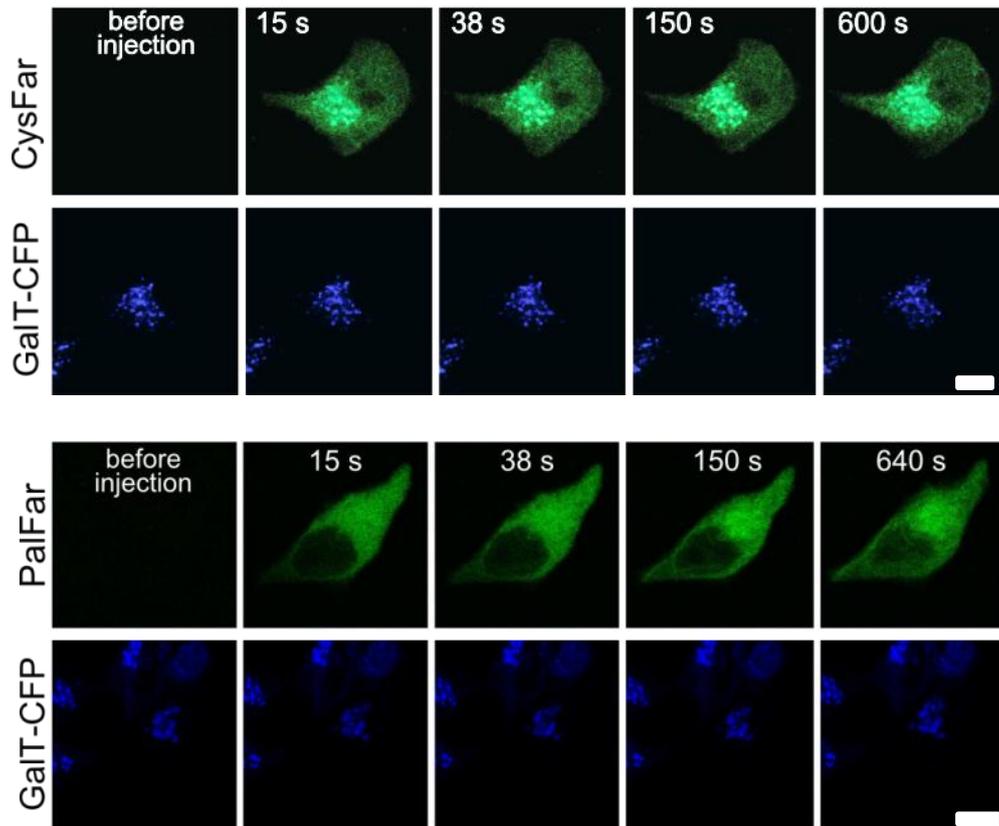
Palmostatin B inhibits depalmitoylation, but not palmitoylation in the acylation cycle Confocal time-lapse images of MDCK cells expressing the Golgi marker GalT-CFP prior and after microinjecton of CysFar or PalFar. Cells were incubated for 80 min with 1 μM Palmostatin B prior to the experiment. CysFar shows accumulation at the Golgi apparatus, however, PalFar shows no specific accumulation instead adopting an HDFar-like aspecific staining. Compare with Figure 2,3 (pg 55-56). Scale bars: 10 μm.

Figure 11
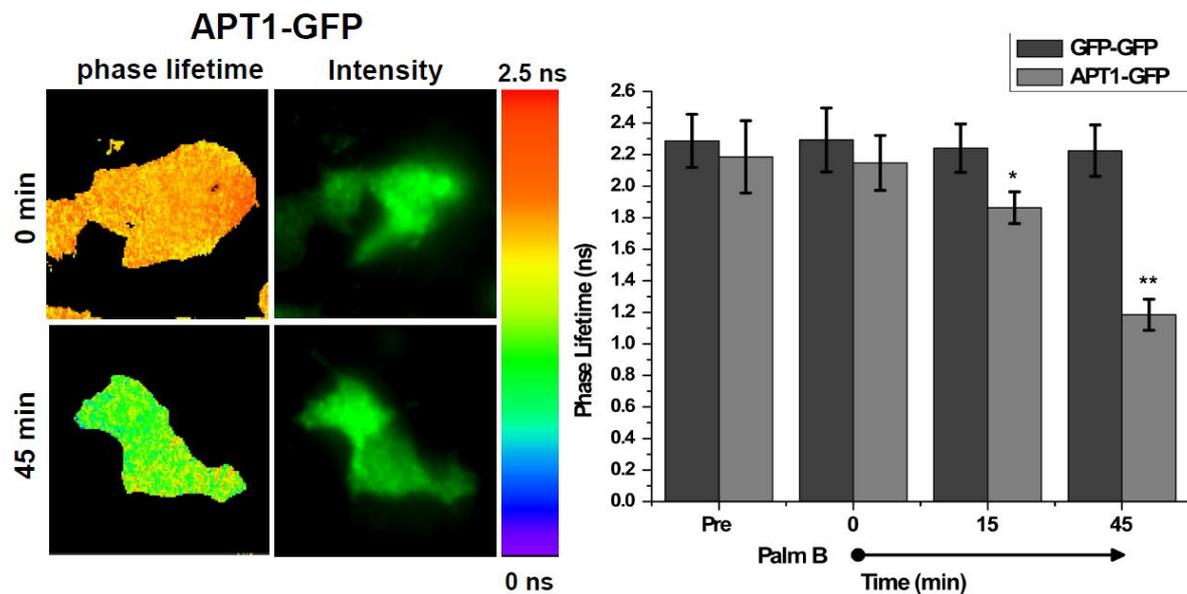
Fluorescence Lifetime Imaging of Live cells showing specific binding of APT1-GFP (donor) to TAMRA-labelled Palmostatin B (acceptor). Lifetime and intensity maps of cells after incubation with acceptor, showing reduction in GFP-fuorescence lifetime of upto 1.26 ns. Graph shows reduction in APT1-GFP lifetime as compared to GFP-GFP (control) lifetime upon incubation with the acceptor. Lower limit for APT1 / Palm B bound fraction is estimated to be 40%.

4.5.3 Palmostatin B affects Ras localization

MDCK cells expressing the fluorescent protein fusion constructs Citrine-NRas and the Golgi marker GalT-CFP were treated with 1 ⎕M Palmostatin B for 100 minutes. Confocal time lapse microscopy showed a dramatic re-distribution of Citrine-NRas to endomembranes over the period of 1h. Quantitative comparison of the localization with Manders' coefficients of yellow fluorescent Citrine-NRas with the solely farnesylated red fluorescent Cherry-C181, 184S HRas mutant, showed that NRas reached a similar random distribution among all cellular membranes similar to that of the monolipidated (farnesylated Ras) (M1 =0.96)(Manders et al, 1993). Here, the partial overlap of Cherry-C181,184S-HRas with the Golgi marker GalT-CFP does not reflect specific accumulation but rather the high density of membranes at this subcellular site.

A similar Palmostatin B induced redistribution was observed in cells expressing Citrine-HRas. This Ras isoform, however, exhibited more persistent, albeit reduced plasma membrane localization after Palmostatin B treatment, expected due to the additional stability of the dual acylation on HRas. The residual Citrine-HRas concentration at the plasma membrane is due to the remaining flux from the secretory pathway that is not completely countered by the slow leaking of the dually acylated HRas from the plasma membrane. Importantly, at shorter times after Palmostatin B incubation there was a clear loss of Golgi-localized HRas due to the remaining unidirectional flux of Ras towards the plasma membrane (PM) via the secretory pathway (Figure 14).

The non-palmitoylated KRas isoform did not exhibit any re-distribution after Palmostatin B treatment of MDCK cells, confirming that this effect of Palmostatin B was due to perturbation of the acylation cycle (Figure 13A). Treatment with 2-BP, on the other hand, leads to a inhibition of the palmitoylation machinery and thus leads to a similar random redistribution. It should be emphasized, however, that Palmostatin B and 2-BP inhibit antagonistic processes, and thus the redistributing species in each case differs in its palmitoylation status. . The Palmostatin B induced redistribution mechanism is similar to that of 2-bromopalmitate. However, in the case of 2-bromopalmitate, palmitoylation at the Golgi is inhibited, and the redistributing species is depalmitoylated (but still farnesylated) Ras. After the initial lag phase in which the cellular palmitate levels drop, the random equilibrium distribution of Citrine-NRas is more rapidly attained, as compared to Palmostatin B incubation. Under 2-bromopalmitate treatment, the more rapid redistribution kinetics are due to the lower hydrophobicity, and thereby, lower affinity for membranes, of solely farnesylated NRas as compared to palmitoylated NRas. Since Palmostatin B has a half-life of about 20 minutes in an aqueous environment, proper localization of Citrine-NRas was restored after overnight incubation. Palmostatin B is therefore not cytotoxic at micromolar concentrations as has been verified elsewhere (Dekker et al, 2010).

In principle, inhibition of the thioesterase activity would have been expected to increase enrichment of Ras on the PM, tilting the kinetic balance in favor of palmitoylation and consequently membrane PM localization. The counterintuitive identical result of increasing

and decreasing palmitoylation of Ras finally reveals the cyclical nature of Ras palmitoylation. Palmitoylation at the Golgi apparatus and transport to the plasma membrane is followed by depalmitoylation by the ubiquitous thioesterases and a return to the rapidly mobile mono-lipidated state. Such molecules have a high stochastic probability of a Golgi encounter, only to be repalmitoylated – thus completing the acylation cycle.

Figure 12
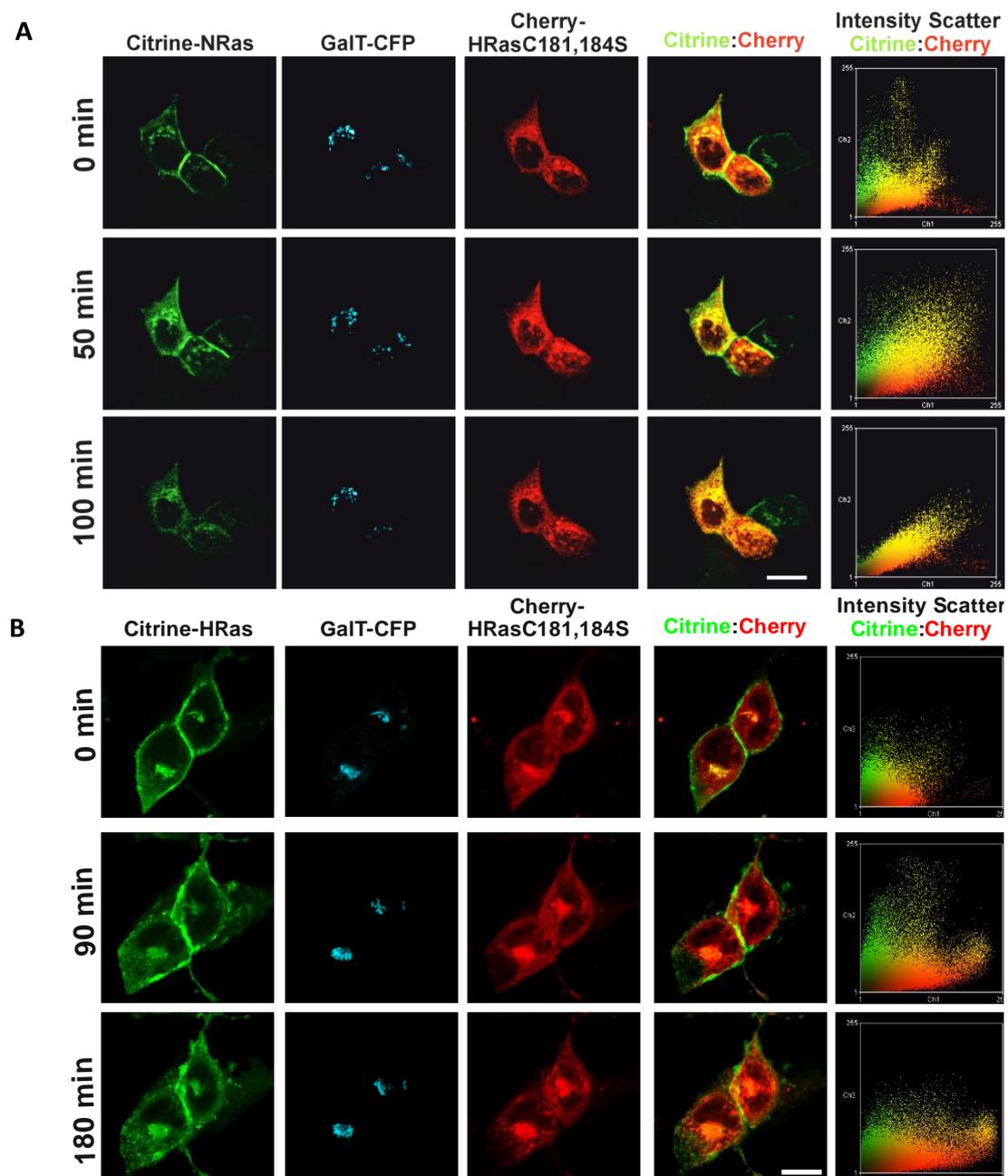
Palmostatin B causes entropy-driven redistribution of palmitoylated Ras isoforms. A Representative example of changes in distribution of Citrine-NRas with respect to Cherry-HRasC181S,C184S in MDCK cells at various time-points after treatment with 1 μM Palmostatin B observed under confocal microscopy. Columns show red-green channel overlays and intensity scatter plots for Citrine-NRas (green) and Cherry-HRasC181S,C184S (red) demonstrating their increase in co-localization over time. Manders' coefficients for colocalization of Citrine-NRas and Cherry-HRasC181S,C184S over time after Palmostatin B treatment approach a value >0.95. **B** Representative example of changes in distribution of Citrine-HRas with respect to Cherry-HRasC181S,C184S in MDCK cells at various time-points after treatment with 10 μM Palmostatin B. Scale bar : 10 μm.

Figure 13

A
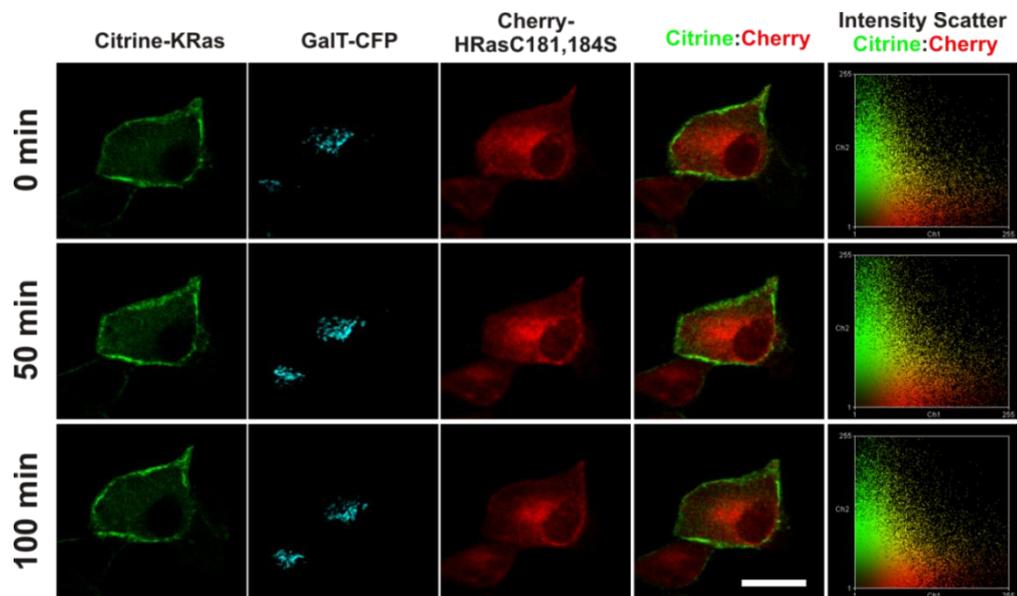
B
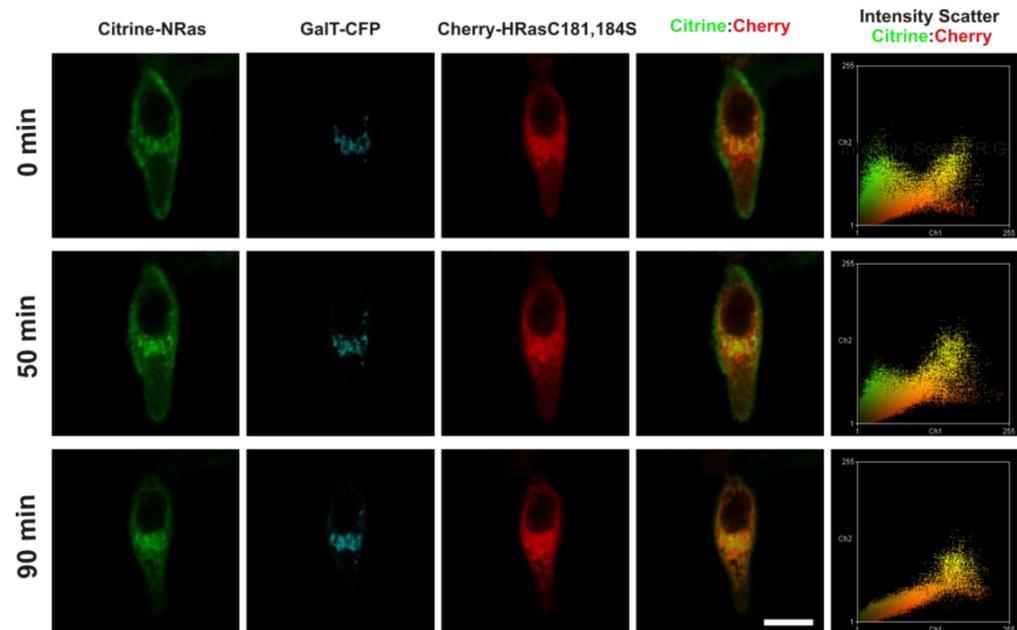
Palmostatin B induced redistribution is Palmitoylation depedent. A Representative example of stable distribution of Citrine-KRas with respect to Cherry-HRasC181S,C184S in MDCK cells at various time-points after treatment with 10 μM Palmostatin B. **B** Inhibition of protein palmitoylation with 2-BP replicates the redistribution of NRas as seen with Palmostatin B. Scale bar : 10 μm.

Figure 14
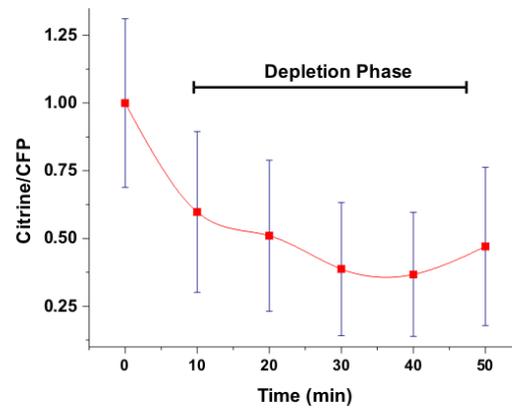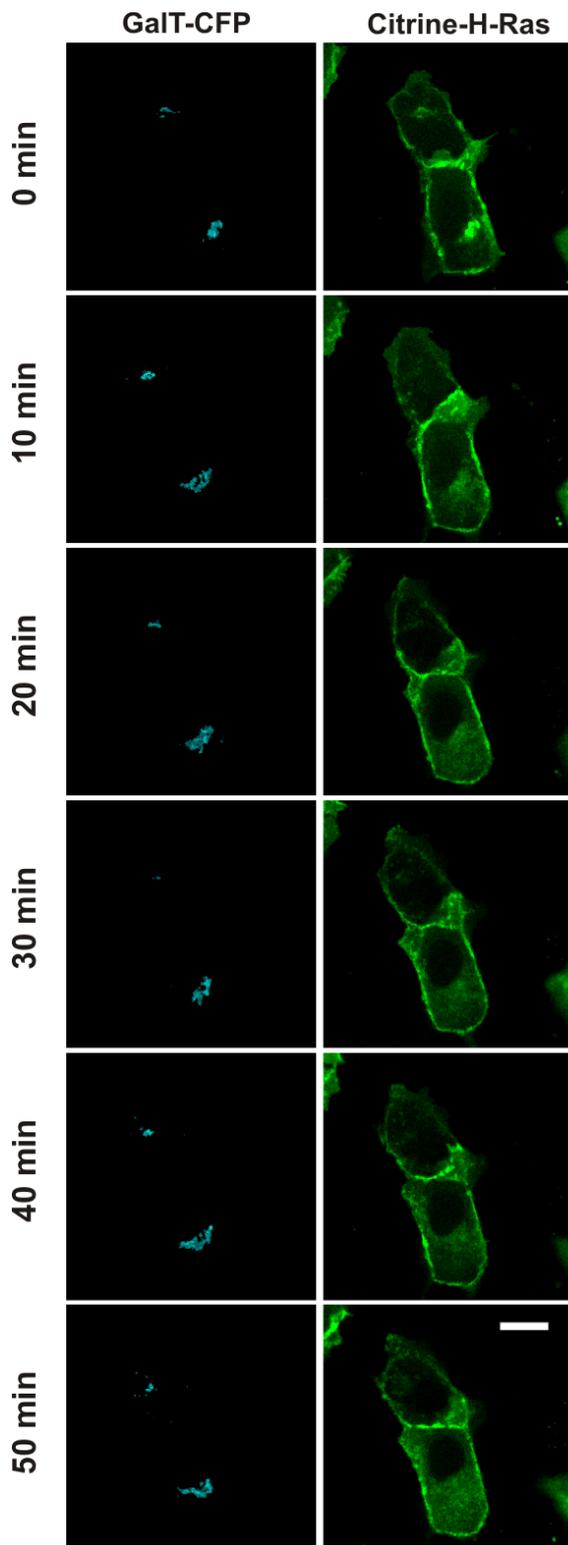
Palmostatin B leads to depletion of Citrine-HRas from the Golgi apparatus at short time scales. MDCK cells expressing Citrine-HRas and the Golgi marker GalT-CFP show depletion of HRas from the Golgi apparatus within a hour of 10 µM Palmostatin B treatment, due to the pumping action of the secretory pathway when influx of HRas through depalmitoylation is blocked. Scale bar: 10 µm

Endocytosis does not play a role in Ras redistribution

In order to rule out the possibility that the observed redistribution of Ras did not occur due to enhanced binding to the PM and subsequent redistribution by membrane processes such as endocytosis, the redistribution experiment was repeated in the presence of Dynasore, an inhibitor of endocytosis (Macia et al, 2006a). Inhibition of endocytosis prevented cellular uptake of high-molecular weight fluorescein labeled Dextran, but did not alter the kinetics of Palmostatin B induced redistribution of NRas (Figure 15). This shows that endocytosis was not the primary mechanism of entropy driven redistribution of palmitoylated Ras.

Figure 15
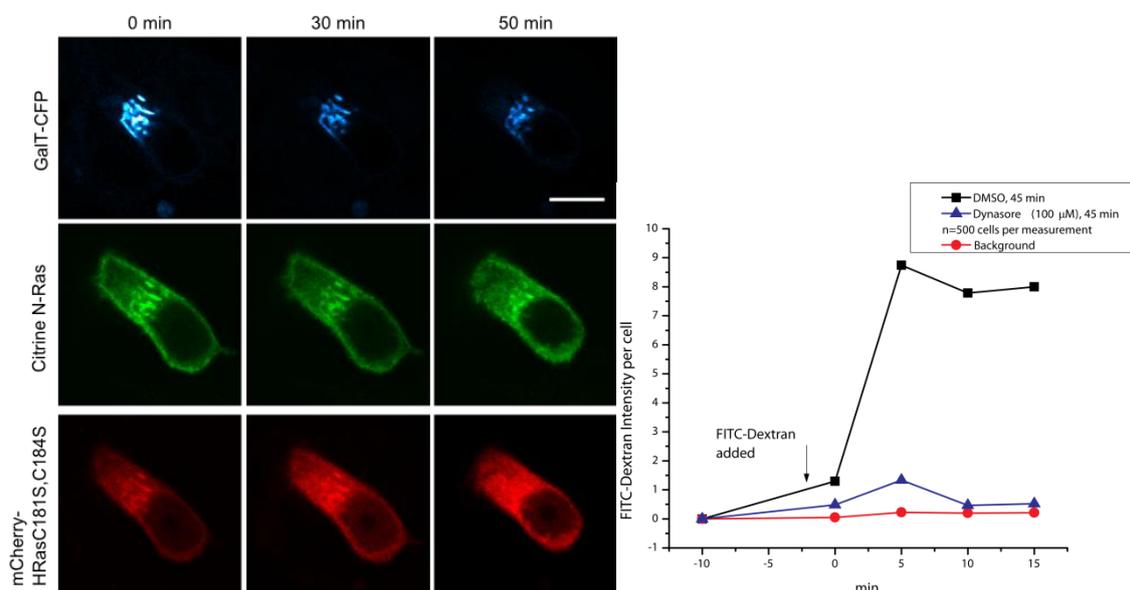
Palmostatin-induced Ras redistribution under Dynasore-imposed Endocytosis block: MDCK cells were cultured and transfected with Citrine-NRas, GalT-CFP and mCherry-HRasC181S,C184S, incubated with 100 ⎵M Dynasore (Macia et al, 2006b) for 20 min and treated with 1 μM Palmostatin B as in the case of the restribution assay described earlier. Restribution was observed over the next 50 min. In order to evaluate the efficacy of Dynasore in inhibiting endocytosis, MDCK cells were incubated with Dynsore or DMSO under similar conditions as the redistribution assay and uptake of 15kD FITC-Dextran (Sigma) into endocytic vesicles was measured over time using wide-field fluorescence microscopy. Mean FITC-Dextran intensities per cell provided a measure of the near complete inhibition of endocytosis due to Dynasore. Scale bar: 20 μm

4.5.4 Down-regulation of APT1 mimics the effect of Palmostatin B

In order to ascertain that APT1 exhibits a thioesterase activity that regulates the Ras acylation cycle in cells, and there are no pleiotropic effects of Palmostatin B playing a role in the observed effects on Ras localization, RNA interference mediated knockdown of APT1 was performed in MDCK cells (Figure 16A). The steady state palmitoylation levels of YFP-NRas were ascertained with the acyl-biotin exchange assay, showing a near doubling of the fraction of palmitoylated NRas (Figure 16B) under a 5 fold downregulation of APT1. Further, this reduction of NRas palmitoylation could be rescued by ectopic expression of human APT1 in MDCK cells (Figure 16D), which is not susceptible to knockdown by Anti-Canine APT1 siRNA.

Since the palmitoylation activity that causes Ras to accumulate at the Golgi is not perturbed by APT1 down-regulation, it is expected the redistribution to endomembranes following a loss of thioesterase activity reduces the fraction of Ras localized to the plasma membrane, resulting in the decrease of the plasma membrane/Golgi fluorescence intensity ratio. This change in membrane partitioning during the redistribution was quantitatively imaged, and a comparison of APT1 knockdown and Palmostatin B treated cells shows the qualitative similarity in the effects of the two methods of reducing thioesterase activity. The thioesterase activity of APT1 therefore is necessary to depalmitoylate Ras proteins.

Together these results confirm that the re-distribution of Ras is indeed due to inhibition of cytoplasmic APT1 activity, that APT1 is a Ras-depalmitoylating thioesterase and is the cellular target of Palmostatin B.

Figure 16
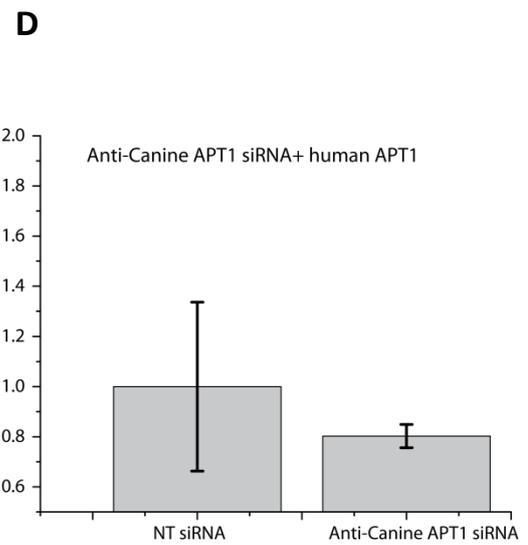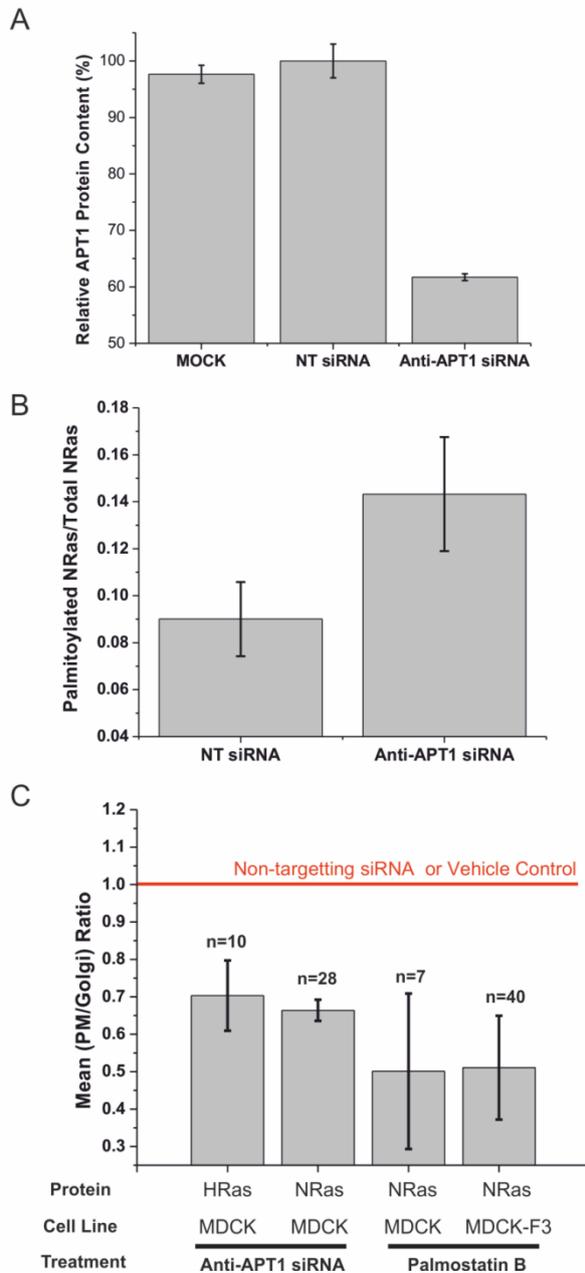
Down-regulation of APT1 increases the steady-state palmitoylation level of Ras. A Efficacy of APT RNAi - The bar graph shows decrease in relative APT1 mRNA content in NRas transfected cells for two siRNA concentrations. RT-qPCR quantification of mRNA APT1 knockdown in MDCK cells treated with 100 nM anti-canine APT1 siRNA $(\Delta(\Delta Ct))=1.8$ cycles w.r.t GAPDH control **B.** Down-regulation of APT1 by RNAi increases the levels of NRas palmitoylation as measured by the acyl-biotin-exchange assay. **C,** Ratiometric image analysis of the redistribution of palmitoylatable Ras isoforms to endomembranes after down regulation of APT1 shows a significant decrease of the PM/Golgi intensity ratio of both Citrine-HRas and Citrine-NRas occurs in cells treated with anti-APT1 siRNA. For Citrine-NRas, cells treated with Palmostatin B showed a similar decrease in PM/Golgi intensity ratio in MDCK and MDCK-F3 cells. PM/Golgi ratios from control cells treated with either NT siRNA or DMSO as vehicle control (indicated by red bar) was used to normalize the data.

4.6 The Acylation Cycle convolutes with Ras Signal transduction

4.6.1 Palmostatin B uncouples Ras signaling from the PM from that on the Golgi

Growth factor stimulation normally leads to a rapid activation of HRas at the plasma membrane and delayed but sustained activity on the Golgi (Rocks et al, 2006). The short-term effect (<1 h) of Palmostatin B incubation on wild-type HRas activity was monitored via the translocation of the mCherry-labeled Ras binding domain of Raf (RafRBD) to Citrine-labeled HRas upon epidermal growth factor (EGF) stimulus. The relatively short time of thioesterase inhibition ensured that HRas maintained its overall localization at the plasma membrane and Golgi in this experiment. Palmostatin B treatment indeed resulted in EGF-induced transient HRas activity at the plasma membrane, while the HRas pool on the Golgi remained inactive (Figure 17). The activity of HRas on the Golgi thus also critically depends on retrograde transport of active protein from the plasma membrane via the acylation cycle. Ihibition of depalmitoylation results in restriction of HRas activity to the plasma membrane. Palmostatin B uncouples Ras signaling from the plasma membrane from Ras signaling on the Golgi.

Since the completion of this work, the long-duration Ras activation on the Golgi has been confirmed to emanate from ER-based RasGEFs that facilitate its activation. This too, depends on the acylation cycle, as without such a cycle, Ras would not pass through a rapidly mobile state that allows ints interaction with the ER. The results of this work are discussed in detail elsewhere (Lorentzen et al, 2010).

Figure 17

Palm B Incubation, 1 μM, 45 min + EGF

Equivalent DMSO, 45 min + EGF
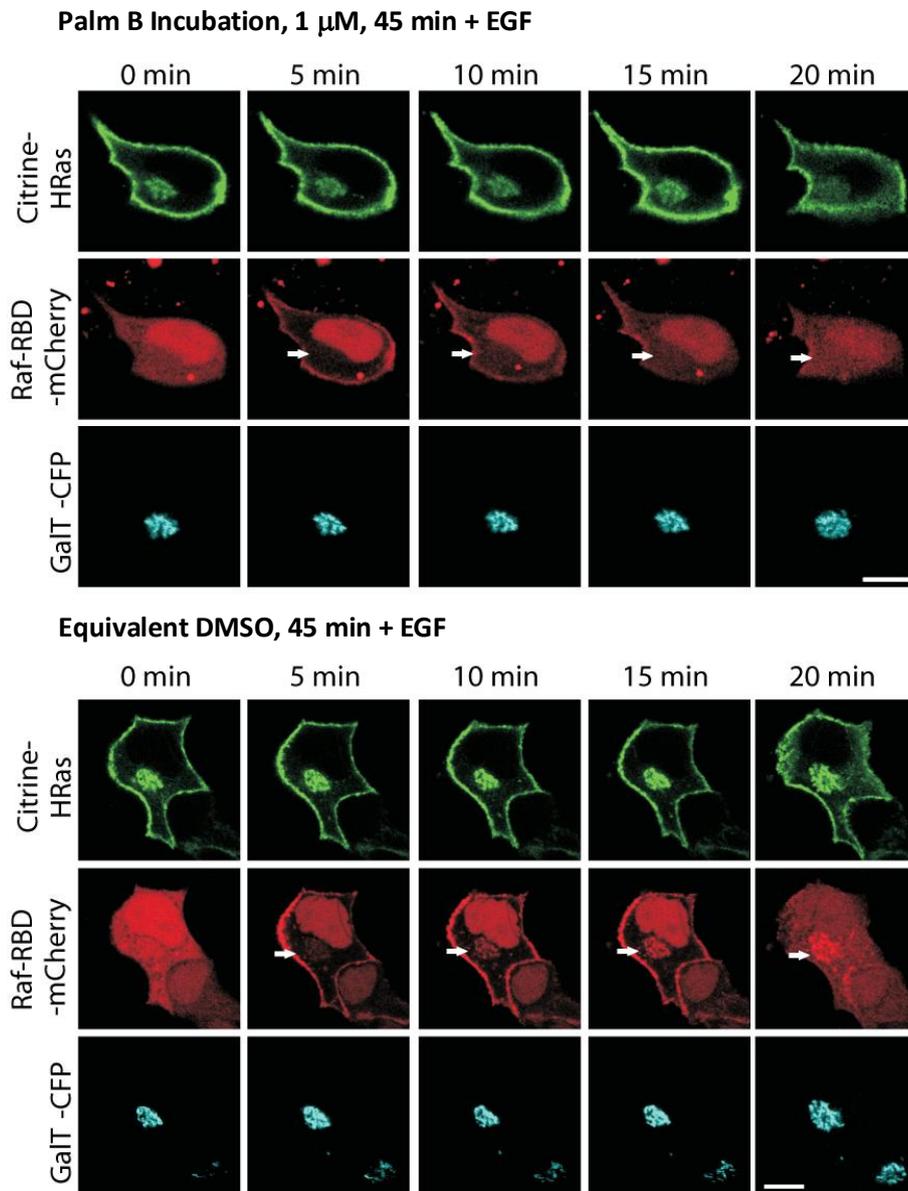
Palmostatin B causes compartment-specific inhibition of Ras activity a, Altered HRas activity profile in Palmostatin B treated cells. Confocal time lapse of EGF-induced membrane translocation of RafRBD-Cherry to Citrine-HRas in MDCK cells co-expressing GalT-CFP in the presence of 1 μM Palmostatin B for 45 min. Scale bar: 10 μm. Arrows indicate absence of activated Citrine-HRas on Golgi as compared to control case. **b,** Representative Control case, showing unperturbed spatial activity profile for HRas after EGF-induction. Arrows indicate accumulation of activated Citrine-HRas on Golgi. Scale bar: 10 μm.

4.6.2 Cellular Phospholipase C-β activity is not inhibited by Palmostatin B

APT1 has been reported to exhibit marginal lysophospholipase activity (Duncan & Gilman, 1998). As such, inhibitors such as Palmostatin B might inhibit phospholipase activities in the cel, with potential implications in signaling and the conclusions of this work. Additionally, Ras may couple into PI3-kinase dependent signaling that depends on phospholipase activities (Yip et al, 2007; Mastrangelo et al, 2000). In order to ascertain that Palmostatin B did not lysophospholipase activites within the cell and that any observed effects downstream of Ras where associated with the Raf-Mek-Erk cascade, the response of Phospholipase C-β activity was tested in MDCK cells. MDCK cells were transfected with Protein Kinase Cα-C1 domain- eGFP fusion protein and mCherry and starved for at least 2 hours prior to experimentation and stimulated with 10 μM Bradykinin (Merck) Bradykinin activates Phospholipase C-β via GPCRs, and results in the formation of diacylglycerol in the plasma membrane. Protein Kinase C (PKC) binds DAG, and is thus recruited to the PM if activation of this signaling pathway occurs. Translocation of the PKCα-C1-GFP to the basal membrane was observed in response to diacylglycerol production (Feng et al, 1998), using TIRF microscope, with and without treatment with Palmostatin B for 1h. No statistical difference could be detected between the PKCα-C1-GFP translocation responses (Figure 18) in either treatment condition, indicating that Palmostatin B does not affect Phospholipase C-β activity. *In vitro* biochemical assays for Phospholipase A, C and D enzymes have confirmed that Palmostatin B does not affect these enzymes (Dekker et al, 2010).

Figure 18
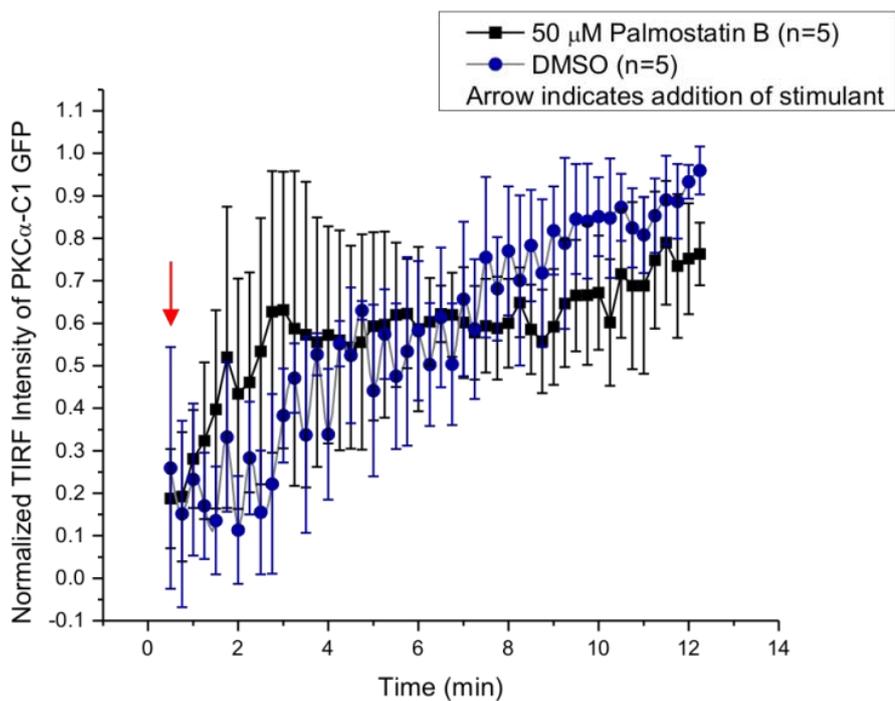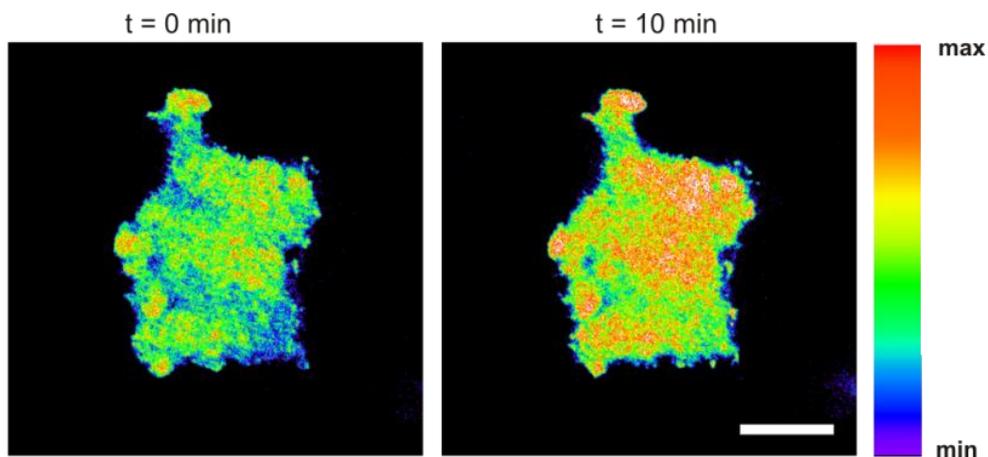
Palmostatin B does not inhibit the activity of Phospholipase C-β. MDCK cells transfected with C1 domain of PKCα tagged with GFP (PKCα-C1-GFP) were incubated with vehicle control (DMSO) or Palmostatin B (50 μM) for 60 minutes. Basal cell membranes were observed by TIRF microscopy following stimulation with bradykinin (10 μM). PKCα-C1-GFP translocates to the basal membrane after diacylglycerol production by activated PLCβ. **a,** Representative cells showing increased PKCα-C1-GFP intensity at the plasma membrane 10 minutes after bradykinin stimulation. Scale bar : 10 μm. **b,** Average response profiles (n=5 for each condition) showing increase in PKCα-C1-GFP intensities after bradykinin stimulation for Palmostatin B treated or control cells.

4.7 Phenotypic effects of modulating the Ras Acylation Cycle

4.7.1 Palmostatin B attenuates oncogenic Ras signaling in transformed MDCK-F3 cells

The subcellular localization of Ras determines its access to effectors that are localized to the PM or to other intracellular organelles. Palmostatin B alters the subcellular localization of both Ras isoforms and has already been shown to alter the characteristic compartmental Ras activation profile. It was therefore of interest to see if Palmostatin B has similar effects on oncogenic Ras signaling.

The effects of Palmostatin B on the HRasG12V-transformed MDCK-F3 cell line were investigated. Upon neoplastic transformation with HRasG12V, MDCK cells undergo an HRas-mediated epithelial-to-mesenchymal phenotype transition (Chen et al, 2010). The resulting MDCK-F3 cells appear spindle-shaped, as opposed to the cuboidal shape of untransformed MDCK cells. The expression of E-cadherin - a epithelial cell specific protein mediated contact inhibition, on the plasma membrane is lost, giving MDCK-F3 cells metastatic invasive characteristics (Onder et al, 2008; Schmidt et al, 2003). Since HRasG12V is a constitutively active from of HRas, the MAPK pathway downstream of Ras in these cells is constantly active, as measured by the phosphorylation of the downstream MAPKs Erk1/2.

Overnight treatment of Citrine HRas transfected MDCK-F3 cells with 50 μM Palmostatin B showed the expected redistribution of HRas. Western blot analysis for Erk phosphorylation showed a marked decrease in the levels of phosphorylated Erk1 and Erk2 over 4h. This Palmostatin B-mediated time-dependant reduction in Erk1/2 phosphorylation correlated significantly well with the time dependency Palmostatin B-induced Ras relocalization indicating that the Ras redistribution effects of Palmostatin B served to uncouple oncogenic Ras from the downstream MAPK cascade (Figure 19, Figure 20B for quantification). In order to confirm that Erk phosphorylation was a result of oncogenic Ras activity, HRasG12V was ectopically expressed in MDCK-F3 cells. As expected, the increased amount of oncogenic Ras caused a significant slowdown of the kinetics of decrease in Erk phosphorylation levels as measured by Western Blot (Figure 19, Figure 20A for quantification).

Concomitantly, Palmostatin B treated MDCK-F3 cells showed a phenotypic reversion to a cuboidal phenotype and growth in an epithelium-like monolayer with well-organized cell-cell contacts and re-establishment of contact inhibition as judged by surface E-cadherin expression that is characteristic for untransformed MDCK cells (Figure 20A). This phenotypic reversion is comparable to that induced by UO126, a potent and specific inhibitor of Mek – another MAPK cascade kinase upstream of Erk.

These phenotypic and Erk phosphorylation effects of Palmostatin B could be subverted by ectopic expression of KRasG12V, and oncogenic by palmitoylation independent isoform mutant of Ras that is localized only to the PM. MDCK-F3 cells transfected with KRasG12V resisted phenotypic reversion as determined by cell-shape, and relative Erk phosphorylation levels we measured to be higher than even those generated by ectopic expression of HRasG12V. The latter observation is likely an effect of the stronger coupling of KRasG12V into the Raf-Mek-Erk cascade, as has been reported previously. Unfortunately, experiments on the effect of KRasG12V expression on E-cadherin expression were not insightful, as KRas is known to have isoform specific effects on E-cadherin expression that are not related to the MAPK cascade (Agbunag & Bar-Sagi, 2004).

Nonetheless, these results show that in MDCK-F3 cells oncogenic HRasG12V induces proliferative Erk1/2 signaling, and that such signaling must occur predominantly from the plasma membrane. Palmostatin B, by the redistribution of HRasG12V to endomembranes, uncouples HRasG12V from the signaling pathway, revealing an avenue for the attenuation of oncogenic Ras signaling in mammalian cells.

Figure 19
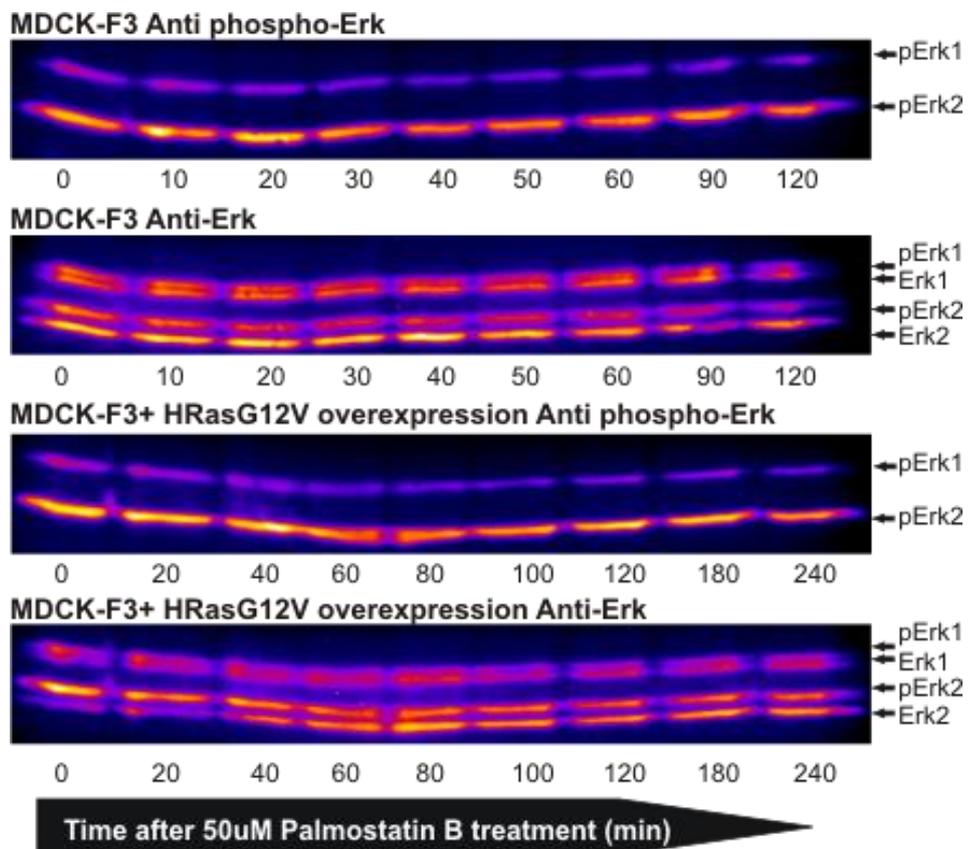
Palmostatin B treatment leads to a reduction in Erk1/2 phosphorylation. Representative Western blots showing reduction in Erk1/2 phosphorylation levels after Palmostatin B treatment as detected by an Erk and phospho-Erk specific antibodies in MDCK-F3 cells. With ectopic expression of HRasG12V in MDCK-F3 cells, attenuation of the Erk phosphorylation signal occurs over a longer time scale. For quantification, see Figure 20B.

Figure 20
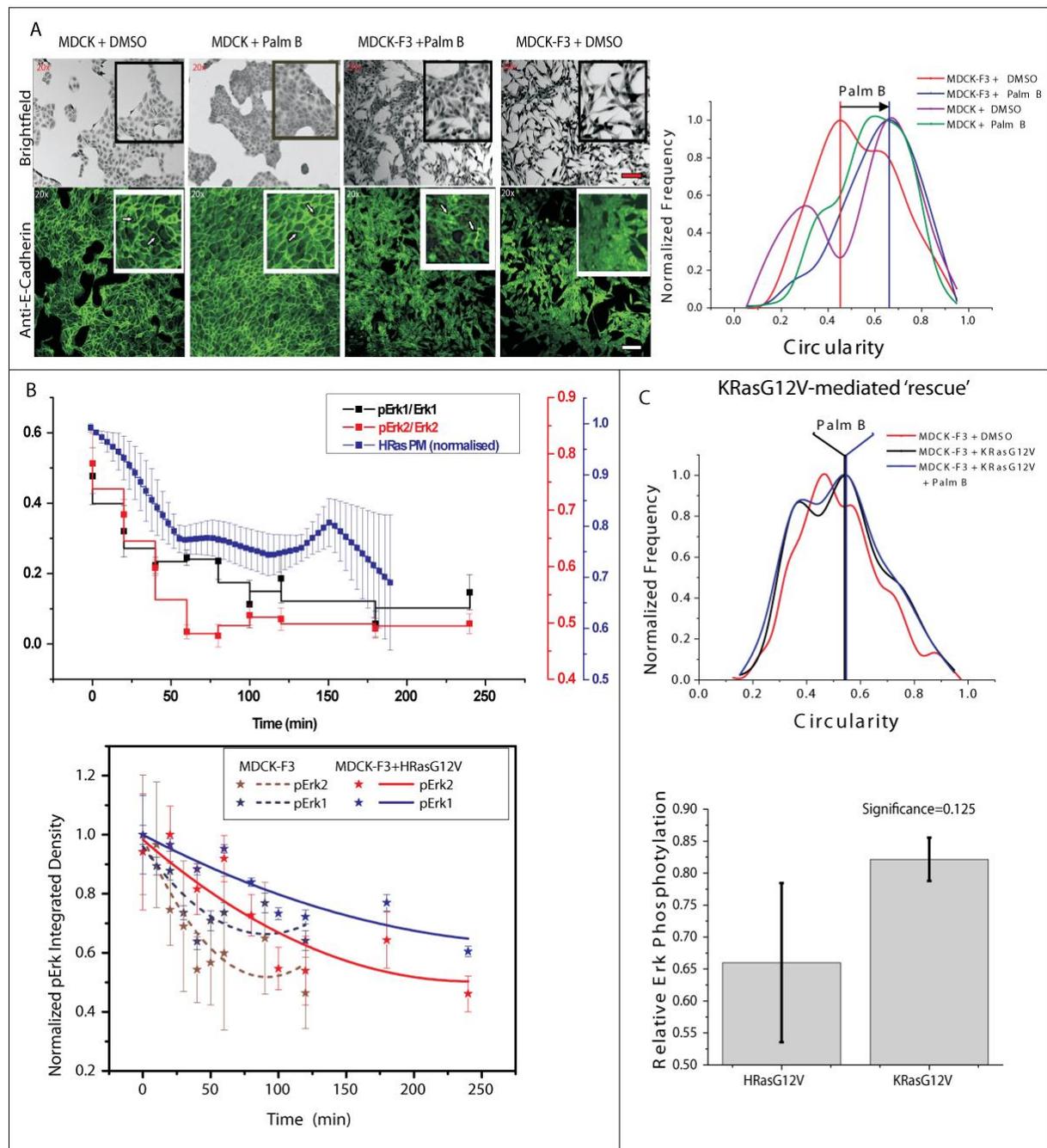
Palmostatin B-induced phenotypic reversion of HRasG12V-transformed MDCK-F3 cells

A, Top-left row: HRasG12V-transformed MDCK-F3 cells show changes in overall cell shape comparable to non-transformed MDCK cells, after overnight treatment with 50 μM Palmostatin B. Bottom-left row: E-cadherin immunostaining of HRasG12V-transformed MDCK-F3 shows restoration of E-cadherin expression at the cell-cell interfaces (arrow-heads) after treatment with 50 μM Palmostatin B. Untransformed MDCK cells treated with Palmostatin B or DMSO (vehicle control) are shown as controls (Supplementary figure 13b). E-cadherin staining at the cell junctions is correlated with contact inhibition [32]. Right panel: cell circularity distribution (n >

400 cells for each case) of HRasG12V-transformed MDCK-F3 cells approaches that of untransformed MDCK cells upon treatment with Palmostatin B. In all cases, 20 μM U0126 treated MDCK-F3 cells serve as positive control for phenotypic reversion (Supplementary figure 13b), while DMSO treated MDCK-F3 cells serve as negative control. Scale bars represent 20μm. **B,** Upper panel : Correlation of Citrine-HRas intensity on PM as detected by live cell imaging (n=7) and Erk activity as detected by densitometric quantification of fraction of phospho-Erk1/2 from gel-shift with Western blots (n=3). Pearson's correlation for HRas PM-fraction (blue) and pErk1 fraction (black): 0.83 (p=0.006), or pErk2 fraction (red): 0.75 (p=0.021). Lower Panel: MDCK-F3 cells as well as MDCK-F3 cells overexpressing Citrine-HRasG12V (Upper and Lower panels respectively) show significant reduction in Erk1/2 phosphorylation, on different time scales, after Palmostatin B treatment. Lines represent trend lines from a parabolic fit for comparison. **C.** KRasG12V mediated rescue of transformed phenotype in Palmostatin B treated cells. Upper panel: circularity distributions (n > 400 cells for each case) of MDCK-F3 cells transfected with KRasG12V did not change significantly upon treatment with Palmostatin B. Lower panel: Relative Erk phosphorylation in HRasG12V and KRasG12V transfected MDCK-F3 cells treated for 100 min with 50 μM Palmostatin B show enhanced Erk phosphorylation in KRasG12V transfected cells (p=0.125, Mann-Whitney-Wilcoxon test).

5 DISCUSSION

5.1 The Acylation Cycle as a General Spatial Pattern Generator

This work started with a description of spatial pattern generators. The simplest spatial cycles of mobile entities originate due to their interactions with substantially slower supramolecular structures(Benson et al, 1993; Benson et al, 1998; Dillon et al, 1994; MAINI et al, 1992). Cellular organelles constituted of membranes, the cytoskeleton and other relatively immobile features, while being dynamic, have a steady state presence that facilitates spatial cycles of relatively rapidly moving molecules that may interact with them. Spatial cycles may therefore be confined to specific locales in the cell, or spread across the cellscape depending on the molecules and physiochemical nature of the supramolecular structures. The interaction between mobile entities and semi-static structures need not be direct, but may be mediated by intervening molecular players.

The net effect is the utilization of free energy to generate a kinetically maintained steady state (De Kepper et al, 1990) that entails an inhomogeneous distribution of molecules in the volume of a cell. The abundance of molecular transport processes, in combination with a ready supply of energy and the specific localization of such activities in biological systems, provides a pre-existing framework for the formation of spatial cycles.

The acylation cycle can be understood as a reaction-diffusion spatial pattern generator, with invididual palmitoylatable protein molecules as the discrete players. As is shown in this work, monolipidated and permanently palmitoylated proteins tend to spread throughout the cell volume, staining endomembranes aspecifically simply due to their affinity towards hydrophobic environments. Their mobility is affected by the strength of this affinity. Reversible S-palmitoylation causes this affinity to membranes to shift between a relatively 'strong' and 'weak' form. However, the locations in the cell where such switching occurs are spatially separated. More specifically, the Golgi apparatus is the site of palmitoylation where low-membrane affinity, rapidly-diffusing monolipidated proteins are palmitoylated and converted to a high-membrane affinity, slow-moving form in the first stage of the acylation cycle. In the second stage, vesicular transport via the secretory pathway transfers these

kinetically trapped palmitoylated proteins to the PM. The unidirectionality of the secretory pathway provides the vectorial component driving the cycle. However, cellular membranes such as the PM are dynamic structures themselves and such proteins would eventually leak, either by membrane fusions or slow diffusion. In general, these homogenizing effects can be attributed to simple entropy. In cells, before such entropic loss of localization leads to complete homogenization, cytoplasm wide thioesterase activities depalmitoylates proteins returning them to their rapidly mobile form. Such proteins now have a high probability of stochastically encountering the Golgi apparatus, where they can be repalmitoylated, thus completing a single turn of the Acylation Cycle. The spatial asymmetry in the location of palmitoylation and depalmitoylation activities , and the unidirectionality of the secretory pathway is thus manifested in the more elaborate dynamic steady-state localization of palmitoylated proteins.
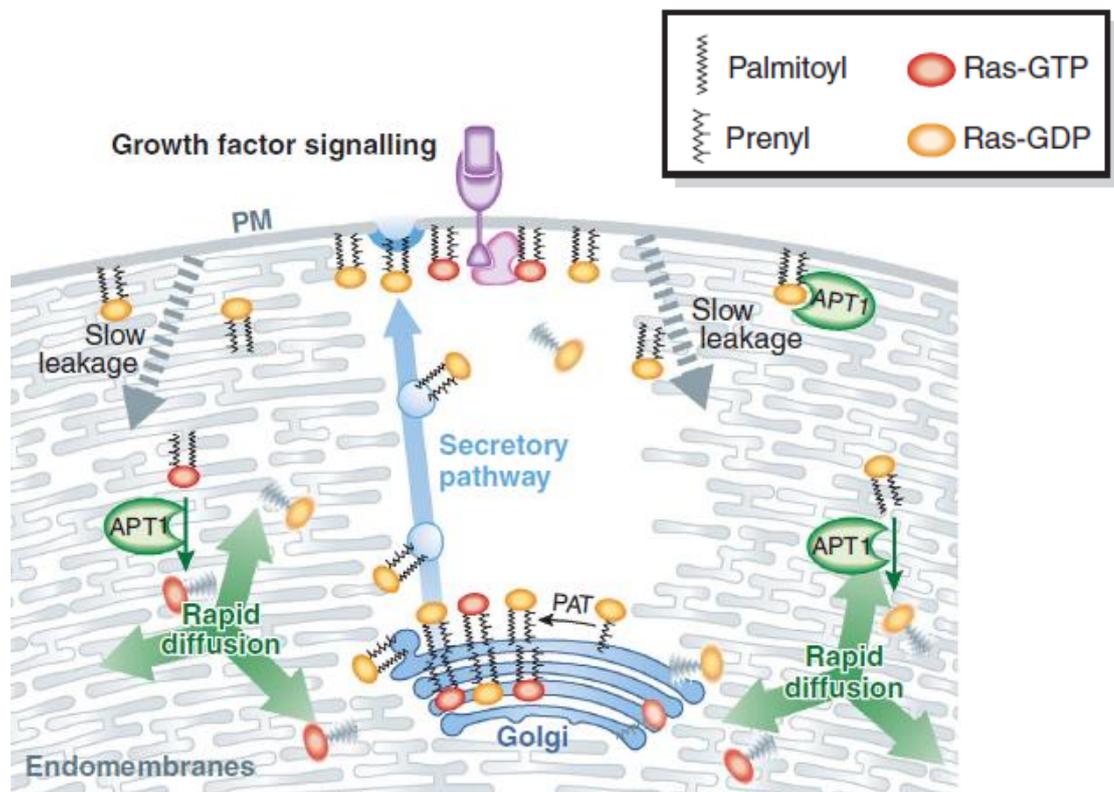
Schematic Representation of the Acylation Cycle and the generation of spatial distribution of Ras proteins.

This mechanistic explanation of the Acylation cycle also explains why inhibition of APT1 by Palmostatin B leads to a homogenous redistribution of palmitoylated Ras that is indistinguishable from that of unpalmitoylated Ras. **The role of the acylation cycle is to counter entropy: the tendency of lipidated proteins to populate all accessible membranes.** Interrupting the acylation cycle leads to an entropy-driven, aspecific spread of Ras molecules throughout the cellular environment. It is worth noting that such a system does not involve receptors on membrane compartments that recognize lipidation states of molecules.

All entropy-countering processes, the acylation cycle must require enthalpic input. For the acylation cycle, energetic contributions are represented by the energy required to palmitoylate proteins. The acyl-donor in the reaction palmitoyl-CoA, is biochemically equivalent to the energy of 2 ATP molecules. Further, the energy expended in the transport of vesicles in the secretory pathway is also what drives the acylation cycle – representing an elegant optimization of energy efficiency in a process that has several other functions than to transport palmitoylated proteins.

5.2 On Palmitoyltransferases and Thioesterases

Palmitoyltransferase (PAT) activity that has been attributed to the zDHHC proteins in yeast and mammalian (Fukata et al, 2004; Bartels et al, 1999; Bijlmakers & Marsh, 2003; Goytain et al, 2008; Iwanaga et al, 2009; Matakatsu & Blair, 2008) systems remains a controversial issue. In this work, we could not detect any local or global substrate specificity for the palmitoylation reaction. (Fukata et al, 2004; Bartels et al, 1999; Bijlmakers & Marsh, 2003; Goytain et al, 2008; Iwanaga et al, 2009; Matakatsu & Blair, 2008). The spontaneous occurrence of the palmitoylation reaction *in* vitro casts even more doubt on the requirement of enzymes to facilitate it in the reducing cellular environment. However, at least for the DHHC proteins claimed to be RasPATs, a consensus sequence could be identified that allows them to be grouped together in cladal analysis and idenitifies the same proteins in a wide variety of mammalian genomes. What the function of this particular

conserved sequence might be remains to be clarified, despite its localization that appears proximal to the DHHC-CRD domain in 3D. It has been reported earlier that the DHHC proteins contain phosphorylatable Tyrosine residues C-terminal of the DHHC-CRD domain. It is tempting to speculate that the conflicts in understanding arise from a failure to take into account the phosphorylation state of DHHC proteins in *in vitro* experiments.

It seems plain that if at all the DHHC proteins are palmitoyltransferases, they are certainly not conventional enzymes. Whatever the identity of the PAT activity, it is clear that the relevant palmitoylation reaction is confined to the cytoplasmic face of the Golgi apparatus . The strict localization of this activity could be due to high concentrations of the acyl-donor palmitoyl-CoA in the Golgi apparatus, though no evidence exists for it. Palmitoyl-CoA was intuitively identified as the acyl donor in the S-palmitoylation reaction by analogy to the fatty-acid biosynthesis pathway. One could extend the analogy further, and deem the DHHC proteins simply palmitate carriers - similar to the Acyl Carrier Protein (ACP) and Condensing Enzyme, which are part of the Fatty Acid Synthase complex (Toomey & Wakil, 1966). ACP and the Condensing enzyme both contain acylated sulfhydryls as part of cofactors or Cysteine residues respectively, and serve to 'hold' the growing acyl chain while it is extended by other enzymatic activities. Eventually, the ACP transfers the completed Acyl chain to Coenzyme A, generating palmitoyl-CoA. S-palmitoylation of proteins could be thought of the same biochemical reaction in reverse, where Golgi-localized DHHC proteins function as the palmitate carriers that sequester activated palmitate groups to the Golgi through reaction with CoA. These palmitate thioesters can then be easily exchanged with other proximal Cysteine residues (on other proteins), as the thioester bond is rather labile. In other words, we hypothesize that DHHC proteins do not catalyze palmitoylation, but simply enhance the local palmitate thioester concentration. Indeed, it has been reported that the Cys residue in DHHC proteins is itself palmitoylated, and that certain DHHC proteins display 'auto-palmitoylation' activity.

Such a mechanism would facilitate the acylation cycle at the Golgi via two modes : (1) Since DHHC proteins are transmembrane and Golgi localized, interactions of monolipidated proteins with weak membrane affinity such Ras with DHHC proteins are far more likely than

with a freely-diffusing small molecule like Palmitoyl-CoA. (2) By localizing palmitoylation activity at the Golgi, such a mechanism allows for a dynamic acylation cycle to generate spatial asymmetry. If palmitoylation and depalmitoylation occurred everywhere within the cytoplasm, the futile cycle would now allow enrichment of such proteins on the PM or Golgi apparatus.

Clearly, DHHC proteins represent a large family of 25 proteins in mammals as compared with <10 in yeast and Dictyostelium. Teleogical argumentation suggests that amplification of the protein family would not occur without a beneficial function to these proteins. Substantial work is needed before the details of the functions of DHHC proteins , and their contribution to the acylation cycle can be fully ascertained.

In order for the acylation cycle to function, depalmitoylation activity must be spread throughout the cytoplasm of the cell. Indeed, acyl protein thioesterase-1 (APT1), a protein now shown to depalmitoylate Ras in this work is present ubiquitously in the cytosol(Hirano et al, 2009b). Incidentally, APT1 and its close homolog APT2 are the only two candidates that may mediate such a depalmitoylation reaction, and are seen to be rather promiscuous in their substrate specificity for the peptide chain as well as for the acyl-chain. This promiscuity is expected, considering that several other proteins besides Ras undergo a similar acylation cycle, but there do not seem to be any other soluble thioesterases in the cytosol. Studies on the X-Ray crystal structure of APT1 have shown APT1 to be a dimer, with large open tubular pockets for binding the acyl-chain. A closely related enzyme APT-like 2 (LYPLAL3) does not possess this acyl-binding pocket and fails to show acyl-protein thioesterase activity. The promiscuity of APT1 therefore stems from the fact that the enzyme recognizes the acyl chain as its substrate rather than the protein the acyl-chain is attached to.

It is however unclear how a cytoplasmic thioesterase gains access to a palmitate group which is embedded into a membrane. Recent work (Ahearn et al, 2011) has shown that at least for HRas, FKBP-catalyzed isomerization of a proline residue in the hypervariable region facilitates its depalmitoylation. The isomerization of proline residues is known to cause conformational changes in the protein. It is possible such mechanisms allow APT1 access to

the attached palmitate group on other proteins as well, and open the door on potential regulatory mechanisms for depalmitoylation.

5.3 Potency of Acylation Cycle perturbations to inhibit Ras Signaling

Spatial cycles occur in the background of signaling events involved in the sustenance of living systems. In recent years, mechanistic analyses of signaling have revealed non-linear phenomena such as bistability(Narula et al, 2010; Sabouri-Ghomi et al, 2008; To & Maheshri, 2010; Kulkarni et al, 2010; Ferrell Jr., 2009; Xiong & Ferrell, 2003; Angeli et al, 2004), temporal dynamics and hysteresis(Takahashi et al, 2010; Kramer & Fussenegger, 2005; Weichsel & Schwarz, 2010; Kholodenko et al, 2010), all of which are found to be critical to the relevant cellular process or structure. While molecular interactions and network topologies explain some aspects of these phenomena, models describing signaling must implicitly include assumptions relating to reaction-diffusion, compartmentalization and other geo-structural features of the cell, such as spatial cycling.

Like all G-Proteins, Ras proteins also have a GTP/GDP cycle and are activated in response to a variety of stimuli: the most commonly studied being growth factor signaling. Transport to the plasma membrane (PM), PM enrichment, rapid diffusion and trapping at the Golgi are all features of the Ras spatial cycle which convolute with its activation mechanisms, conferring it with unique signal propagation characteristics. For example, the canonical RasGEF Son of Sevenless (SOS) requires Ras to be membrane tethered before it can be activated(Freedman et al, 2006). Additionally, SOS contains binding domains towards adapter proteins such as Grb2 that bind to activated receptor tyrosine kinases(Jang et al, 2010) via phosphotyrosines and towards plasma membrane lipids such as phosphatidic acid(Zhao et al, 2007) and phosphatidylinositol. Combined, these specificities indicate that SOS almost exclusively activates Ras at the plasma membrane(Innocenti et al, 2002). The localized activation of Ras is further amplified due to a positive feedback mediated by the allosteric activation of SOS by Ras-GTP, and to some extent due to further membrane recruitment of SOS by Ras. For example, dampening effects on the MAPK response due to

abolished allosteric binding in SOS mutants have been shown to be rescued by independent membrane targeting of such SOS mutants through recombination with the Ras C-terminus, subjecting them to the same acylation cycle as Ras. These experiments highlight the role the acylation cycle plays in the generation of robust Ras activation on the plasma membrane. Ras activity on the plasma membrane, however, is transient despite the amplifying effects of the positive feedback on SOS. The adaptive response of Ras activity on the plasma membrane may be attributed to several factors such as recruitment of RasGAPs(Ding & Lengyel, 2008; Smida et al, 2007), internalization of the growth factor receptor over longer time scales(Goh et al, 2010), or negative feedback on SOS via its phosphorylation by Erk(Chen§ et al, 1996; Waters et al, 1995). On short time scales, the acylation cycle exerts a modulatory effect. Since Ras is constantly being depalmitoylated and thus diffuses away, its total concentration on the plasma membrane is maintained at a certain steady-state level, while allowing the spread of active Ras in other regions of the cell (Harvey et al, 2008). Such a system clearly contributes to the non-linear MAPK response characteristics observed upon stimulation with different growth factors in living cells (Santos et al, 2007).

Consider the case of the dominant oncogenic RasG12V mutants: The presence of feedbacks such as the one mentioned above means constitutively active Ras will tend to activate the normal wild type Ras present in these cells, explaining why such mutations are dominant. Thus, even if the gene dosage of oncogenic Ras is 50%, the protein activity level of Ras is far higher. The presence of the constitutively active G12V mutation in a single allele of a Ras gene can catapult the MAPK cascade into a permanent 'on' state due to positive feedbacks that activate even the wild type (wt) Ras expressed from the other allele. The 'gain-of-function' mutant Ras generates an offset in the Ras dose-response relationship that might trigger full activation of the wt Ras dependent on its expression level. By down-modulating the amount of mutant Ras that can effectively couple into effectors, the feedback strength is weakened thereby putting the system into a regime with only partially activated Ras and a phenotype that still has regulated growth factor responses. Inhibition of constitutively active signaling on the level of Ras is extremely challenging, as is evidenced by the complete lack of any known Ras inhibitors. Therefore, the Ras spatial cycle is a lucrative target for the modulation of oncogenic Ras signaling. Palmostatin B treatment of untransformed MDCK

cells shows no apparent toxicity or morphological changes. It should be noted that while oncogenic Ras redistributes over all membranes after Palmostatin B treatment, it is still GTP-loaded. It is, however, unable to effectively couple into the downstream MAPK cascade indicating that oncogenic MAPK signaling originates primarily from the oncogenic factors on the plasma membrane (Matallanas et al, 2006). The fact that several oncogenic proteins reside on the plasma membrane seems to corroborate this hypothesis. The author believes that the effects on MAPK signaling and dramatic phenotypic reversion described in this work are likely to stem from attenuation of the positive feedbacks of the sort Ras and SOS-like GEFs, rather than the obvious decrease of Ras partitioning onto the PM.

In addition to these processes, phenomena such as activity-dependent clustering of Ras proteins in the plasma membrane(Tian et al, 2007), or specific partitioning to lipid rafts(Prior et al, 2001) add an additional layer of spatial complexity to Ras signaling dynamics.

In the context of Ras effectors that are not located on the plasma membrane, the dynamic cycling of Ras molecules allows for a 'clutch and gear' framework, where activity is transmitted via the energy used to maintain the spatial cycle. Transmission of Ras-signals after growth factor activation to different cellular locations can occur by the generation of an activated Ras pulse into the pre-existing spatially cycling population. The acylation cycle allows the rapid diffusion of activated Ras throughout the cytoplasm until it is enriched at the Golgi via (re-)palmitoylation, enabling access to effectors spread throughout the cytoplasm. Since Golgi encounters are stochastic, the pulse-like Ras activation response at the plasma membrane is widened at the Golgi, while its amplitude is reduced (Peyker et al, 2010). Ras effectors such as RIG1(Tsai et al, 2007) and MAPK scaffolds such as Sef and BIT1(Philips, 2004; Yi et al, 2010), which are restricted to the ER or Golgi complex, teliologically imply a function for Ras mediated signaling on these cellular compartments. The precise nature of this signaling remains open for study but multiple lines of evidence indicate that phenotypic effects on cells require Ras activation on specific cellular compartments(Chiu et al, 2002; Inder et al, 2008). In the context of the acylation cycle there

is little doubt that effectors on internal membranes experience a Ras temporal activation profile that is substantially different from that seen by effectors on the plasma membrane.

5.4 Modulation of spatial cycles in potential therapeutic applications

Conventional cancer drug therapy in particular depends either on inactivation of hyper-activated molecules, as is seen in the case of inhibitors of tyrosine kinases(Klohs et al, 1997) or, at the other extreme, on essentially harnessing a pleiotropic effect to cause apoptotic death, as is the case with cytoskeleton targeting drugs(Calligaris et al, 2010). The manipulation of spatial cycles to alter signaling presents an exciting opportunity to control cellular dynamics in a rational manner. While the approach is not devoid of pleiotropic phenomena, the fact that the intended target molecule is far removed in the interaction network from the site of drug action allows for fine-tuning of the inhibition to reduce oncogenic signaling below a certain threshold level. Since spatial cycles work in tandem with activation cycles of proteins, and exert an indirect effect, they present the opportunity for finer control of signaling activities at the expense of sensitivity - the so-called 'Hormetic dose-response' (Scott, 2004; Calabrese & Baldwin, 2003; Preston, 2005). In particular contexts, where basal activities of signaling molecules are essential for cell survival, as is often the case for neurological and oncogenic diseases, the manipulation of spatial cycles provides a gentler approach in manipulating cellular signaling network states.

The intimate relationships between spatial cycles of G-Proteins and their activity in signaling networks reveals an avenue for signaling response manipulation by altering the steady state localization of such molecules. Strategies to interfere with pathological cellular signaling have focused largely on inhibition of hyperactive signaling pathways. However, since conserved cellular signaling modules like the MAPK cascade are utilized for the transmission of multiple signaling cues to various effectors(Chavel et al, 2010; Roberts et al, 2000), complete inhibition of signaling leads to several undesirable effects due to the acute perturbation of important branches of a signaling network. For example, the potent Mek inhibitor UO126 effectively terminates downstream MAPK signaling, but results in

widespread toxicity (Cheng & Force, 2010; Finegan et al, 2009) due to the collateral inhibition of survival signaling. Modulation of spatial cycles however as described in this work, may allow leveraging of non-linear signaling responses to nudge signaling networks into a desirable parameter regime (Gomez-Uribe et al, 2007), in order to selectively attenuate pathological phenotypic effects on the cell.

5.6 Future Directions

The perturbation of spatial cycles for manipulating cellular processes may be expanded beyond Ras proteins. The ensemble of proteins displaying spatial cycling is large. Heterotrimeric G-proteins, most Src family kinases, secreted enzymes, signaling molecules such as Sonic Hedgehog, the Huntington protein, several proteins involved in synaptic trafficking display the Ras-like palmitoylation based spatial cycle. Transmembrane receptors have spatial cycles based on endocytic sorting. Arf-GTPases that modulate ER-Golgi traffic seem to have spatial cycles akin, and the Rab proteins which regulate vesicular transport are reported to have spatial cycles relying on GDI proteins to convert them to a high-mobility soluble state, although spatiotemporal dynamics are not well understood. Rho, Rac and Cdc42 GTPases have activity gradients and GDI proteins akin to Rab whose effects have been discussed elsewhere (Rajnicek et al, 2006). Indications are that KRas itself is targeted dynamically, based on a spatial cycle that counters its entropic mislocalization. The effect of cellular size and shape has been theoretically postulated to have a substantial effect on signaling activities due to the relative scale of activity gradients and cycles and their respective temporal properties (Meyers et al, 2006). The modulation of the activities of these proteins has implications in oncogenesis, development, neuropathology, immune responses and possibly on several biological phenomena that remain to be discovered. As probing and detection methods have improved over the last ten years in their temporal and spatial resolution, at the same time becoming more and more non-invasive, empirical observation of spatial cycles of proteins in living cells has become more accessible. Small molecule inhibitors such as Palmostatin B have the potential to effect minute non-toxic modifications on protein activities, simply because they do not involve dramatic inhibition

or activation, but a finely resolved manipulation of protein activities. Efforts to develop such small molecules will provide iterative growth in the understanding of the dynamics of living systems, with simultaneous therapeutic promises.

The development of high-throughput adaptations of advanced microscopy techniques (Grecco et al, 2010) , coupled with similar high-throughput detection of signaling activities and networks(Olsen et al, 2010), along with progress in the mathematical modeling of cellular processes (Bressloff, 2006) sets the stage for the exploitation of spatial cycles in tinkering with biology.

SUMMARY

This work combines advanced microscopy methods with chemical biology techniques, conventional biochemistry and molecular biology, to elucidate the players and role of the acylation cycle in generating spatial patterning of proteins and its effect of Ras-mediated cellular signaling.

Monolipidated peripheral-membrane proteins were shown to have rapid mobility within the cell by measuring fluorescence loss after photo-activation of paGFP-fusions of a myristoylated or a prenylated protein. Confocal imaging showed that mono-lipidated proteins display aspecific weak affinity to all cellular membranes, reflecting only membrane density within the cell without specific enrichment. Total internal fluorescence imaging showed that monolipidated proteins also have access to the plasma membrane, without significant enrichment. Palmitoylation of these proteins must therefore significantly contribute to the hydrophobicity of these proteins and thus increase membrane affinity.

The acylation cycle was shown to be a spatial reaction-diffusion cycle of peripheral membrane proteins that consists of (1) S-palmitoylation at the Golgi apparatus with a concomitant increase in membrane affinity, (2) vesicular transport of high-membrane affinity species to the plasma membrane (3) Ubiquitous depalmitoylation and (4) Rapid diffusion until stochastic encounter of the Golgi apparatus, leading to re-palmitoylation. Each of these processes is summarized below.

Palmitoylation is known to occur at the Golgi apparatus from previous studies involving the microinjection of semi-synthetic palmitoylation substrates. The DHHC-proteins reported to be facilitating this S-palmitoylation, i.e., palmitoyl transferases (PATs) were shown to have broad specificity, if any at all. A consensus sequence for previously reported so-called Ras-specific PATs was identified using Hidden Markov Models, but Ras palmitoylation activity was demonstrated in Dictyostelium discoideum, an organism lacking any of the so-called Ras-specific PATs. Any specificity reported previously is therefore likely to be a feature of the experimental procedure followed or an underlying effect of unknown functions of these DHHC proteins not related to palmitoylation. Further, it was shown that steady state

distribution of Ras depends solely on the number and position of palmitoylation events and the Ras G-domain does not affect the spatial distribution of Ras within the cell through ratiometric imaging of full-length and truncated Ras proteins.

The steady state distribution of some peripheral palmitoylated proteins such as Fyn maybe affected by distal regions on the proteins, unlike in the case of Ras. However, a secretory pathway block through cooling induced a clear retardation of these proteins on the Golgi apparatus, indicating that they follow a similar acylation cycle, irrespective of their wild-type localization. It is apparent that their localization is either different due to additional factors specific to those proteins overlaying the acylation cycle, or that their steady state partitioning over membranes is only quantitatively but not qualitatively different from that generated by the acylation cycle.

APT1 was identified as a cellular thioesterase that depalmitoylates Ras in vivo. APT1 expression was confirmed to be cytosolic, in line with the requirement of ubiquitous depalmitoylation according the model of the acylation cycle shown above.

Palmostatin B, a newly developed inhibitor of APT1 was shown bind APT1 directly through Fluorescence Lifetime Imaging (a FRET assay) of GFP-APT1 fusions and Rhodamine-labeled versions of the inhibitor. Palmostatin B blocks depalmitoylation activity and was shown to increase the steady state fraction of palmitoylated protein through biochemical measurement with the acyl-biotin exchange assay.

Confocal time-lapse microscopy after treatment with Palmostatin B led to redistribution of N-Ras localization, counter-intuitively leading to aspecific distribution over all membranes on longer time scales, that was indistinguishable from that of solely prenylated Ras, However, FRAP studies showed that this redistributed species has high-membrane affinity and is not rapidly mobile like solely prenylated Ras. The redistribution is attributed simply to entropy - slow leakage from the membrane, and membrane fusion events themselves, leading to a mislocalization of Ras over time. The mislocalized Ras, however, being still in its palmitoylated high-membrane affinity form, is effectively trapped aspecifically on all membranes, in the absence of thioesterase activity.

Removal of thioesterase inhibition led to a recovery of the usual steady-state distribution of NRas. The depalmitoylation activity of APT1 thus provides a reset mechanism in the acylation cycle that allows mislocalized palmitoylated proteins to regain rapid mobility and encounter the Golgi apparatus, with palmitoylation and vesicular transport restoring the specific enrichment on the Golgi apparatus and plasma membrane.

The acylation cycle determines the amount and residence time of Ras proteins on the plasma membrane. Since growth factor mediated signaling occurs via receptors on the plasma membrane, the acylation cycle affects the probability that Ras molecules are available for participation in the MAPK signaling cascade through their GTPase cycle. Treatment with inhibitors such as Palmostatin B, which lead to an effective trapping of Ras molecules away from the plasma membrane, causes an attenuation of MAPK signaling output as measured by phosphorylation of the downstream kinases ERK1/2, which is activated in response to EGF signaling.

As a logical step, the inhibitor Palmostatin B was applied to oncogenic Ras-transformed MDCK-F3 cells, which exhibit loss of contact inhibition, invasiveness and a mesenchymal-like phenotype compared to untransformed MDCK cells which are contact inhibited, display growth in islands and have an epithelial phenotype. Overnight Palmostatin B treatment caused a phenotypic reversion of MDCK-F3 to epithelial-like phenotype, as measured with cell shape determination and restoration of E-cadherin expression on the plasma membrane (the absence of which is a diagnostic marker of metastatic tumors). The phenotypic reversion caused by Palmostatin B could be blocked in cells transformed with KRas-G12V, an oncogenic but acylation-cycle-independent version of Ras.

It was noted however that Palmostatin B displayed no toxicity towards MDCK cells for the duration of the experiment at the concentrations used. Thus, the phenotypic reversion was an effect of the interruption of the acylation cycle, which attenuated oncogenic Ras signaling in transformed cells down to levels sufficient for reversion to an untransformed-like phenotype. The attenuation was subtle enough, however, to not block survival signals, which also are Ras-mediated.

In conclusion, this work describes the generation of spatially asymmetric protein distributions within the cell through a general reaction-diffusion mechanism. The acylation cycle depends on a localized conversion of proteins to a high-membrane affinity form, directional transport, and ubiquitous return to a low-affinity form. Functionally, the acylation cycle counters the effect of entropy in the distribution of proteins. In the case of Ras proteins, the acylation cycle convolutes with their GTPase cycle and modulates cellular MAPK signaling. It was possible to attenuate MAPK signaling by interrupting the acylation cycle without causing toxicity, providing a therapeutic avenue where cellular signaling can be manipulated beneficially while avoiding deleterious effects.

REFERENCES

Agbunag C & Bar-Sagi D (2004) Oncogenic K-ras Drives Cell Cycle Progression and Phenotypic Conversion of Primary Pancreatic Duct Epithelial Cells. *Cancer Res* **64:** 5659-5663 Available at: [Accessed November 25, 2008]

Ahearn IM, Tsai FD, Court H, Zhou M, Jennings BC, Ahmed M, Fehrenbacher N, Linder ME & Philips MR (2011) FKBP12 Binds to Acylated H-Ras and Promotes Depalmitoylation. *Molecular Cell* **41:** 173-185 Available at: [Accessed 10:43:09]

Alberts AW, Majerus PW & Vagelos PR (1965) Acyl Carrier Protein. VI. Purification and Properties of β-Ketoacyl Acyl Carrier Protein Synthetase*. *Biochemistry* **4:** 2265-2274 Available at: [Accessed March 14, 2011]

Angeli D, Ferrell JE & Sontag ED (2004) Detection of multistability, bifurcations, and hysteresis in a large class of biological positive-feedback systems. *Proc Natl Acad Sci U S A* **101:** 1822-1827

Antonarakis S & Van Aelst L (1998) Mind the GAP, Rho, Rab and GDI. *Nat Genet* **19:** 106-108 Available at: [Accessed March 30, 2010]

Apolloni A, Prior IA, Lindsay M, Parton RG & Hancock JF (2000) H-ras but Not K-ras Traffics to the Plasma Membrane through the Exocytic Pathway. *Mol. Cell. Biol.* **20:** 2475-2487 Available at: [Accessed June 2, 2010]

Arredondo J, Chernyavsky AI, Jolkovsky DL, Pinkerton KE & Grando SA (2006) Receptor-mediated tobacco toxicity: cooperation of the Ras/Raf-1/MEK1/ERK and JAK-2/STAT-3 pathways downstream of α7 nicotinic receptor in oral keratinocytes. *The FASEB Journal* **20:** 2093 -2101 Available at: [Accessed March 14, 2011]

Baker TL, Booden MA & Buss JE (2000) S-Nitrosocysteine Increases Palmitate Turnover on Ha-Ras in NIH 3T3 Cells. *Journal of Biological Chemistry* **275:** 22037 -22047 Available at: [Accessed March 14, 2011]

Bartels DJ, Mitchell DA, Dong X & Deschenes RJ (1999) Erf2, a Novel Gene Product That Affects the Localization and Palmitoylation of Ras2 in Saccharomyces cerevisiae. *Mol. Cell. Biol.* **19:** 6775-6787 Available at: [Accessed June 2, 2010]

Benson DL, Maini PK & Sherratt JA (1993) Analysis of pattern formation in reaction diffusion models with spatially inhomogenous diffusion coefficients. *Mathematical and Computer Modelling* **17:** 29-34 Available at: [Accessed June 2, 2010]

Benson DL, Maini PK & Sherratt JA (1998) Unravelling the Turing bifurcation using spatially varying diffusion coefficients. *Journal of Mathematical Biology* **37:** 381-417 Available at: [Accessed June 2, 2010]

Bijlmakers M-J & Marsh M (2003) The on–off story of protein palmitoylation. *Trends in Cell Biology* **13:** 32-42 Available at: [Accessed February 4, 2009]

Bivona TG, Quatela SE, Bodemann BO, Ahearn IM, Soskis MJ, Mor A, Miura J, Wiener HH, Wright L & Saba SG (2006) PKC Regulates a Farnesyl-Electrostatic Switch on K-Ras that Promotes its Association with Bcl-Xl on Mitochondria and Induces Apoptosis. *Molecular Cell* **21:** 481-493 Available at: [Accessed June 2, 2010]

Bizzozero OA, McGarry JF & Lees MB (1987a) Autoacylation of myelin proteolipid protein with acyl coenzyme A. *Journal of Biological Chemistry* **262:** 13550-13557 Available at: [Accessed March 14, 2011]

Bizzozero OA, McGarry JF & Lees MB (1987b) Acylation of endogenous myelin proteolipid protein with different acyl-CoAs. *Journal of Biological Chemistry* **262:** 2138-2145 Available at: [Accessed March 14, 2011]

Bourne HR, Sanders DA & McCormick F (1991) The GTPase superfamily: conserved structure and molecular mechanism. *Nature* **349:** 117-127 Available at: [Accessed June 2, 2010]

Bressloff PC (2006) Stochastic model of protein receptor trafficking prior to synaptogenesis. *Phys Rev E Stat Nonlin Soft Matter Phys* **74:** 031910 Available at: [Accessed June 2, 2010]

Brunet A, Roux D, Lenormand P, Dowd S, Keyse S & Pouysségur J (1999) Nuclear translocation of p42/p44 mitogen-activated protein kinase is required for growth factor-induced gene expression and cell cycle entry. *EMBO J* **18:** 664-674 Available at: [Accessed March 14, 2011]

Buglino JA & Resh MD (2008) Hhat Is a Palmitoylacyltransferase with Specificity for N-Palmitoylation of Sonic Hedgehog. *Journal of Biological Chemistry* **283:** 22076 -22088 Available at: [Accessed March 14, 2011]

Calabrese EJ & Baldwin LA (2003) The Hormetic Dose-Response Model Is More Common than the Threshold Model in Toxicology. *Toxicol. Sci.* **71:** 246-250 Available at: [Accessed June 2, 2010]

Calligaris D, Verdier-Pinard P, Devred F, Villard C, Braguer D & Lafitte D (2010) Microtubule targeting agents: from biophysics to proteomics. *Cell. Mol. Life Sci* **67:** 1089-1104 Available at: [Accessed June 2, 2010]

Caron RW, Yacoub A, Li M, Zhu X, Mitchell C, Hong Y, Hawkins W, Sasazuki T, Shirasawa S, Kozikowski AP, Dennis PA, Hagan MP, Grant S & Dent P (2005) Activated forms of H-RAS and K-RAS differentially regulate membrane association of PI3K, PDK-1, and AKT and the effect of therapeutic kinase inhibitors on cell survival. *Mol Cancer Ther* **4:** 257-270 Available at: [Accessed November 7, 2008]

Chavel CA, Dionne HM, Birkaya B, Joshi J & Cullen PJ (2010) Multiple Signals Converge on a Differentiation MAPK Pathway. *PLoS Genet* **6:** e1000883 Available at: [Accessed June 2, 2010]

Chen Y-S, Mathias RA, Mathivanan S, Kapp EA, Moritz RL, Zhu H-J & Simpson RJ (2010) Proteomic profiling of MDCK plasma membranes reveals Wnt-5a involvement during oncogenic H-Ras/TGF- -mediated epithelial-mesenchymal transition. *Molecular & Cellular Proteomics* Available at:

http://www.mcponline.org/content/early/2010/05/28/mcp.M110.001131.abstract [Accessed July 29, 2010]

Chen§ D, Waters§ SB, Holt KH & Pessin JE (1996) SOS Phosphorylation and Disassociation of the Grb2-SOS Complex by the ERK and JNK Signaling Pathways. *Journal of Biological Chemistry* **271::** 6328 -6332 Available at: [Accessed July 9, 2010]

Cheng H & Force T (2010) Molecular Mechanisms of Cardiovascular Toxicity of Targeted Cancer Therapeutics. *Circ Res* **106:** 21-34 Available at: [Accessed June 2, 2010]

Chiu VK, Bivona T, Hach A, Sajous JB, Silletti J, Wiener H, Johnson RL, Cox AD & Philips MR (2002) Ras signalling on the endoplasmic reticulum and the Golgi. *Nat Cell Biol* **4:** 343-350 Available at: [Accessed April 6, 2009]

Coleman RA, Rao P, Fogelsong RJ & Bardes ES (1992) 2-Bromopalmitoyl-CoA and 2-bromopalmitate: promiscuous inhibitors of membrane-bound enzymes. *Biochim Biophys Acta* **1125:** 203-9 Available at: [Accessed April 6, 2009]

Crouthamel M, Thiyagarajan MM, Evanko DS & Wedegaertner PB (2008) N-terminal polybasic motifs are required for plasma membrane localization of G[alpha]s and G[alpha]q. *Cellular Signalling* **20:** 1900-1910 Available at: [Accessed October 29, 2008]

Dasgupta P, Chattopadhyay S, Chaudhuri PP & Sengupta I (2001) Cellular automata-based recursive pseudoexhaustive test pattern generator. *Computers, IEEE Transactions on* **50:** 177-185

Dawson G, Schroeder C & Dawson PE (2010) Palmitoyl:protein thioesterase (PPT1) inhibitors can act as pharmacological chaperones in infantile Batten disease. *Biochem. Biophys. Res. Commun* **395:** 66-69 Available at: [Accessed March 14, 2011]

De Kepper P, Ouyang Q, Boissonade J & Roux JC (1990) Sustained coherent spatial structures in a quasi-1D reaction-diffusion system. *Reaction Kinetics and Catalysis Letters* **42:** 275-288 Available at: [Accessed June 2, 2010]

Dekker FJ, Koch MA & Waldmann H (2005) Protein structure similarity clustering (PSSC) and natural product structure as inspiration sources for drug development and chemical genomics. *Current Opinion in Chemical Biology* **9:** 232-239 Available at: [Accessed April 6, 2009]

Dekker FJ, Rocks O, Vartak N, Menninger S, Hedberg C, Balamurugan R, Wetzel S, Renner S, Gerauer M, Schölermann B, Rusch M, Kramer JW, Rauh D, Coates GW, Brunsveld L, Bastiaens PIH & Waldmann H (2010) Small-molecule inhibition of APT1 affects Ras localization and signaling. *Nat Chem Biol* **6:** 449-456 Available at: [Accessed May 25, 2010]

DeSouza S, Fu J, States BA & Ziff EB (2002) Differential Palmitoylation Directs the AMPA Receptor-Binding Protein ABP to Spines or to Intracellular Clusters. *J. Neurosci.* **22:** 3493-3503 Available at: [Accessed February 4, 2009]

Dietrich LEP & Ungermann C (2004) On the mechanism of protein palmitoylation. *EMBO Rep* **5:** 1053-1057 Available at: [Accessed September 16, 2010]

Dillon R, Maini PK & Othmer HG (1994) Pattern formation in generalized Turing systems. *Journal of Mathematical Biology* **32:** 345-393 Available at: [Accessed June 2, 2010]

Ding B & Lengyel P (2008) p204 protein is a novel modulator of ras activity. *J. Biol. Chem* **283:** 5831-5848 Available at: [Accessed June 2, 2010]

Drisdel RC & Green WN (2004) Labeling and quantifying sites of protein palmitoylation. *Biotechniques* **36:** 276-85 Available at: [Accessed April 6, 2009]

Duncan JA & Gilman AG (1998) A Cytoplasmic Acyl-Protein Thioesterase That Removes Palmitate from G Protein alpha �Subunits and p21RAS. *J. Biol. Chem.* **273:** 15830-15837 Available at: [Accessed April 6, 2009]

Edgar RC (2004) MUSCLE: multiple sequence alignment with high accuracy and high throughput. *Nucl. Acids Res.* **32:** 1792-1797 Available at: [Accessed September 7, 2009]

Feng X, Zhang J, Barak LS, Meyer T, Caron MG & Hannun YA (1998) Visualization of Dynamic Trafficking of a Protein Kinase C beta II/Green Fluorescent Protein Conjugate Reveals Differences in G Protein-coupled Receptor Activation and Desensitization. *J. Biol. Chem.* **273:** 10755-10762 Available at: [Accessed April 6, 2009]

Ferrell Jr. JE (2009) Signaling Motifs and Weber's Law. *Molecular Cell* **36:** 724-727 Available at: [Accessed July 7, 2010]

Finegan KG, Wang X, Lee E-J, Robinson AC & Tournier C (2009) Regulation of neuronal survival by the extracellular signal-regulated protein kinase 5. *Cell Death Differ* **16:** 674-683 Available at: [Accessed June 2, 2010]

Freedman TS, Sondermann H, Friedland GD, Kortemme T, Bar-Sagi D, Marqusee S & Kuriyan J (2006) A Ras-induced conformational switch in the Ras activator Son of sevenless. *Proceedings of the National Academy of Sciences* **103:** 16692-16697 Available at: [Accessed May 19, 2010]

Freedman TS, Sondermann H, Kuchment O, Friedland GD, Kortemme T & Kuriyan J (2009) Differences in Flexibility Underlie Functional Differences in the Ras Activators Son of Sevenless and Ras Guanine Nucleotide Releasing Factor 1. *Structure* **17:** 41-53 Available at: [Accessed May 19, 2010]

Fukata M, Fukata Y, Adesnik H, Nicoll RA & Bredt DS (2004) Identification of PSD-95 Palmitoylating Enzymes. *Neuron* **44:** 987-996 Available at: [Accessed May 20, 2009]

Fukata Y & Fukata M (2010) Protein palmitoylation in neuronal development and synaptic plasticity. *Nat. Rev. Neurosci* **11:** 161-175 Available at: [Accessed June 2, 2010]

Garber M, Guttman M, Clamp M, Zody MC, Friedman N & Xie X (2009) Identifying novel constrained elements by exploiting biased substitution patterns. *Bioinformatics* **25:** i54-62 Available at: [Accessed June 12, 2009]

Gelb MH, Brunsveld L, Hrycyna CA, Michaelis S, Tamanoi F, Van Voorhis WC & Waldmann H (2006) Therapeutic intervention based on protein prenylation and associated modifications. *Nat Chem Biol* **2:** 518-528 Available at: [Accessed March 14, 2011]

Goh LK, Huang F, Kim W, Gygi S & Sorkin A (2010) Multiple mechanisms collectively regulate clathrin-mediated endocytosis of the epidermal growth factor receptor. *J. Cell Biol* **189:** 871-883 Available at: [Accessed June 2, 2010]

Gomez-Uribe C, Verghese GC & Mirny LA (2007) Operating Regimes of Signaling Cycles: Statics, Dynamics, and Noise Filtering. *PLoS Comput Biol* **3:** e246 Available at: [Accessed March 23, 2010]

Gonnord P, Delarasse C, Auger R, Benihoud K, Prigent M, Cuif MH, Lamaze C & Kanellopoulos JM (2009) Palmitoylation of the P2X7 receptor, an ATP-gated channel, controls its expression and association with lipid rafts. *The FASEB Journal* **23:** 795 -805 Available at: [Accessed March 14, 2011]

Goytain A, Hines RM & Quamme GA (2008) Huntingtin-interacting Proteins, HIP14 and HIP14L, Mediate Dual Functions, Palmitoyl Acyltransferase and Mg2+ Transport. *J. Biol. Chem.* **283:** 33365-33374 Available at: [Accessed May 26, 2009]

Grecco HE, Roda-Navarro P, Girod A, Hou J, Frahm T, Truxius DC, Pepperkok R, Squire A & Bastiaens PIH (2010) In situ analysis of tyrosine phosphorylation networks by FLIM on cell arrays. *Nat Meth* **advance online publication:** Available at: http://dx.doi.org/10.1038/nmeth.1458 [Accessed May 14, 2010]

Gulbins E, Coggeshall KM, Langlet C, Baier G, Bonnefoy-Berard N, Burn P, Wittinghofer A, Katzav S & Altman A (1994) Activation of Ras in vitro and in intact fibroblasts by the Vav guanine nucleotide exchange protein. *Mol. Cell. Biol* **14:** 906-913 Available at: [Accessed March 14, 2011]

Harding A & Hancock J (2008) Using plasma membrane nanoclusters to build better signaling circuits. *Trends in Cell Biology* **18:** 364-371 Available at: [Accessed March 14, 2011]

Harvey CD, Yasuda R, Zhong H & Svoboda K (2008) The Spread of Ras Activity Triggered by Activation of a Single Dendritic Spine. *Science* **321:** 136-140 Available at: [Accessed April 22, 2010]

Hayashi T, Thomas GM & Huganir RL (2009) Dual Palmitoylation of NR2 Subunits Regulates NMDA Receptor Trafficking. *Neuron* **64:** 213-226 Available at: [Accessed March 14, 2011]

Herz J, Willnow TE & Farese RV (1997) Cholesterol, hedgehog and embryogenesis. *Nat Genet* **15:** 123-124 Available at: [Accessed March 14, 2011]

Hirano T, Kishi M, Sugimoto H, Taguchi R, Obinata H, Ohshima N, Tatei K & Izumi T (2009a) Thioesterase activity and subcellular localization of acylprotein thioesterase 1/lysophospholipase 1. *Biochimica et Biophysica Acta (BBA) - Molecular and Cell Biology of Lipids* **1791:** 797-805 Available at: [Accessed October 7, 2010]

Hirano T, Kishi M, Sugimoto H, Taguchi R, Obinata H, Ohshima N, Tatei K & Izumi T (2009b) Thioesterase activity and subcellular localization of acylprotein thioesterase 1/lysophospholipase 1. *Biochim. Biophys. Acta* **1791:** 797-805 Available at: [Accessed June 2, 2010]

Hofman EG, Bader AN, Voortman J, van den Heuvel DJ, Sigismund S, Verkleij AJ, Gerritsen HC & van Bergen en Henegouwen PMP (2010) Ligand-induced EGF Receptor Oligomerization Is Kinase-dependent and Enhances Internalization. *Journal of Biological Chemistry* **285:** 39481 -39489 Available at: [Accessed March 14, 2011]

Hou H, Peter ATJ, Meiringer C, Subramanian K & Ungermann C (2009) Analysis of DHHC Acyltransferases Implies Overlapping Substrate Specificity and a Two-Step Reaction Mechanism. *Traffic* **9999:** Available at: http://dx.doi.org/10.1111/j.1600-0854.2009.00925.x [Accessed June 1, 2009]

Hougland JL & Fierke CA (2009) Getting a handle on protein prenylation. *Nat Chem Biol* **5:** 197-198 Available at: [Accessed March 14, 2011]

Inder K, Harding A, Plowman SJ, Philips MR, Parton RG & Hancock JF (2008) Activation of the MAPK Module from Different Spatial Locations Generates Distinct System Outputs. *Mol. Biol. Cell*: E08-04-0407 Available at: [Accessed October 6, 2008]

Innocenti M, Tenca P, Frittoli E, Faretta M, Tocchetti A, Fiore PPD & Scita G (2002) Mechanisms through Which Sos-1 Coordinates the Activation of Ras and Rac. *The Journal of Cell Biology* **156:** 125-136 Available at: [Accessed March 10, 2009]

Ireland CM (1989) Activated N-ras oncogenes in human neuroblastoma. *Cancer Res* **49:** 5530-5533 Available at: [Accessed March 14, 2011]

Iwanaga T, Tsutsumi R, Noritake J, Fukata Y & Fukata M (2009) Dynamic protein palmitoylation in cellular signaling. *Progress in Lipid Research* **48:** 117-127 Available at: [Accessed June 5, 2009]

Iwanaga T, Tsutsumi R, Noritake J, Fukata Y & Fukata M Dynamic protein palmitoylation in cellular signaling. *Progress in Lipid Research* **In Press, Corrected Proof:** Available at: http://www.sciencedirect.com/science/article/B6TBP-4VNH3NT-1/2/0daa5531edd53cb3c6a9502cf4a8f676 [Accessed May 20, 2009]

Jang IK, Zhang J, Chiang YJ, Kole HK, Cronshaw DG, Zou Y & Gu H (2010) Grb2 functions at the top of the T-cell antigen receptor-induced tyrosine kinase cascade to control thymic selection. *Proc Natl Acad Sci U S A* Available at: http://www.ncbi.nlm.nih.gov/pubmed/20498059 [Accessed June 2, 2010]

Jennings BC, Nadolski MJ, Ling Y, Baker MB, Harrison ML, Deschenes RJ & Linder ME (2009) 2-Bromopalmitate and 2-(2-hydroxy-5-nitro-benzylidene)-benzo[b]thiophen-3-one inhibit DHHC-mediated palmitoylation in vitro. *J. Lipid Res.* **50:** 233-242 Available at: [Accessed April 6, 2009]

Johnson L, Greenbaum D, Cichowski K, Mercer K, Murphy E, Schmitt E, Bronson RT, Umanoff H, Edelmann W, Kucherlapati R & Jacks T (1997) K-ras is an essential gene in the mouse with partial functional overlap with N-ras. *Genes Dev* **11:** 2468-2481

Karaguni I-M, Herter P, Debruyne P, Chtarbova S, Kasprzynski A, Herbrand U, Ahmadian M-R, Glusenkamp K-H, Winde G, Mareel M, Möröy T & Müller O (2002) The New Sulindac

Derivative IND 12 Reverses Ras-induced Cell Transformation. *Cancer Res* **62:** 1718-1723 Available at: [Accessed June 15, 2009]

Kholodenko BN, Hancock JF & Kolch W (2010) Signalling ballet in space and time. *Nat Rev Mol Cell Biol* **11:** 414-426 Available at: [Accessed May 31, 2010]

Klohs WD, Fry DW & Kraker AJ (1997) Inhibitors of tyrosine kinase. *Curr Opin Oncol* **9:** 562-568 Available at: [Accessed June 2, 2010]

Kolch W (2005) Coordinating ERK/MAPK signalling through scaffolds and inhibitors. *Nat Rev Mol Cell Biol* **6:** 827-837 Available at: [Accessed March 14, 2011]

Kramer BP & Fussenegger M (2005) Hysteresis in a synthetic mammalian gene network. *Proc. Natl. Acad. Sci. U.S.A* **102:** 9517-9522 Available at: [Accessed July 2, 2010]

Kulkarni VV, Kareenhalli V, Malakar P, Pao LY, Safonov MG & Viswanathan GA (2010) Stability analysis of the GAL regulatory network in Saccharomyces cerevisiae and Kluyveromyces lactis. *BMC Bioinformatics* **11 Suppl 1:** S43 Available at: [Accessed July 2, 2010]

Lemmon MA & Schlessinger J (2010) Cell Signaling by Receptor Tyrosine Kinases. *Cell* **141:** 1117-1134 Available at: [Accessed June 28, 2010]

Liang X, Lu Y, Neubert TA & Resh MD (2002) Mass spectrometric analysis of GAP-43/neuromodulin reveals the presence of a variety of fatty acylated species. *Journal of Biological Chemistry* **277:** 33032-33040 Available at: [Accessed March 14, 2011]

Lindenmayer A (1968) Mathematical models for cellular interactions in development II. Simple and branching filaments with two-sided inputs. *Journal of Theoretical Biology* **18:** 300-315 Available at: [Accessed March 14, 2011]

Linder ME & Deschenes RJ (2007) Palmitoylation: policing protein stability and traffic. *Nat Rev Mol Cell Biol* **8:** 74-84 Available at: [Accessed March 14, 2011]

Lorentzen A, Kinkhabwala A, Rocks O, Vartak N & Bastiaens PIH (2010) Regulation of Ras Localization by Acylation Enables a Mode of Intracellular Signal Propagation. *Sci. Signal.* **3:** ra68 Available at: [Accessed September 22, 2010]

Lowenstein E (1992) The SH2 and SH3 domain-containing protein GRB2 links receptor tyrosine kinases to ras signaling. *Cell* **70:** 431-442 Available at: [Accessed March 14, 2011]

Macia E, Ehrlich M, Massol R, Boucrot E, Brunner C & Kirchhausen T (2006a) Dynasore, a Cell-Permeable Inhibitor of Dynamin. *Developmental Cell* **10:** 839-850 Available at: [Accessed March 16, 2009]

Macia E, Ehrlich M, Massol R, Boucrot E, Brunner C & Kirchhausen T (2006b) Dynasore, a cell-permeable inhibitor of dynamin. *Dev. Cell* **10:** 839-850 Available at: [Accessed 16:28:49]

Maeda A, Okano K, Park PS-H, Lem J, Crouch RK, Maeda T & Palczewski K Palmitoylation stabilizes unliganded rod opsin. *Proceedings of the National Academy of Sciences* Available at:

http://www.pnas.org/content/early/2010/04/07/1000640107.abstract [Accessed March 6, 2011]

MAINI PK, BENSON DL & SHERRATT JA (1992) Pattern formation in reaction-diffusion models with spatially inhomogeneous diffusion coefficients. *Math Med Biol* **9:** 197-213 Available at: [Accessed June 2, 2010]

Manders EEM, Verbeek FJ & Aten JA (1993) Measurement of co-localisation of objects in dual-colour confocal images. *J.Microscopy***:** 375-382

Martin BR & Cravatt BF (2009) Large-scale profiling of protein palmitoylation in mammalian cells. *Nat Meth* **6:** 135-138 Available at: [Accessed June 2, 2010]

Martin DDO, Beauchamp E & Berthiaume LG (2011) Post-translational myristoylation: Fat matters in cellular life and death. *Biochimie* **93:** 18-31 Available at: [Accessed March 14, 2011]

Mastrangelo AM, Downward J, Ginsberg M & LaFlamme SE, with Allison L. Berrier (2000) Activated R-Ras, Rac1, Pi 3-Kinase and PKCε Can Each Restore Cell Spreading Inhibited by Isolated Integrin β1 Cytoplasmic Domains. *The Journal of Cell Biology* **151:** 1549-1560 Available at: [Accessed March 14, 2011]

Matakatsu H & Blair SS (2008) The DHHC Palmitoyltransferase Approximated Regulates Fat Signaling and Dachs Localization and Activity. *Current Biology* **18:** 1390-1395 Available at: [Accessed October 29, 2008]

Matallanas D, Sanz-Moreno V, Arozarena I, Calvo F, Agudo-Ibanez L, Santos E, Berciano MT & Crespo P (2006) Distinct Utilization of Effectors and Biological Outcomes Resulting from Site-Specific Ras Activation: Ras Functions in Lipid Rafts and Golgi Complex Are Dispensable for Proliferation and Transformation. *Mol. Cell. Biol.* **26:** 100-116 Available at: [Accessed June 2, 2010]

Maurer-Stroh S, Eisenhaber B & Eisenhaber F (2002) N-terminal N-myristoylation of proteins: prediction of substrate proteins from amino acid sequence. *Journal of Molecular Biology* **317:** 541-557 Available at: [Accessed March 14, 2011]

Maurer-Stroh S & Eisenhaber F (2005) Refinement and prediction of protein prenylation motifs. *Genome Biol* **6:** R55 Available at: [Accessed March 14, 2011]

McGeady P, Kuroda S, Shimizu K, Takai Y & Gelb MH (1995) The Farnesyl Group of H-Ras Facilitates the Activation of a Soluble Upstream Activator of Mitogen-activated Protein Kinase. *Journal of Biological Chemistry* **270:** 26347 -26351 Available at: [Accessed March 14, 2011]

Meyers J, Craig J & Odde DJ (2006) Potential for Control of Signaling Pathways via Cell Size and Shape. *Current Biology* **16:** 1685-1693 Available at: [Accessed July 7, 2010]

Milenkovic L & Scott MP (2010) Not Lost in Space: Trafficking in the Hedgehog Signaling Pathway. *Sci. Signal.* **3:** pe14 Available at: [Accessed April 19, 2010]

Morris DL, O'Neil SP, Devraj RV, Portanova JP, Gilles RW, Gross CJ, Curtiss SW, Komocsar WJ, Garner DS, Happa FA, Kraus LJ, Nikula KJ, Monahan JB, Selness SR, Galluppi GR, Shevlin KM, Kramer

JA, Walker JK, Messing DM, Anderson DR, et al (2010) Acute lymphoid and gastrointestinal toxicity induced by selective p38alpha map kinase and map kinase-activated protein kinase-2 (MK2) inhibitors in the dog. *Toxicol Pathol* **38:** 606-618 Available at: [Accessed March 14, 2011]

Nadolski MJ & Linder ME (2009) Molecular recognition of the palmitoylation substrate VAC8 by its palmitoyltransferase PFA3. *J. Biol. Chem.***:** M109.005447 Available at: [Accessed May 18, 2009]

Narula J, Smith AM, Gottgens B & Igoshin OA (2010) Modeling reveals bistability and low-pass filtering in the network module determining blood stem cell fate. *PLoS Comput. Biol* **6:** e1000771 Available at: [Accessed July 2, 2010]

Navarro-Lerida I, Alvarez-Barrientos A, Gavilanes F & Rodriguez-Crespo I (2002) Distance-dependent cellular palmitoylation of de-novo-designed sequences and their translocation to plasma membrane subdomains. *J Cell Sci* **115:** 3119-3130 Available at: [Accessed March 14, 2011]

Newton R, Cambridge L, Hart LA, Stevens DA, Lindsay MA & Barnes PJ (2000) The MAP kinase inhibitors, PD098059, UO126 and SB203580, inhibit IL-1[beta]-dependent PGE2 release via mechanistically distinct processes. *Br J Pharmacol* **130:** 1353-1361 Available at: [Accessed February 20, 2009]

Norton JD, Connor J & Avery RJ (1984) Genesis of Kirsten murine sarcoma virus: sequence analysis reveals recombination points and potential leukaemogenic determinant on parental leukaemia virus genome. *Nucleic Acids Res* **12:** 6839-6852 Available at: [Accessed March 14, 2011]

Ohno Y, Kihara A, Sano T & Igarashi Y (2006) Intracellular localization and tissue-specific distribution of human and yeast DHHC cysteine-rich domain-containing proteins. *Biochimica et Biophysica Acta (BBA) - Molecular and Cell Biology of Lipids* **1761:** 474-483 Available at: [Accessed May 28, 2009]

Olsen JV, Vermeulen M, Santamaria A, Kumar C, Miller ML, Jensen LJ, Gnad F, Cox J, Jensen TS, Nigg EA, Brunak S & Mann M (2010) Quantitative Phosphoproteomics Reveals Widespread Full Phosphorylation Site Occupancy During Mitosis. *Sci. Signal.* **3:** ra3 Available at: [Accessed June 2, 2010]

Onder TT, Gupta PB, Mani SA, Yang J, Lander ES & Weinberg RA (2008) Loss of E-Cadherin Promotes Metastasis via Multiple Downstream Transcriptional Pathways. *Cancer Res* **68:** 3645-3654 Available at: [Accessed 22:29:02]

Pan YH, Nuzum EO, Hanson LA & Beer DG (1990) Ki-ras activation and expression in transformed mouse lung cell lines. *Mol. Carcinog* **3:** 279-286 Available at: [Accessed March 14, 2011]

Parada LF, Tabin CJ, Shih C & Weinberg RA (1982) Human EJ bladder carcinoma oncogene is homologue of Harvey sarcoma virus ras gene. *Nature* **297:** 474-478 Available at: [Accessed October 11, 2010]

Peyker A, Kinkhabwala A, Rocks O, Vartak N & Bastiaens P (2010) Spatial Regulation of Ras Reveals a Novel Mode of Intracellular Signal Propagation. *Accepted, In Press, Science Signaling*

Peyssonnaux C & Eychène A (2001) The Raf/MEK/ERK pathway: new concepts of activation. *Biology of the Cell* **93:** 53-62 Available at: [Accessed March 14, 2011]

Pfaffl MW (2001) A new mathematical model for relative quantification in real-time RT-PCR. *Nucl. Acids Res.* **29:** e45 Available at: [Accessed April 6, 2009]

Philips MR (2004) Sef: A MEK/ERK Catcher on the Golgi. *Molecular Cell* **15:** 168-169 Available at: [Accessed May 6, 2010]

Polack F & Stepney S (2005) Emergent Properties Do Not Refine. *Electronic Notes in Theoretical Computer Science* **137:** 163-181 Available at: [Accessed March 14, 2011]

Preston RJ (2005) Bystander effects, genomic instability, adaptive response, and cancer risk assessment for radiation and chemical exposures. *Toxicology and Applied Pharmacology* **207:** 550-556 Available at: [Accessed June 2, 2010]

Prior I & Hancock J (2001) Compartmentalization of Ras proteins. *J Cell Sci* **114:** 1603-1608 Available at: [Accessed March 14, 2011]

Prior IA, Harding A, Yan J, Sluimer J, Parton RG & Hancock JF (2001) GTP-dependent segregation of H-ras from lipid rafts is required for biological activity. *Nat Cell Biol* **3:** 368-375 Available at: [Accessed July 7, 2010]

Quatela SE, Sung PJ, Ahearn IM, Bivona TG & Philips MR (2008) Analysis of K-Ras phosphorylation, translocation, and induction of apoptosis. *Meth. Enzymol* **439:** 87-102 Available at: [Accessed June 2, 2010]

Quinlan MP & Settleman J (2009) Isoform-specific ras functions in development and cancer. *Future Oncol* **5:** 105-116 Available at: [Accessed March 14, 2011]

Rajnicek AM, Foubister LE & McCaig CD (2006) Temporally and spatially coordinated roles for Rho, Rac, Cdc42 and their effectors in growth cone guidance by a physiological electric field. *J Cell Sci* **119:** 1723-1735 Available at: [Accessed July 7, 2010]

Rak A, Pylypenko O, Durek T, Watzke A, Kushnir S, Brunsveld L, Waldmann H, Goody RS & Alexandrov K (2003) Structure of Rab GDP-Dissociation Inhibitor in Complex with Prenylated YPT1 GTPase. *Science* **302:** 646-650 Available at: [Accessed June 2, 2010]

Reid TS, Terry KL, Casey PJ & Beese LS (2004) Crystallographic analysis of CaaX prenyltransferases complexed with substrates defines rules of protein substrate selectivity. *J. Mol. Biol* **343:** 417-433 Available at: [Accessed March 14, 2011]

Resh MD (2006) Trafficking and signaling by fatty-acylated and prenylated proteins. *Nat Chem Biol* **2:** 584-590 Available at: [Accessed March 14, 2011]

Roberts CJ, Nelson B, Marton MJ, Stoughton R, Meyer MR, Bennett HA, He YD, Dai H, Walker WL, Hughes TR, Tyers M, Boone C & Friend SH (2000) Signaling and Circuitry of Multiple MAPK Pathways Revealed by a Matrix of Global Gene Expression Profiles. *Science* **287:** 873-880 Available at: [Accessed June 2, 2010]

Rocks O, Gerauer M, Vartak N, Koch S, Huang Z-P, Pechlivanis M, Kuhlmann J, Brunsveld L, Chandra A, Ellinger B, Waldmann H & Bastiaens PIH (2010) The Palmitoylation Machinery Is a Spatially Organizing System for Peripheral Membrane Proteins. *Cell* **141:** 458-471 Available at: [Accessed February 9, 2011]

Rocks O, Peyker A & Bastiaens PI (2006) Spatio-temporal segregation of Ras signals: one ship, three anchors, many harbors. *Current Opinion in Cell Biology* **18:** 351-357 Available at: [Accessed April 6, 2009]

Rocks O, Peyker A, Kahms M, Verveer PJ, Koerner C, Lumbierres M, Kuhlmann J, Waldmann H, Wittinghofer A & Bastiaens PIH (2005) An Acylation Cycle Regulates Localization and Activity of Palmitoylated Ras Isoforms. *Science* **307:** 1746-1752 Available at: [Accessed April 6, 2009]

Roth AF, Feng Y, Chen L & Davis NG (2002) The yeast DHHC cysteine-rich domain protein Akr1p is a palmitoyl transferase. *J. Cell Biol* **159:** 23-28 Available at: [Accessed June 2, 2010]

Roth AF, Wan J, Bailey AO, Sun B, Kuchar JA, Green WN, Phinney BS, III JRY & Davis NG (2006) Global Analysis of Protein Palmitoylation in Yeast. *Cell.* **125:** 1003–1013 Available at: [Accessed May 26, 2009]

Sabouri-Ghomi M, Ciliberto A, Kar S, Novak B & Tyson JJ (2008) Antagonism and bistability in protein interaction networks. *J. Theor. Biol* **250:** 209-218 Available at: [Accessed July 2, 2010]

Salaun C, Greaves J & Chamberlain LH (2010) The intracellular dynamic of protein palmitoylation. *The Journal of Cell Biology* **191:** 1229 -1238 Available at: [Accessed March 14, 2011]

Santillo M, Mondola P, Gioielli A, Serù R, Iossa S, Annella T, Vitale M & Bifulco M (1996) Inhibitors of Ras Farnesylation Revert the Increased Resistance to Oxidative Stress in K-rasTransformed NIH 3T3 Cells. *Biochemical and Biophysical Research Communications* **229:** 739-745 Available at: [Accessed March 14, 2011]

Santos SDM, Verveer PJ & Bastiaens PIH (2007) Growth factor-induced MAPK network topology shapes Erk response determining PC-12 cell fate. *Nat Cell Biol* **9:** 324-330 Available at: [Accessed June 2, 2010]

Sato I, Obata Y, Kasahara K, Nakayama Y, Fukumoto Y, Yamasaki T, Yokoyama KK, Saito T & Yamaguchi N (2009) Differential trafficking of Src, Lyn, Yes and Fyn is specified by the state of palmitoylation in the SH4 domain. *J Cell Sci* **122:** 965-975 Available at: [Accessed March 14, 2011]

Schmidt CR, Washington MK, Gi YJ, Coffey RJ, Beauchamp RD & Pearson AS (2003) Dysregulation of E-cadherin by oncogenic Ras in intestinal epithelial cells is blocked by inhibiting MAP kinase. *Am J Surg* **186:** 426-30 Available at: [Accessed November 25, 2008]

Scott BR (2004) A biological-based model that links genomic instability, bystander effects, and adaptive response. *Mutation Research/Fundamental and Molecular Mechanisms of Mutagenesis* **568:** 129-143 Available at: [Accessed June 2, 2010]

Shields J (2000) Understanding Ras: "it ain"t over "til it"s over'. *Trends in Cell Biology* **10:** 147-154 Available at: [Accessed March 14, 2011]

Silvius JR & l'Heureux F (1994) Fluorometric Evaluation of the Affinities of Isoprenylated Peptides for Lipid Bilayers. *Biochemistry* **33:** 3014-3022 Available at: [Accessed September 16, 2010]

Smida M, Posevitz-Fejfar A, Horejsi V, Schraven B & Lindquist JA (2007) A novel negative regulatory function of the phosphoprotein associated with glycosphingolipid-enriched microdomains: blocking Ras activation. *Blood* **110:** 596-615 Available at: [Accessed June 2, 2010]

Smyth P (1997) Clustering Sequences with Hidden Markov Models. *ADVANCES IN NEURAL INFORMATION PROCESSING SYSTEMS* **9:** 648--654 Available at: [Accessed September 7, 2009]

Soumpasis D (1983) Theoretical analysis of fluorescence photobleaching recovery experiments. *Biophysical Journal* **41:** 95-97 Available at: [Accessed March 14, 2011]

Swarthout JT, Lobo S, Farh L, Croke MR, Greentree WK, Deschenes RJ & Linder ME (2005) DHHC9 and GCP16 Constitute a Human Protein Fatty Acyltransferase with Specificity for H- and N-Ras. *Journal of Biological Chemistry* **280:** 31141-31148 Available at: [Accessed June 2, 2010]

Takahashi K, Tănase-Nicola S & ten Wolde PR (2010) Spatio-temporal correlations can drastically change the response of a MAPK pathway. *Proceedings of the National Academy of Sciences* **107:** 2473-2478 Available at: [Accessed July 2, 2010]

Tian T, Harding A, Inder K, Plowman S, Parton RG & Hancock JF (2007) Plasma membrane nanoswitches generate high-fidelity Ras signal transduction. *Nat Cell Biol* **9:** 905-914 Available at: [Accessed July 7, 2010]

To T-L & Maheshri N (2010) Noise can induce bimodality in positive transcriptional feedback loops without bistability. *Science* **327:** 1142-1145 Available at: [Accessed July 2, 2010]

Tomatis VM, Trenchi A, Gomez GA & Daniotti JL Acyl-Protein Thioesterase 2 Catalizes the Deacylation of Peripheral Membrane-Associated GAP-43. *PLoS One* **5:**

Toomey RE & Wakil SJ (1966) Studies on the Mechanism of Fatty Acid Synthesis. *Journal of Biological Chemistry* **241:** 1159 -1165 Available at: [Accessed March 14, 2011]

Tsai F-M, Shyu R-Y & Jiang S-Y (2007) RIG1 suppresses Ras activation and induces cellular apoptosis at the Golgi apparatus. *Cellular Signalling* **19:** 989-999 Available at: [Accessed May 6, 2010]

Ulsh LS & Shih TY (1984) Metabolic turnover of human c-rasH p21 protein of EJ bladder carcinoma and its normal cellular and viral homologs. *Mol. Cell. Biol* **4:** 1647-1652 Available at: [Accessed March 14, 2011]

Valdez-Taubas J & Pelham H (2005) Swf1-dependent palmitoylation of the SNARE Tlg1 prevents its ubiquitination and degradation. *EMBO J* **24:** 2524-2532 Available at: [Accessed March 14, 2011]

Vetter IR & Wittinghofer A (2001) The guanine nucleotide-binding switch in three dimensions. *Science* **294:** 1299-1304 Available at: [Accessed March 14, 2011]

Wang A, Johnson CA, Jones Y, Ellisman MH & Dennis EA (2000) Subcellular localization and PKC-dependent regulation of the human lysophospholipase A/acyl-protein thioesterase in WISH cells. *Biochim. Biophys. Acta* **1484:** 207-214 Available at: [Accessed March 14, 2011]

Wang Q, Villeneuve G & Wang Z (2005) Control of epidermal growth factor receptor endocytosis by receptor dimerization, rather than receptor kinase activation. *EMBO Rep* **6:** 942-948 Available at: [Accessed March 14, 2011]

Waters SB, Holt KH, Ross SE, Syu L-J, Guan K-L, Saltiel AR, Koretzky GA & Pessin JE (1995) Desensitization of Ras Activation by a Feedback Disassociation of the SOS-Grb2 Complex. *Journal of Biological Chemistry* **270::** 20883 -20886 Available at: [Accessed July 9, 2010]

Watson RT, Furukawa M, Chiang S-H, Boeglin D, Kanzaki M, Saltiel AR & Pessin JE (2003) The Exocytotic Trafficking of TC10 Occurs through both Classical and Nonclassical Secretory Transport Pathways in 3T3L1 Adipocytes. *Mol. Cell. Biol.* **23:** 961-974 Available at: [Accessed March 14, 2011]

Weichsel J & Schwarz US (2010) Two competing orientation patterns explain experimentally observed anomalies in growing actin networks. *Proc. Natl. Acad. Sci. U.S.A* **107:** 6304-6309 Available at: [Accessed July 2, 2010]

Wennerberg K, Rossman KL & Der CJ (2005) The Ras superfamily at a glance. *J Cell Sci* **118:** 843-846 Available at: [Accessed December 8, 2009]

Wittinghofer A, Scheffzek K & Ahmadian MR (1997) The interaction of Ras with GTPase-activating proteins. *FEBS Lett* **410:** 63-67 Available at: [Accessed September 16, 2010]

Xiong W & Ferrell JE (2003) A positive-feedback-based bistable /`memory module/' that governs a cell fate decision. *Nature* **426:** 460-465 Available at: [Accessed July 7, 2010]

Yeung T, Gilbert GE, Shi J, Silvius J, Kapus A & Grinstein S (2008) Membrane Phosphatidylserine Regulates Surface Charge and Protein Localization. *Science* **319:** 210-213 Available at: [Accessed April 15, 2010]

Yi P, Nguyen DT, Higa-Nishiyama A, Auguste P, Bouchecareilh M, Dominguez M, Bielmann R, Palcy S, Liu JF & Chevet E (2010) MAPK scaffolding by BIT1 in the Golgi complex modulates stress resistance. *J Cell Sci* **123:** 1060-1072 Available at: [Accessed May 6, 2010]

Yip S-C, El-Sibai M, Coniglio SJ, Mouneimne G, Eddy RJ, Drees BE, Neilsen PO, Goswami S, Symons M, Condeelis JS & Backer JM (2007) The distinct roles of Ras and Rac in PI 3-kinase-dependent protrusion during EGF-stimulated cell migration. *J Cell Sci***:** jcs.005298 Available at: [Accessed March 14, 2011]

Zha J, Weiler S, Oh KJ, Wei MC & Korsmeyer SJ (2000) Posttranslational N-Myristoylation of BID as a Molecular Switch for Targeting Mitochondria and Apoptosis. *Science* **290:** 1761 -1765 Available at: [Accessed March 14, 2011]

Zhang B, Zhang Y, Shacter E & Zheng Y (2005) Mechanism of the guanine nucleotide exchange reaction of Ras GTPase--evidence for a GTP/GDP displacement model. *Biochemistry* **44:** 2566-2576 Available at: [Accessed June 2, 2010]

Zhao C, Du G, Skowronek K, Frohman MA & Bar-Sagi D (2007) Phospholipase D2-generated phosphatidic acid couples EGFR stimulation to Ras activation by Sos. *Nat. Cell Biol* **9:** 706-712 Available at: [Accessed May 25, 2010]

Zhong H, Wade SM, Woolf PJ, Linderman JJ, Traynor JR & Neubig RR (2003) A Spatial Focusing Model for G Protein Signals. *Journal of Biological Chemistry* **278:** 7278-7284 Available at: [Accessed April 20, 2010]

ACKNOWLEDGEMENTS

PUBLICATIONS AND PRESENTATIONS

Results and methodologies presented in this thesis have contributed to the following peer-reviewed publications:

- Dekker FJ, Rocks O, Vartak N, Menninger S, Hedberg C, Balamurugan R, Wetzel S, Renner S, Gerauer M, Schölermann B, Rusch M, Kramer JW, Rauh D, Coates GW, Brunsveld L, Bastiaens PIH & Waldmann H (2010) Small-molecule inhibition of APT1 affects Ras localization and signaling. *Nat Chem Biol* **6:** 449-456
- Lorentzen A, Kinkhabwala A, Rocks O, Vartak N & Bastiaens PIH (2010) Regulation of Ras Localization by Acylation Enables a Mode of Intracellular Signal Propagation. *Sci. Signal.* **3:** ra68
- Rocks O, Gerauer M, Vartak N, Koch S, Huang Z-P, Pechlivanis M, Kuhlmann J, Brunsveld L, Chandra A, Ellinger B, Waldmann H & Bastiaens PIH (2010) The Palmitoylation Machinery Is a Spatially Organizing System for Peripheral Membrane Proteins. *Cell* **141:** 458-471
- Vartak N & Bastiaens P (2010) Spatial cycles in G-protein crowd control. *EMBO J* **29:** 2689-2699
- Christian H, Dekker F, Rusch M, Renner S, Wetzel S, Vartak N, Gerding-Reimers C, Bon R, Bastiaens PIH, Waldmann H (2011) Development of Highly Potent Inhibitors of the Ras-Targeting Human Acyl Protein Thioesterases Based on Substrate Similarity Design. *Angewandte Chemie International Edition* (in review)

The work was presented at the following conferences :

- IMPRS-CB Symposium 2010 – "Spatial Organization of Palmitoylated Proteins"
- Sonderforchungsbereit 642 Annual Meets, Ruhr-Universitaet, Bochum

CURRICULUM VITAE

Name : Nachiket Vartak

Address : Appartment 11, Hohe Str. 98, 44139 Dortmund, Germany

Telephone : +49-176-630-31139

Email : nash@vartak.org

Date of Birth : 05 Dec 1983

Nationality : Indian

University Matriculation Number : 113912 (TU Dortmund)

Education :

July 2001-July 2004 - Bachelor of Science (Life sciences and Biochemistry)
Institution: St.Xavier's College, University of Mumbai
Grade : First Class with Distinction at 81.00%

July 2004- August 2006 – Master of Science (Biotechnology)
Institution: Indian Institute of Technology , Mumbai
Grade/CPI – 9.3 /10

August 2006- Jan 2007 – Training in advanced Biological Imaging
Instituion: Cell Biology Unit, European Molecular Biology

Current Occupation (Jan 2007-present)
Ph.D student at the Department of Systemic Cell Biology, Max Planck Inst. For Molecular
Physiology, Dortmund, in the group of Prof.Dr. Philippe Bastiaens.

ABBRIEVIATIONS

2-BP	2 Bromopalmitate
ABE	Acyl-Biotin Exchange Assay
APT	Acyl Protein Thioesterase
Asp	Aspartate
BMCC	1-biotinamido-4-[4´(maleimidomethyl)cyclohexanecarboxamido]butane
CRD	Cysteine Rich Domain
Cys	Cysteine
EGF/R	Epidermal Growth Factor/ Receptor
ER	Endoplasmic Reticulum
FLIM	Fluorescence Lifetime Imaging Microscopy
FRET	Foerster Resonance Energy Transfer
MAPK	Mitogen Activated Protein Kinase
Met	Methionine
Palm B	Palmostatin B
PAT	Palmitoyltransferase
PM	Plasma Membrane
RTK	Receptor Tyrosine Kinase
RT-qPCR	Reverse Transcriptase Quantitative Polymerase Chain Reaction
Ser	Serine
Thr	Threonine
TIRF	Total Internal Reflection Fluorescence
Tyr	Tyrosine